THE JOURNAL
OF
CHEMICAL PHYSICS

VOLUME 5 JANUARY, 1937 NUMBER 1

The Analysis of Isotopic Mixtures of Deuteromethanes and Ethanes by Infrared Absorption Spectra

W. S. BENEDICT, KIYOSHI MORIKAWA, R. BOWLING BARNES AND H. S. TAYLOR, *Princeton University, Princeton, N. J.*

(Received October 16, 1936)

The infrared absorption spectra of a large number of deuterium-containing methane samples, and a few of ethane, have been studied with a rocksalt spectrometer. All the observable fundamental frequencies of each individual methane isotope have been identified, and from the relative intensity of absorption at various characteristic wave-lengths the composition of any mixture of these isotopes may be determined. The infrared spectra of deuteroethanes including C_2D_6 have been observed.

THE exchange reactions between deuterium and various hydrogen-containing compounds have yielded much information of chemical interest concerning the stability of these compounds. In several preliminary notes[1] we have given the chief results of such studies on the simplest hydrocarbons, methane and ethane. In the present paper, one of a series of more detailed communications, the others of which are appearing in the *Journal of the American Chemical Society*, we will describe the general method of analysis of our samples, involving the infrared spectra of these compounds, some of which have not been previously reported. A subsequent paper will deal with the theoretical and experimental determination of the equilibrium of the reactions

$$CH_4+nD_2\rightleftarrows CH_{4-2n}D_{2n}+nH_2, \text{ etc.}$$

The use of infrared spectroscopy for the analysis of isotope exchanges appears to be new. The advantage of absorption spectroscopy in analyzing isotopic mixtures is that the presence of each individual isotopic molecule is made known by its characteristic absorption bands. Infrared absorption is made necessary in the case of saturated hydrocarbons by the absence of any banded absorption in the visible or ultraviolet regions, which made the semiquantitative analysis of exchange in ammonia[2] and benzene[3] so convenient. The comparative tedium of the infrared technique is more than compensated, however, by the quantitative accuracy obtainable; and after experience and a number of calibrating analyses throughout the entire infrared spectrum have disclosed the few wave-lengths at which the absorption is most significant, a complete analysis giving the composition of a mixture of deuteromethanes to within 1 or 2 percent for each isotopic constituent is a matter of a very few hours.

PREPARATION OF SAMPLES

In addition to determining the infrared absorption of a large number of "unknown"

[1] Taylor, Morikawa and Benedict, J. Am. Chem. Soc. **57**, 383 (1935); ibid. **57**, 592 (1935); ibid. **57**, 2735 (1935).

[2] Taylor and Jungers, J. Chem. Phys. **2**, 373 (1934).

[3] Bowman, Benedict and Taylor, J. Am. Chem. Soc. **57**, 960 (1935).

samples of methane of varying D content the preparation of which forms the subject of other papers, "standard" samples were prepared as follows.

CH_4 and CD_4 were prepared by reduction of CO with H_2 or D_2 on a nickel catalyst. The preparation of the catalyst and the purification of the gases are described in detail elsewhere.[4] The resulting CD_4 contained small amounts of CD_3H, which could be estimated from the spectra. The samples used varied from 93 to 98.4 percent C−D content. Samples containing $33\frac{1}{3}$ percent, 50 percent and $66\frac{2}{3}$ percent C−D were also prepared by reduction of CO with the appropriate $H_2 : D_2$ mixtures. The composition of the resulting gases is subject to a slight uncertainty, due to the possibilities of dilution with H or D excess present on the catalyst, and differential isotope exchange in the reaction. Equilibrium mixtures of methanes not subject to these uncertainties were prepared by bringing a mixture of CH_4 and CD_4 in the desired proportions to equilibrium on a nickel catalyst at 302°. The catalyst had been previously washed with a $H_2 : D_2$ mixture of the same proportions. Two samples of each mixture were prepared and gave concordant results. In this way equilibrium mixtures of 9.5, 18.1, 79.8 and 88.6 percent C−D content were secured. Correction was made for the H content of the CD_4 samples used.

CH_3D was prepared by the Grignard reaction, using CH_3I and D_2O. It was subjected several times to fractional extraction at liquid-air temperatures. The product was spectroscopically free from CH_2D_2, but contained a small amount of CH_4.

To prepare CH_2D_2, CH_2I_2 was added drop by drop to $C_2H_5OD+D_2O+Zn$ dust.[5] The reaction being highly exothermic, it was necessary to cool the mixture at first, later raising the temperature. The gas was collected in a liquid-air trap and subjected to repeated fractionation. The C_2H_5OD was prepared from $(C_2H_5O)_3Al$ and D_2O, according to directions suggested by Dr. John Turkevich. The resulting gas was far from pure CH_2D_2 containing considerable CH_3D, as well as smaller amounts of CHD_3 and CH_4.

A similar method was attempted in the preparation of CHD_3, using a mixture of CHI_3 and $CHCl_3$ in place of CH_2I_2. Again the resulting gas contained considerable amounts of CH_2D_2, CH_3D and CD_4, though preponderantly CHD_3.

To prepare C_2H_6, tank ethylene was fractionated, the middle fraction hydrogenated on nickel catalyst at room temperature, and excess hydrogen removed by Cu−CuO at 302° as water.

To prepare C_2D_6, purified tank ethylene was hydrogenated with D_2 and then subjected to the exchange reaction with twice the quantity of D_2 seven times on nickel catalyst. Details are described in another paper.[4b] The resulting C_2D_6 showed only very weak absorption due to C_2D_5H and may be estimated as containing 95–98 percent C−D bonds.

Infrared Spectra

Technique

For infrared analysis, the gaseous samples were transferred at known pressures into cylindrical Pyrex absorption cells, with rocksalt windows. Two such cells were used in the present work, 20.6 and 24.4 cm in optical length, respectively. The spectrometer was a rocksalt prism instrument of the Wadsworth type, described by Barnes.[6] The high magnification of the photorelay made possible the use of comparatively narrow slits and high accuracy of absorption measurements even to long wave-lengths. At 10μ the galvanometer deflections due to the energy spectrum reached 500 mm reproducible to 2 mm, and the working limit of the spectrum was 16μ. The absorption cell was raised and lowered in and out of the light beam, alternate readings in, out, out and in being taken at each wave-length. At some times the galvanometer zero showed a steady drift; hence the average of the deflections obtained on raising and lowering the shutter was taken. The deflections obtained were to a slight extent a function of the position of the galvanometer zero, due to nonlinearity of the amplification; hence the zero was brought back to approximately the same position for each reading; and to ensure further the accuracy of the ratio of the absorbed to the unabsorbed deflections, the latter was raised by a factor of two at

[4] Morikawa, Benedict and Taylor, J. Am. Chem. Soc. (a) **58**, 1445 (1936); (b) **58**, 1795 (1936).
[5] Sabanejew, Ber. 9 (1870).
[6] Barnes, Brattain and Seitz, Phys. Rev. **48**, 582 (1935).

any given important wave-length. Using all these precautions for quantitative accuracy, the percentage absorption of a given sample, or of similar samples at different times, was reproducible to 1 percent. For absorption under average conditions, the accuracy is 2–3 percent. In the earliest experiments the accuracy is considerably less, as at that time there was no device for raising and lowering the absorption cell. The energy spectrum was first mapped with the cell in; then with it out; and smoothed curves for each were plotted, and then the ratio was taken.

Correction for the effect of rocksalt window

The observed transmission ratio of energy: cell-in/energy: cell-out must be corrected for the absorptions and reflections of the rocksalt windows. This depends on wave-length and the position of the cell in its carrier. The following procedure was adopted: Wave-lengths were found at which there was zero absorption, as proven both by experiment at high gas pressures, and backed by theory. The transmission was always observed at these wave-lengths; the transmission of the cell at intermediate wave-lengths, where there was gas absorption, was determined from these by plotting a smooth curve, in accordance with measurements made on an evacuated cell. For the methane experiments, the reference wave-lengths were 25.05 scale divisions = 3400 cm^{-1}; 24.45 = 2520 cm^{-1}; 23.60 = 1900 cm^{-1}; and 17.00 = 850 cm^{-1}. From evacuated-cell measurements, trans 3000 cm^{-1} = $(\text{trans}_{3400}+\text{trans}_{2520})/2$, and trans 2250 cm^{-1} = $(2.\text{trans}_{2520}+\text{trans}_{1700})/3$. Similar standard procedure prevailed for other wave-lengths.

Absorption coefficient and pressure

The percent absorption, $1-(I/I_0)$, then was given by 1 − (observed transmission/calc. cell transmission). To correct for the effect of gas density and cell length, these are converted into extinction coefficients, $K=(-\log_{10} I/I_0/pl)$, where p is the gas pressure in mm Hg, corrected to 25°C; and l is the cell length in cm. That K is rarely a true constant, but varies with pressure, i.e., that Beer's law does not hold, is a familiar phenomenon in infrared work.[7] This is particularly true when using a rocksalt spectrometer and spectra consisting of unresolved single lines. Here the slit width is much greater than the true line width, and the observed transmission is the average of narrow peaks of true absorption and wide valleys of transmission. When the absorption of the peaks is already high, increasing the pressures does not increase the over-all absorption linearly. Moreover, the effects of pressure broadening on line shapes are often appreciable. However, for low absorptions and for moderate absorptions in bands where the lines are numerous and closely spaced (i.e., the unsymmetrical methanes), Beer's law should be expected to hold. This is indeed the case, experimentally. The K's determined from $I/I_0>70$ percent, or those for the unsymmetrical methanes (except the 1300 cm^{-1} band of CH_3D) up to $I/I_0>50$ percent are nicely constant; for higher gas pressures K falls with pressures to perhaps 70 percent of its true value. In practice, therefore, the pressure was chosen to bring as many points as possible between the limits of absorption too low to be accurately measured $I/I_0>95$ percent and too high to obey Beer's law. Since this could not be attained for all wave-lengths, the pressure of a series of corresponding samples was kept constant, so that even though the K's might fall below their true values, they would be directly comparable one with another.

Effect of H_2 or D_2 pressure

Many of the unknown samples contained H_2 or D_2 in addition to methanes. The effect of such nonabsorbing foreign gas on the absorption coefficients was therefore tested on the 18.1 percent D sample. Addition of 190 mm D_2 to the 190 mm sample had no effect greater than 10 percent on K for any wave-lengths although such an increase was observed in some bands. Hence deviations from Beer's law due to pressure broadening by H_2 are of no great consequence.

Absorption coefficients and mole fraction

The K's observed were computed on the bases of the total pressure of methane of whatever isotopic nature in the cell. If several methanes are present, $K_{obs}=\Sigma K_i x_i$, where K_i is K for any pure constituent and x_i its mole fraction. The accuracy of this expression is testified to by the

[7] von Bahr, Ann. d. Physik **29**, 780 (1909); Bartholome, Zeits. f. physik. Chemie **23**, 131 (1933).

coherence of all the observed data. The K for any given sample is quite accurately decomposable for all wave-lengths into the sum of the K's for the pure components, and their mole fractions, due allowance being made for Beer's law deviations.

The wave-length calibration curve of the instrument was obtained from the known absorption bands of various substances. One calibration point, the energy minimum due to atmospheric CO_2 absorption at 2353 cm^{-1}, was rechecked for every run.

Observed spectra

The observed absorption spectra of the methanes may for convenience be divided into two regions, those of the "valence" vibrations, 2000–3200 cm^{-1}, and of the "deformation" vibrations, 1500–900 cm^{-1}.

(1) *Region 2000–3200 cm^{-1}.*—In the first region, the fundamental frequencies correspond closely to two values, one characteristic of the C–H band, 3000 cm^{-1}, and one to the C–D band, 2250 cm^{-1}. In all the methanes, the bands of strongest absorptive power lie within 50 cm^{-1} of these values, so that, under the low resolving power of a rocksalt spectrometer in this region, the absorption of samples of widely different C–D-content show only these two bands roughly similar in position and structure, but differing in intensity. Because of the similarity and the low resolution, no curves of the absorption in this region will be presented. The values of the extinction coefficient at the two maxima of absorption, designated by K_H and K_D, respectively, are given with the plots of absorption in the second region. The position of the K_H maximum was constant, within the accuracy at this region of ± 40 cm^{-1}, at 3020 cm^{-1}, with the exception of the very weak band observed in the CD_4 of highest purity. Here, of course, there should be no absorption corresponding to a C–H fundamental. Actually there is a weak, broad band, with a badly defined maximum at about 3200 cm^{-1}, as well as some absorption at 3000 cm^{-1} due to the small percentage of CD_3H remaining in the sample. The 3200 cm^{-1} absorption is undoubtedly due to the CD_4 molecule, and corresponds to the CH_4 absorption at 4300 cm^{-1}, due to "combination" bands of valence and deformation frequencies. In the 2250 cm^{-1} region, the accuracy of wave-length determination is somewhat improved, so that the maximum of samples of lowest D content is found at 2210 cm^{-1}, the position of the single CH_3D, C–D fundamental. CH_2D_2 and CHD_3 each have two fundamentals in this region, but those at 2255 and 2270 cm^{-1}, respectively, appear by far the stronger, as the maximum occurs there, with only a slight asymmetry of the band, lower frequencies indicating the presence of the other fundamentals, known from Raman measurements[8] to occur at 2139 and 2141 cm^{-1}. Similarly, the weaker C–H frequencies, CH_3D, 2922 cm^{-1} and CH_2D_2, 2974 cm^{-1} do not appear strong enough to shift the maximum observably.

(2) *Region 1500–900 cm^{-1}.*—Representative curves of absorption in the second region are presented in Figs. 1–3. Frequencies in cm^{-1} are plotted

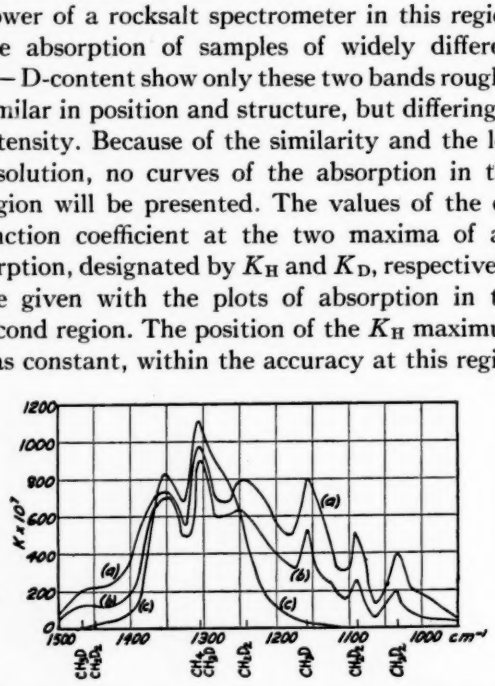

FIG. 1. Absorption spectra of equilibrium methanes of low C–D content. $P = \sim 180$ mm. (a) 18.1 percent; (b) 9.5 percent; (c) 0.4 percent.

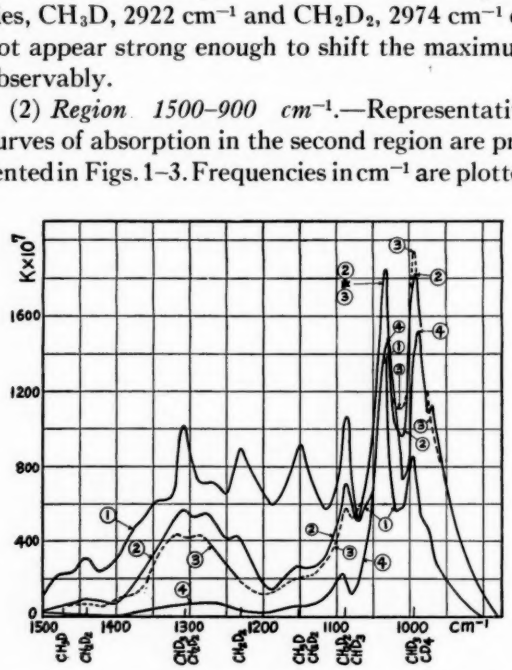

FIG. 2. Absorption spectra of equilibrium methanes of high C–D content. (1) 46 percent; (2) 79.8 percent; (3) 88.6 percent; (4) 98.2 percent.

[8] MacWood and Urey, J. Chem. Phys. **4**, 402 (1936).

TABLE I. *K of individual isotopes.*

MOLECULE ν CM^{-1}→	3020	2250	1460	1305	1180–1160	1090	1035
CH_4	380	—	—	1110	80–0	—	—
CH_3D	1200	300	350	800	1100–1900	550	—
CH_2D_2	1200	1500	500	500	700–700	2400	2400
CHD_3	733	2200	—	1400	300–300	400	2500
CD_4	70	450	—	—	—	250	1400

against $K\times10^7$. The gradual appearance and disappearance of bands C−D, as the percent expressed in the form (C−D/C−H+C−D)×100, increases, in Figs. 1 and 2, is the justification for their assignment to individual molecules, at the foot of the figures. These assignments are corroborated by the curves of Fig. 3, which represent the absorption of the samples prepared to give the pure individual isotopes. As can easily be seen, the desired goal was not achieved. The CH_3D is quite free from other isotopes, but the "CH_2D_2" and "CHD_3" curves show bands due to both molecules, as well as CH_3D.

In order further to demonstrate how the observed absorption may be represented as the sum of the contributions of each individual isotopic molecule, we may plot, for any desired wave-length, K against the percent C−D. The mol fractions of each molecular species may be calculated, given the equilibrium constants of the equations $CH_4+CH_2D_2\rightleftarrows2CH_3D$, $CH_3D+CHD_3\rightleftarrows2CH_2D_2$, and $CH_2D_2+CD_4\rightleftarrows2CHD_3$ and the total percent C−D. The equilibrium constants are obtained, and the mol fractions calculated therefrom, in a later paper. The result is given in Fig. 10, where the heavy lines represent the resulting mole fractions. These are seen to deviate but slightly from the classical result, if all the equilibrium constants equal 1, given by the broken lines. Given the mole fractions, K_i's may now be found so that $K_{obs}=\Sigma X_iK_i$. This has been done, and the results plotted, for significant wave-lengths of maximum absorption, K_H and K_D are given in Fig. 4, and K_{1460}, K_{1305}, $K_{1180-1160}$, K_{1090} and K_{1035} in Figs. 5–9. The light lines in Fig. 4 are X_iK_i computed from the X_i's of Fig. 10 and the K_i's of Table I, the heavy lines are the resultant K's. The observed points, as shown in Figs. 4–9, are marked by circles.

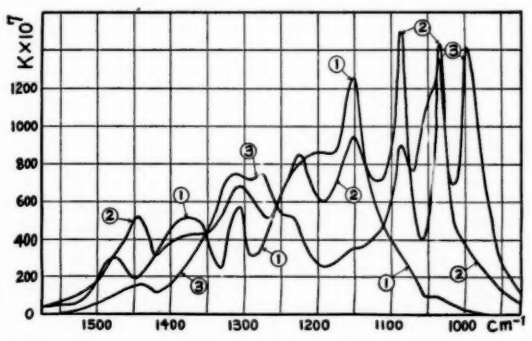

FIG. 3. Absorption spectra of methanes prepared by reduction of halides. (1) CH_3D; (2) CH_2D_2; (3) CHD_3.

Analysis of mixtures

Figs. 4–9 thus gives a series of calibration curves, obtained both experimentally and theoretically from which it is possible to determine the percent C−D of any unknown sample, assuming equilibrium distribution among the methanes. This has been done many times (see the other papers[1, 4]) always with gratifying concordance among the results obtained from various wave-lengths. It must be admitted that the observed K's for all the wave-lengths given do not fall on the curves, if the pressure of the sample differs too much from the $p\cong170$ mm obtaining in the standard samples, due to the deviations from Beer's law mentioned above. In such cases, however, it has been feasible to apply concordant corrections, such that the values then fall on the curves. For example, for samples in the neighborhood of 50 percent C−D, the observed results for K_H and K_D fall uniformly below the values plotted in Fig. 4. The ratio K_H/K_D is then a good measure of the percent C−D in the sample. Similarly, if it be attempted to estimate the composition of the samples whose curves are plotted in Fig. 3 (taken at higher pressures), the result will not add up to 100 percent. It is believed, however, that the ratios of one isotopic molecule to the other obtained from the K's of Table I are substantially correct.

Also, the calibration curve for 1305 cm^{-1} could not be relied upon in the range 0–60 percent C−D,

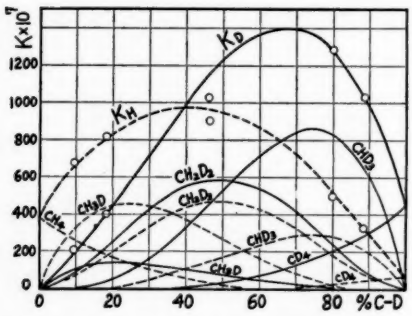

FIG. 4. Contribution of individual isotopes to K_H (3020 cm^{-1}) and K_D (2250 cm^{-1}).

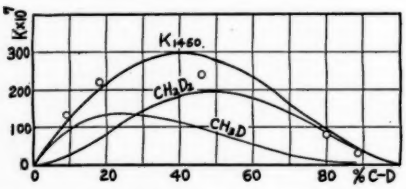

FIG. 5. Contributions of individual isotopes to K_{1460} cm^{-1}.

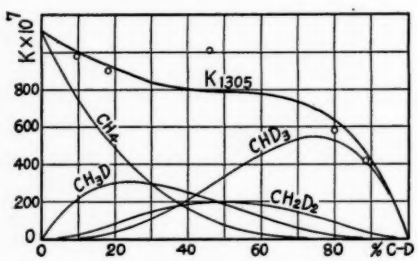

FIG. 6. Contribution of individual isotopes to K_{1305} cm^{-1}.

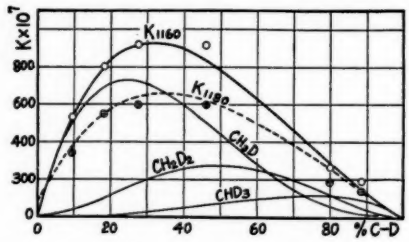

FIG. 7. Contributions of individual isotopes to K_{1160} cm^{-1}.

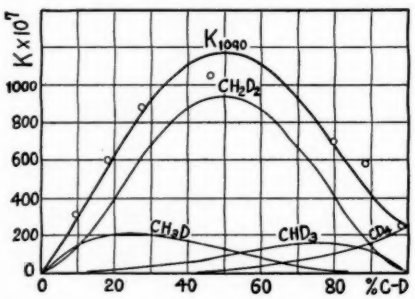

FIG. 8. Contribution of individual isotopes to K_{1090} cm^{-1}.

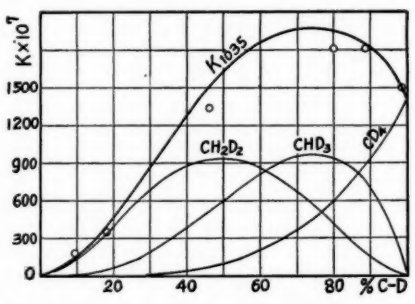

FIG. 9. Contribution of individual isotopes to K_{1035} cm^{-1}.

as seen from the bad agreement of observed and computed points. This is believed due to the abnormally large Beer's law variations for the 1305 cm^{-1} band of CH_4. In the range 60–100 percent C−D, where CD_3H is the principal absorber, the calibration curve may be relied upon, as results obtained were consistent with those from other wave-lengths.

In practice, it sufficed to measure K_H and K_D with the utmost accuracy, and to dispense with further measurements, unless it was believed that nonequilibrium conditions prevailed. This was done in most of the early work on the attainment of equilibrium on catalytic surfaces. Nonequilibrium samples were found under several conditions, however. For example, CH_4 and CD_4 were mixed on catalytic surfaces for times less than that corresponding to equilibrium. If percent conversion, X, is understood to be the fractional amount by which both CH_4 and CD_4 have approached the equilibrium state, this may easily be found by drawing new plots similar to Figs. 4–9 in which the abscissa, X, runs from 0–100 percent and the ordinates are the average of the K's corresponding to percent C−D = $X/2$ and percent C−D = percent C−D in $CD_4 - X/2$. Again the results from varying wave-lengths were concordant. In other cases, mentioned in the catalytic papers,[4] the reaction CH_4+D_2 sometimes progressed with the heavier isotopes, CH_2D_2 and CHD_3 appearing in quantities beyond the equilibrium amounts. Recourse to the curves will always make possible estimates of the composition of any mixture, however, once the necessity for taking absorption readings at a number of wave-lengths is established.

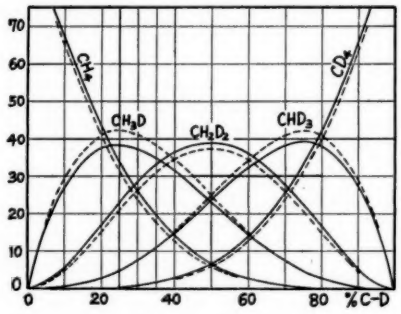

FIG. 10. Mole percentages of individual isotopic molecules: — Equilibrium at 302°. --- Ideal equilibrium (infinitely high temp.).

Effects of ethanes on absorption coefficients of methanes

Another series of discrepancies between the percent C−D estimated from K_H and K_D and from the other K's appeared in certain photochemical experiments (the results of which will appear later in this Journal) in which K_H and K_D were higher than expected from the percent C−D estimated from K_{1160}, for example. Since the C_2H_6 molecule has a K_H much higher than CH_4 it was thought that there might be traces of $C_2H_xD_{6-x}$ present; the abnormally high values of K_{1460} in these samples corroborated this view, as C_2H_6 also has a strong band at 1460 cm^{-1}. Subsequent chemical analysis of similarly prepared samples proved the presence of the ethanes, etc. It was hardly possible to estimate the ethane quantitatively from the absorption coefficients, however, as the small amounts of ethane involved contributed markedly only to K_H and K_D, and there was no guarantee that the percent C−D was the same in the methane and the ethane. Accordingly, the percent C−D of the methane was determined from the curves of Fig. 6–9, and the differences between the observed and calculated values of K_H and K_D serve as a semi-quantitative indication of the amount of ethane. In some of the early experiments only K_H and K_D were measured; for these runs the percent C–D in the methane can be roughly found by assuming ethane absorption equal to that determined for analogous samples by the more exact later measurements.

Ethane spectra

Although no attempt was made to prepare and analyze the entire range of deuteroethane samples as we have done for deuteromethane, absorption curves were run for several catalytically prepared deuteroethane samples, including one of nearly pure C_2D_6. These are presented in Fig. 11. The exact percentage C−D in samples 2, 3 and 4 was not measured, but may be estimated from the spectra. In C_2H_6 there are three main regions of

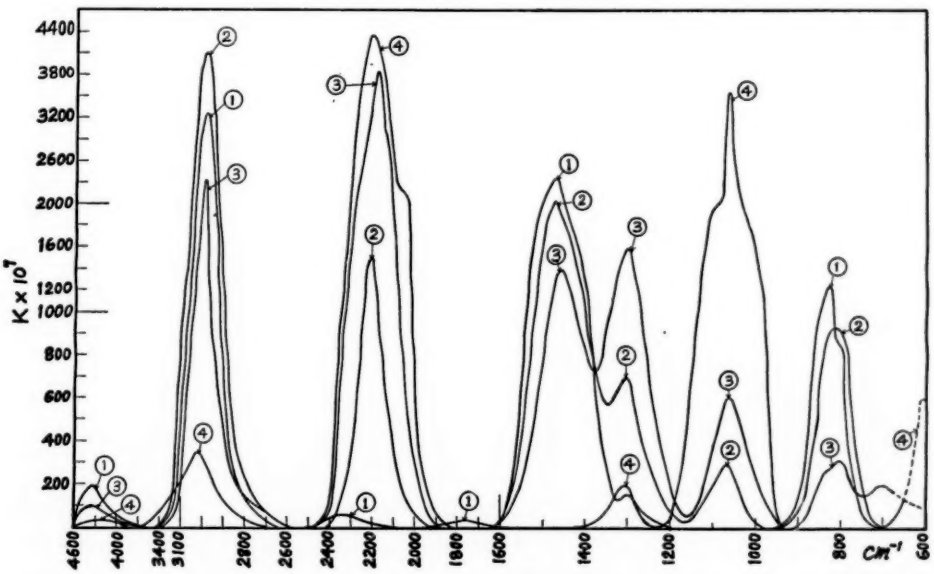

FIG. 11. Absorption spectra of ethanes of varying C−D contents. (1) 0 percent (C_2H_6); (2) ∽15 percent; (3) ∽45 percent; (4) ∽95 percent.

absorption, 2980 cm^{-1}, 1470 cm^{-1} and 827 cm^{-1}, corresponding, respectively, to C−H valence, C−H deformation, and C−C deformation vibrations, to adopt Mecke's[9] terminology. The first two regions have been shown, under high resolution[10] to be composite, each corresponding to several infrared active modes of vibration. In addition to these strong bands we observe, with gas pressures of one atmosphere, weak bands at 4280, 2350, 1770 and 1305 cm^{-1}. The first is $\nu_H+\delta_H$; the second and third do not appear to have been previously reported, but may readily be ascribed to combination bands $\nu_{C-C}+\delta_H$ and $\nu_{C-C}+\delta_C$. (ν_{C-C} is well known from Raman spectra and equals 990 cm^{-1}.) The 1305 cm^{-1} absorption is probably due to a trace of CH_4 as impurity.

Deuteroethanes spectra

Now in spectrum No. 2 these same bands are present, not noticeably shifted in position but in addition new bands have appeared at 2210 cm^{-1} (ν_D) 1300 cm^{-1} (δ_{H-D}), and 1070 cm^{-1} (δ_D). The K_H has increased slightly, and $K_D=0.4\ K_H$. In spectrum No. 3, the new bands have increased appreciably in intensity, ν_D shifting to 2180 cm^{-1}, with $K_D=1.5\ K_H$, $K_{1300}>K_{1480}$, and with much weaker and very irregular absorption in the region <900 cm^{-1}. Obviously here the characteristic bands of C_2H_6 have almost completely disappeared, the observed absorption being a composite of bands of the many possible deuteroethanes of intermediate composition. The simplicity of absorption in the regions of shorter wave-length is another instance of the paradoxical fact that the more complicated the molecule the simpler the vibrational spectrum, in that the vibrations within radicals preserve closely their characteristic values, interradical forces being small. Thus 1470 cm^{-1} is a characteristic frequency of CH_3 or CH_2 radicals, whether in CH_3X, CH_3D, CH_3-CH_3, CH_2D_2, or CH_2D-CH_2D; 1305 cm^{-1} is characteristic of CHD; and 1070 cm^{-1} of CD_3 or CD_2. The ν_H and ν_D absorptions show the same characteristic as in CH_4, namely, that the wave-length shifts but slightly with changing percent D; but that the K increases as asymmetry increases. As $K_D>K_H$ in No. 3, we may conclude that the percent C−D corresponds to equilibrium, as this sample was prepared from 1 C_2H_6 : 2 D_2, or equilibrium of ~45 percent C−D. From relative intensities No. 2 is then between 10 and 20 percent C−D.

In spectrum 4, the purest C_2D_6, the simplicity of the C_2H_6 spectrum is almost but not quite reattained. ν_D is now at 2210 cm^{-1} and the greater resolution obtainable here gives unmistakable evidence that a second fundamental lies at about 2080 cm^{-1}. δ_D is a sharp band at 1067 cm^{-1}, and δ_{C-C} has shifted to wave-lengths just beyond the reach of the instrument, absorption being manifest at ~600 cm^{-1}, but the energy being insufficient to establish the position of the maximum with any accuracy. Other weak bands appear at 1305 cm^{-1} (δ_{H-D}); 3020 cm^{-1}, a combination of $\nu_D+\delta_D$ and ν_H; and 4300 cm^{-1} ($2\nu_D$). From the weakness of the first two ($K\delta_D : K\delta_H=16 : 1$ and $K_D : K_H \leqq 25 : 1$) we may estimate that the sample contains 95–98 percent C−D.

Discussion of methane spectra

The results reported in this paper make nearly complete the tabulation of all the fundamental frequencies of all the methane isotopes. Those of CH_4 have been long known; those of CH_3D and some of CH_2D_2 are known from the accurate infrared work of Ginsburg and Barker;[11] while MacWood and Urey[8] have recently reported on the Raman spectra of all the methanes. In one or two cases these last results disagree with the infrared measurements. The observed values for the frequencies are tabulated in Table II, where the nomenclature follows that of previous authors. The calculated values are taken from a forthcoming paper by one of us, and include corrections for the harmonic terms in the energy, taken so as to give exact agreement with the CH_4 and CD_4 frequencies; hence the somewhat better agreement than with previous calculated values.[12]

The agreement of the Raman and infrared measurements is good, with one or two exceptions. The line found by MacWood and Urey in CH_3D at 1330 cm^{-1} is hard to explain, as the origin of ν_{4ab} is unquestionably the strong zero branch found by Ginsburg and Barker at 1307 cm^{-1} and confirmed in this work. Similarly, the line found by them in CH_2D_2 at 1333 cm^{-1} is out

[9] Mecke, Zeits. f. physik. Chemie **B16**, 409 (1932).
[10] Leven and Meyer, J. Am. Chem. Soc. **16**, 137 (1928).
[11] Ginsburg and Barker, J. Chem. Phys. **3**, 668 (1935).
[12] Dennison and Johnson, Phys. Rev. **47**, 93 (1935).

TABLE II. *Frequencies of the deuteromethanes.*

FREQUENCY	ν_1	$\nu_2(2)$	$\nu_3(3)$	$\nu_4(3)$
CH_4, OBS. AND CALC.	2915 (RAM.)	1519	3020 (RAM. I–R)	1306 (I–R)
CH_3D OBS. I–R (G–B)	2950 (?)	1474	3031 2205	1156 1307
CH_3D OBS. RAM.		$2\nu_2=2921.7$	2199.5	$2\nu_{4c}=2314.8$ 1330(?)
CH_3D CALC.	2961	1458	3032 2193	1147 1311
CH_2D_2 OBS. I–R (G–B)		1450	←3020 2255→	1035 1091 1235
CH_2D_2 OBS. RAM.	2139.0	$2\nu_2=2916$ 1285.6	2974.2	1033.1 $2\nu_{4c}=2179.6$ 1333(?)
CH_2D_2 CALC.	2144	1450 1290	3027 2980 2265	1038 1085 1227
CHD_3 OBS. I–R (THIS PAPER)		1290	3000 2260	988 988(?)
CHD_3 OBS. RAM.	2141	1299.2	2268.6	$2\nu_{4ab}=1963.4$ $2\nu_{4c}=2092.8$
CHD_3 CALC.	2127	1293	3015 2263	995 997
CD_4, OBS. AND CALC.	2085 (RAM.)	1052	2258 (RAM. AND THIS PAPER)	988 (THIS PAPER)

of place in our scheme, as we confirm the occurrence of ν_{4a} at 1235 cm^{-1}, thus making the Raman line at 1285.6 be ν_{2a}, in agreement with calculation. Reference to Ginsburg and Barker's curves will show the complete agreement with ours of all maxima attributed to CH_3D and CH_2D_2. The relative intensity of our bands also agrees with their curves; and, as far as it is possible to calculate extinction coefficients from their data, rough agreement is also obtained. The grating intensities are somewhat higher, as should be expected from the narrower slits used. For CHD_3, we prefer to interpret the two strong absorption peaks at 988 and 1035–1040 cm as being the Q and R branches of both ν_{4cb} and ν_{4c}, the origin of both bands being at 988 cm^{-1}, although perhaps the Q branch of ν_{4c} is at 1035, as suggested by the Raman assignments. A justification of our assignment, based on the expected envelopes of the bands, will be given in the forthcoming paper. That the Q branch of CD_4 is located at 988 cm^{-1} cannot be questioned, as the similarity in envelope with ν_4 of CH_4 is apparent. The weak absorption appearing at 1095 cm^{-1} in CD_4 must be attributed to a difference band, $\nu_1-\nu_4=2085-988=1097$ cm^{-1}.

The relative intensities of the methane bands is a matter of some interest. As we have emphasized, not too much importance can be attached to absolute intensities, because of the low resolving power of the apparatus; thus the apparent greater intensity of ν_D over ν_H in CH_2D_2. or in CD_4 over CH_4, may not be real, as the band width is much greater compared with the slit width at 2250 cm^{-1} than at 3000 cm^{-1}. There can be no question, however, that K_H and K_D are much greater for the unsymmetrical methanes than for CH_4 and CD_4, as Fig. 4 clearly and startlingly indicates. This result is all the more surprising, as in CH_2D_2 the weight of the active upper state is only two (and practically only one, as we have seen that the bands at 3020 and 2255 contribute most to the absorption), compared with three for the tetrahedrally symmetric molecules. Moreover, a simple calculation of the expected intensities, assuming a dipole in each C−H or C−D band, $\mu=\mu_0+\mu_1\partial dr$, indicates that the intensities should be roughly equal for each active fundamental, and be less for a ν_D than a ν_H, because of the smaller amplitudes involved. The peculiar relations observed can only be explained by assuming a complicated behavior of the dipole moment as a function of the C−H distance, and probably interaction terms between the separate C−H bands play a role also. No satisfactory quantitative explanation has been obtained. It is of interest to note that the few samples of heavy ethanes observed showed a similar though somewhat smaller increase of K_H for the intermediate molecules, pointing to a definite property of the C−H dipole in all hydrocarbons. Accurate absolute intensity measurements and further calculations on this point would be of interest.

The Raman Spectra of Some Simple Molecules in Solution*

W. WEST AND PAUL ARTHUR†, *Chemistry Department, Washington Square College, New York University, New York City*

(Received October 12, 1936)

The Raman spectra of HCl, HBr, SO_2 and NH_3 in various nonionizing solvents indicate vibrational frequencies in the solute molecules of lower value than in the corresponding gaseous states, the relative diminution amounting, in the hydrogen halides dissolved in some solvents, to 3 percent of the gas frequencies. The frequency shift is smaller for the two polyatomic molecules. There seems to be a definite relation between the relative frequency displacement and the dielectric constant of the solvent for the dissolved molecules of HCl and HBr. $\Delta\nu/\nu$ increases with solvent dielectric constant to a limiting value of 0.03. A similar trend is shown in SO_2 and for NH_3 it seems that other factors than the dielectric constant of the solvent are effective in determining the frequency displacement. Concentrated solutions of HCl and HBr in several ionizing solvents have no features in their Raman spectra which can be identified as vibrations in HCl or HBr molecules. The bearing of these results on the dissociation process of HCl in solvents is discussed.

THE great power of spectroscopic investigations in furthering the development of the theory of molecular structure in the gaseous state naturally suggests the utility of similar studies in the effort to gain an understanding of molecular properties in liquids and solutions. It is soon apparent, however, that in leaving the gaseous state for the condensed phase we nearly always lose one of the most important aids in the elucidation of molecular structure, the rotational structure associated with rotational-vibrational bands; for in all except molecules of very small moment of inertia, the frequency of rotation characteristic of the isolated molecule is less than the frequency of collision with other molecules in the liquid state and no well defined rotational frequencies are to be expected. But in spite of lack of unambiguous knowledge on such matters as internuclear distances and moments of inertia imposed by this handicap, it is still probable that since any changes in the energy states of molecules will be reflected in their spectra, valuable information may be obtained from spectral studies on the condition of molecules in liquids and on their interactions with their neighbors.

Our program included the investigation of the Raman spectra of the diatomic molecules HCl and HBr, and of the polyatomic molecules SO_2 and NH_3 in a number of nonionizing solvents and in a few ionizing solvents. At the same time it was realized that while the examination of the Raman spectra might afford a quick and easy way of surveying the problem generally, the relatively small dispersion of the instruments available for this purpose kept precision low, and therefore, to confirm the Raman results with higher precision, as well as to observe any further phenomena which might exist, a detailed study has been made of the absorption spectra of HCl in a number of solvents in the near infrared by means of a grating spectrometer of high resolving power.

Woodward,[1] in the course of an investigation of the Raman spectra of solutions, had already examined the spectrum of HCl dissolved in carbon tetrachloride without observing any feature characteristic of HCl, a result he attributed to the low concentration of HCl in the solution he used. By using a temperature of $-65°C$ we have prepared solutions of sufficient concentration to show the Raman line of the solute. Where the nature of the solvent permitted, the HCl concentration was determined by direct titration by means of standard alkali; in other cases solutions of given concentration were prepared with sufficient accuracy by measuring the volume of solvent and of solution in the calibrated Raman cell, assuming the volume of solution to be additive, and using the value of the density of liquid HCl at the temperature in question.[2]

HCl gas was prepared, with due precautions as to purity and dryness, (P_2O_5), by dropping concentrated sulphuric acid into concentrated hydrochloric acid. Hydrogen bromide was pre-

* A preliminary report of some of the experimental observations in this paper was made at the meeting of the American Chemical Society held in New York, April 1935.

† Now at Oklahoma Agricultural and Mechanical College, Stillwater, Oklahoma.

[1] L. A. Woodward, Physik. Zeits. **32**, 212 (1931).

[2] Landolt-Börnstein, Tabellen. II., p. 297.

pared by warming potassium bromide with phosphoric acid from which most of the water had been removed by boiling, freed from traces of bromine by means of moist red phosphorus, dried by P_2O_5, condensed, fractionally distilled into a second receiver, from which it was distilled into the solvent. Special precautions were here necessary to avoid photo-oxidation during the exposure, as the resulting bromine absorbs the exciting and the scattered radiation. The air in the apparatus was displaced by oxygen-free nitrogen before the beginning of the generation. Sulphur dioxide and ammonia were obtained from commercial tanks.

The solutions were prepared by passing the gas into the solvent, contained in the Raman tube, 6″ long, placed in a large Dewar containing dry ice; the temperature was kept at $-67°\pm3°C$ by adjusting the supply of refrigerant. A 6″ 220-volt mercury arc was focused on the cell, through a dilute iodine filter in CCl_4 to minimize the continuous radiation, and a potassium nitrite solution to absorb the ultraviolet. Two cameras were used in the spectrograph, one giving a dispersion of 270 cm^{-1} per mm, the other 90 cm^{-1} per mm at 4600A. Eastman Hyper Press Plates were used.

Results

The results are summarized in Table I, in which D is the dielectric constant of the solvent, ν is the Raman frequency, that is the wave number difference between the exciting and the incoherently scattered line, and $\Delta\nu/\nu$ the ratio of the difference in Raman frequencies of gas and solution to the Raman frequency of the gas. The Raman bands of HCl and HBr in solution are not sharp and in most solvents extend over some 30 cm^{-1} or more and some doubt exists as to which feature of the band should be measured. In HCl gas, for instance, the most intense feature of the Raman spectrum is the unresolved Q branch, the long wave limit of which represents the origin of the branch, but in liquids or solutions the nature of the spectrum is too little understood to justify our attaching a similar importance to the long wave limit. The Raman bands of HCl and HBr in solution are decidedly asymmetrical, with a maximum intensity nearer the long wave than the short wave edge and, somewhat arbitrarily, the measurements reported are for this maximum. Sulphur dioxide and ammonia have sharper and more symetrical lines, and for these solutions the measurements refer to the centers of the lines.

In addition to the solutions listed in Table I, none of which conduct the electric current appreciably, certain electrically conducting solutions of HCl and HBr were examined. Along with all others who have reported the Raman spectrum of concentrated aqueous hydrochloric acid solutions we have found no feature in the spec-

Table I.

Solvent	D	ν cm^{-1}	$\Delta\nu/\nu$
HCl solutions			
HCl gas[1]		2886	
$SiCl_4$	2.5 calc.	2860	−0.009
PCl_3	4.2	2828	−0.020
$CHCl_3$	7.0	2826	−0.021
HCl liquid[1]	8.85(−90°C)	2800	−0.030
SO_2	22.4	2798	−0.031
C_2H_5Br	14	2797	−0.031
$CH_3CO.Cl$	20.3	2804	−0.028
HBr solutions			
HBr gas[1]		2559	
$CHCl_3$	7.0	2500	−0.023
HBr liquid[1]	6.29(−80°C)	2487	−0.028
C_2H_5Br	14	2471	−0.034

Solvent	D	ν_1	ν_2	ν_3	$\Delta\nu_2/\nu_2$	
NH_3 Solutions[2]						
NH_3 gas			3336			
Hexane	1.8	3220	3315	3389	−0.006	
$CHCl_3$	7.0	3211	3317	3382	− .006	
NH_3 liquid[3]	25.4₋₇₇	3210	3310	3380	− .008	
CH_3OH(20°C)	31	3207	3315	3389	−0.006	
H_2O(20°C)	80	3230	3311	3390	− .008	
		ν_δ	ν_π	ν_σ	$\Delta\nu_\pi/\nu_\pi$	$\Delta\nu_\sigma/\nu_\sigma$
SO_2 solutions						
SO_2 gas[4]		525	1153	1361		
$C_6H_5.CH_3$	2.5		1149	1342	−0.003	−0.014
$CHCl_3$	7.0		1153	1347	.000	− .010
HCl	7.77		1152	1345	− .000	− .010
SO_2 liquid	22.4	522	1153	1346	+ .001	− .011
CH_3OH	51.2	522	1147	1341	− .005	− .014
H_2O(20°C)	80(20°C)		1138	1342	− .013	− .014
$CH_3.COCl$	20.3		1143	1329	− .009	− .024
$(CH_3)_2CO$	28.9		1138	1334	− .013	− .020

** See also W. West and P. Arthur, this journal **2**, 215 (1924).
[1] E. O. Salant and A. Sandow, Phys. Rev. **37**, 373 (1931).
[2] Cf. G. Jung and H. Gude, Zeits. f. physik. Chemie **B18**, 380 (1932).
[3] P. Daure, Ann. d. Physik **12**, 375 (1929).
[4] C. R. Bailey, A. B. D. Cassie and W. R. Angus, Proc. Roy. Soc. **A130**, 133 (1930).

trum which can be identified with an HCl vibration, nor with an HBr vibration in hydrobromic acid solution. Long exposures on HCl in cold (−65°C) concentrated alcohol, and ether, and in acetic acid at room temperature were equally without result and it seems that even in concentrated solutions of HCl in these ionizing solvents not more than a small fraction of HCl can be left as diatomic molecules.

General Results

All four of the solute molecules studied, when dissolved in nonionizing solvents, show Raman spectra of the same general type as the corresponding gases; that is they perform vibrations of about the same frequency as in the gaseous state. The vibrational frequency is diminished in solutions to a greater or less extent compared with that in the gas. In HCl and HBr solutions, there seems a definite connection between the frequency shift and the dielectric properties of the solvent; the relative shift, $\Delta\nu/\nu_{\text{gas}}$, increases with increasing dielectric constant of the solvent, reaching, however, a limiting value of about 0.03 in the hydrogen halides, at a solvent dielectric constant of about 14 beyond which increase in dielectric constant produces no further shift. The polyatomic molecules show several Raman frequencies which are differently affected by solutes.[3] The shifts here are smaller than for the diatomic molecules; for SO_2 there is a trend toward greater shifts with increasing solvent dielectric constant, but with marked irregularities, particularly in the ionizing solvents methyl alcohol and water. In ammonia solutions, the relative shift in the vibration common to the gas and solution is small, nor do either our data on the Raman spectra nor the more complete data of Jung and Gude[4] on the third, fourth and fifth overtones in absorption show any relation between the shift and the dielectric constant of the solvent.

It is of some interest to note how the different frequencies of SO_2 are affected by solvents. The three fundamental vibrations of this molecule are all active in the Raman spectrum, although the slow "bending" frequency, ν_δ, in which the two oxygen atoms move symmetrically perpendicularly to the direction of the S−O bonds, is sometimes too feeble to measure. When observed, this frequency is very slightly altered by the solvent. ν_π, the frequency of the symetrical motion of the oxygen atoms along the bond direction while the sulphur moves symmetrically toward the oxygen, is less influenced by solvents than the corresponding antisymmetrical vibration ν_σ.

Discussion

It will be observed that the change in frequency in passing from gas to solution is the same order of magnitude and may be numerically greater than the change in passing from a gas to the corresponding pure liquid. The solutions employed in the Raman investigation were relatively concentrated (mole fraction 0.2) and it is arguable that in the solvents of lower dielectric constant especially, the observed shift may largely have been attributable to the HCl itself. In fact, however, we shall show in the next paper that the shifts observed in the infrared absorption spectra of much more dilute solutions of HCl are within the limits of error the same as those observed in the Raman spectra whence we conclude that the shift, for the most part, is the result of solvent action on dissolved HCl molecules. It was very early noticed in Raman investigations that molecules possessing a permanent dipole undergo considerable diminution in vibrational frequency in changing from gas to liquid while those with no dipole moment are changed very little. For example, the vibrational frequencies of H_2, O_2, N_2, CH_4, CO_2 are almost the same in the gaseous and liquid states, while the liquefaction of HCl, HBr and HI is accompanied by a diminution of the vibrational frequency of about 3 percent of its value in the gas. It may be mentioned that we have found the frequencies of the nonpolar molecule CCl_4 to be unchanged on dissolving it in solvents of different dielectric constants. The diminution in frequency of polar molecules in solvents of high dielectric constant can probably therefore be correlated with the shift brought about by liquefaction, although in the latter case quantum-mechanical resonance effects may be superimposed on dielectric interaction. J. C.

[3] Cf. A. F. Brodskii and A. M. Sack, this journal **3**, 449 (1935).

[4] G. Jung and H. Gude, Zeits. f. physik. Chemie **B18**, 380 (1932).

Kirkwood has given a theory capable of accounting for the essential observations in connection with frequency shifts in diatomic dipole molecules in solution, but as its discussion can be amplified from observations on the absorption spectra we shall postpone it to the next paper. Here we shall point out some qualitative conclusions of general interest which seem capable of being drawn from the observations.

In interpretation of the frequency shift it becomes important to settle the nature of the oscillator; i.e., whether it is an HCl molecule exposed to the fields of its neighbors or an oscillator in an associated $(HCl)_n$ molecule or in a compound of HCl with solvent molecules. What physico-chemical data exist point to the existence of simple molecules in these solutions. Liquid hydrogen chloride itself seems largely to consist of simple molecules; its Trouton constant is nearly normal, although the Eötvös constant is lower than the normal value; and the equilibrium diagram for the $HCl-SO_2$ system shows no sign of a compound between these components. Although we have been unable to find complete equilibrium data for the other solvents, the low solubility, which does not differ greatly from the ideal, in these solvents is indicative of lack of compound formation.

If then we assume the reduced mass of the oscillator to be unaffected in solution, the diminution in vibrational frequency points to a diminution of force constant; the restoring force tending to prevent displacement of the H and Cl nuclei is diminished in solution by an amount, in the limiting case, of some 6 percent of its value in the gaseous state. It is also probable that this diminution of force constant is accompanied by an increase in the equilibrium internuclear distance; if the empirical rule of Morse, $\omega_0 r^3 = \text{constant}$, is applicable to HCl in the gaseous and dissolved states, the internuclear distance at equilibrium will increase from 1.279A in the gas to 1.292A in solution of high dielectric constant.

It may be noticed that there is a certain resemblance between the effects of dielectric interaction on simple polar molecules which we have deduced as existing from the observed action of the solvent on the vibrational frequency, and the well-known effect of the dielectric constant of a solvent in diminishing the force of attraction between oppositely charged ions, postulated by J. J. Thomson and W. Nernst in explanation of the high ionizing power of solvents of high dielectric constant. But an essential result of the spectral observations is that the diminution in interatomic attraction caused by dielectric action on dissolved dipoles cannot exceed a value of, in the hydrogen halides, about 6 percent of the attractive force prevailing in the isolated molecule, however high the dielectric constant, i.e., no process of dissociation in these molecules can occur by purely electrostatic actions, and when electrolytic dissociation of HCl does actually occur, other actions must be in play. It is well known, of course, that HCl functions as a good electrolyte in ether ($D=4.3$ at 20°C) whereas in solvents of much higher dielectric constant, which contain no atom capable of combining with a proton, as nitromethane ($D=39.4$ at 20°) it is a nonelectrolyte.[5] Although then our experiments throw no light on the mechanism of ionization of HCl in solution except insofar as they show what does not happen, our interpretation of the frequency shift in these solutions is in accord with those views of the electrolytic dissociation of HCl which see as the essential process the association of a hydrogen ion to some atom in the solvent molecule, usually the oxygen atom, by a definite homopolar chemical bond. Moreover, in the usual solvents in which HCl does act as an electrolyte, water, ether, alcohols, the absence of HCl Raman lines, and more conclusively, because of lower concentrations of HCl required for detection in absorption, the absence of infrared absorption bands of HCl, indicate that even in very concentrated solutions the electrolytic equilibrium is characterized by an almost complete absence of molecules of HCl.

[5] We have observed a Raman line in nitromethane solutions of HCl, displaced as in other solutions of high dielectric constant. As however, slow precipitation of a crystalline compound takes place from this solution, we have not included the frequency in our discussion, though, in fact, it behaves quite normally.

The Infrared Absorption Spectrum of Hydrogen Chloride in Solution

WILLIAM WEST AND ROY T. EDWARDS, *Chemistry Department, Washington Square College, New York University, New York City*

(Received October 12, 1936)

The near infrared absorption bands of HCl in nonionizing solvents in the neighborhood of 3.5μ and 1.8μ, measured with a 3600 line per inch grating, have the following characteristics; they show no rotational structure; they usually have two components of unequal intensities; the absorption region is displaced towards lower frequencies compared with the gas. The displacement is independent of concentration up to mole fraction 0.1, but increases with diminishing temperature in certain solvents. The interval between the components varies directly with the dielectric constant of the solvent. In solution, the relative displacement of the more intense component from the origin of the gas band is approximately the same for the 3.5μ and 1.8μ bands, as is also the interval between components. A simple relation exists approximately between the frequency displacement from the gas origin and the dielectric constant of the solvent, of the form $\Delta\nu/\nu = C[(D-1)/(2D+1)]$, a deduction of which formula has been made by J. G. Kirkwood. The more intense component, whose relative shift from the gas origin is within the limits of error the same as the corresponding shift in the Raman spectrum, is interpreted as originating in the internuclear vibration, and it is tentatively suggested that the other component represents a combination between such vibrational transitions and some slow intermolecular vibration between HCl and solvent molecules. The effect of the medium on the anharmonic character of the mechanical and electrical vibrations in the HCl molecule is qualitatively discussed.

THIS investigation was undertaken for the sake of confirming with greater precision the results of the previous communication on the influence of solvents on the vibrational frequencies of simple polar molecules and to extend the observations to higher vibrational transitions than the first. Absorption spectra are also much more sensitive at low concentrations than Raman spectra, making it possible to use much lower concentrations of solute, and therefore to study the influence of solvent on solute uncontaminated by possible interactions between the solute molecules themselves; and finally, as it has turned out, new information on the structure of the HCl absorption bands, of which no hint was given by the Raman spectra, has been secured. The nature of absorption spectra, however, places more limitations on the choice of solvent than are presented by Raman spectra; for while the Raman lines of a pure liquid are often quite sharp, absorption bands increase greatly in intensity and width as the thickness and concentration of absorbing layer increases, with the result that, while it is relatively easy to find compounds with no lines too near the HCl Raman line, most organic compounds interfere in the infrared. The "C−H bands" centered about 3.3μ and their overtones at 1.7μ may easily spread so as to cover the HCl absorptions centered at about 3.5μ and 1.76μ. Even if very thin layers of concentrated HCl solutions in organic compounds are used, the HCl absorption is, at best, superposed on a region of rapidly varying solvent absorption, a condition not conducive to accuracy in the determination of the maximum or of any structure in the solute band. Except, then, in cases in which we purposely wished to measure the absorption of thin layers of concentrated solutions, we have avoided organic solvents containing more than one hydrogen atom, but, at the same time, the smaller concentrations necessary for absorption have enabled us to use certain inorganic solvents whose freezing points did not permit cooling to a sufficiently low temperature to obtain an adequate concentration of solute for Raman work.

Besides the Raman results of the previous paper, the information from previous work relevant to the investigation of HCl solutions is to the effect that the fundamental of liquid HCl has a single maximum displaced by about 100 cm^{-1} to lower frequencies than the origin of the gas band;[1] that the first overtone of liquid HCl has a single maximum similarly displaced by 125 cm^{-1};[2] no absorption corresponding to gaseous absorption of HCl is present in aqueous solution,[3] while recently, with fluorite prism dispersion, Plyler and Williams have found a

[1] G. Hettner, Zeits. f. Physik **89**, 234 (1934).
[2] E. O. Salant and W. West, Phys. Rev. **37**, 108 (1931).
[3] E. K. Plyler and E. S. Barr, J. Chem. Phys. **2**, 306 (1934).

single maximum for HCl dissolved in benzene at about 3.4μ.[4]

Apparatus

A grating spectrometer was used along with a rough prism monochromator for removal of higher orders of wave-lengths shorter than those under investigation. The grating, ruled by Professor R. W. Wood to concentrate light in the first order of 3.5μ, had 3600 lines per inch and a ruled surface 5 in.$\times$4 in. The light from the entrance slit was collimated and thrown on the grating, and the diffracted light focused on the exit slit by separate mirrors, of 50 cm focal length and aperture $f/3$. A single junction thermopile was used, made by Dr. J. D. Hardy of the Russell Sage Institute of Pathology, New York. The galvanometer was a Leeds and Northrup HS, sometimes used in conjunction with a Moll thermorelay amplifier. The monochromator prism for work on the first overtone was a 30° glass prism, and for the fundamental two 20° rocksalt prisms were used through which the light was passed twice. The whole instrument was enclosed in a galvanized iron box covered with Celotex. As light source, a 500-watt tungsten-filament projection lamp was used at 1.7μ, and a Nernst glower, consuming about 70 watts, at 3.5μ. In the course of the investigation of the fundamental it developed that special care had to be taken to prevent the entrance into the grating slit of spurious light of wave-length 1.7μ, which, in the light from the Nernst glower, is far more intense than light of wave-length 3.5μ. For this purpose a Pfund filter of zinc oxide on mica of the required transmission characteristics was interposed near the monochromator slit,[5] and the efficacy of the filter-monochromator arrangement proved by our obtaining the theoretical intensity relationships between the P and R rotational lines of the gas.

The instrument was calibrated by measuring the HCl gas rotational-vibrational lines with the use of Meyer and Levin's values for the frequencies.[6] Slit widths covering a spectral range of 4 cm^{-1} were used at 1.7μ and 6 cm^{-1} at 3.5μ.

In the region of the first overtone, glass windows were used on the absorption cells, in some cells fused on, in others clamped liquid light without the use of grease or cements. According to the experiment, the cell length for solutions in this region varied from about 5 to 25 cm; the diameter was 5 cm. The overtone of liquid hydrogen chloride was observed in a quartz cell 1 mm thick and 5 cm diameter. This cell was made like a Baly cell by fusing windows to quartz tubes, one sliding within the other, separating the two windows by a ring of platinum wire 1 mm in diameter, and fusing together the two tubes at the end remote from the windows. Inlet and outlet tubes were fused to the outer tube. The length of the absorption path can be altered by cutting open the seal, separating the windows to the desired distance, and resealing.

Quartz windows were used at 3.5μ. The cell here was 1 cm long and 4 cm in diameter provided with inlet and outlet tubes. Such cells can easily be made by cutting Pyrex rings of the desired length, drawing out with the help of a pointed flame a small cone in the side which can be fashioned into a small hole, on which is fused, without subsequent working, the very hot end of a narrow bore side tube. The ends are now ground and polished and the windows pressed on by clamping (Fig. 1).

In low temperature experiments, condensation of ice on the windows was prevented in the manner illustrated in the diagram (Fig. 2). The P_2O_5 prevented condensation on the cell windows, and the heating wire prevented cooling of the other two below the dew point. Sufficiently constant temperature of $-65°C$ was secured in the cell by packing the vessel with dry ice and occasionally replenishing during an experiment. Temperatures were read by means of a copper-constantan couple inclosed in a tube immersed in the solution.

Transmissions were determined by evaluating immediately after each other at a given grating setting the galvanometer deflections for the substance under investigation and for a blank in an identical cell; the blank was air in determining the transmission of the pure solvents, and in calibrating by means of HCl gas, and the

[4] E. K. Plyler and D. Williams, Phys. Rev. **49**, 215 (1936).
[5] A. H. Pfund, Phys. Rev. **36**, 71 (1930).
[6] C. F. Meyer and A. A. Levin, Phys. Rev. **34**, 44 (1929).

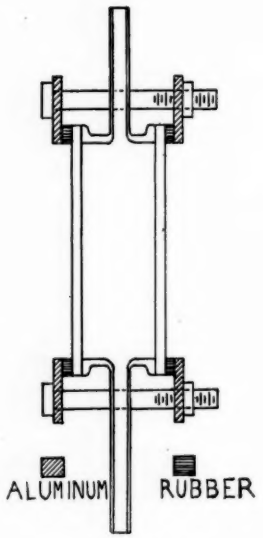

FIG. 1. 1 cm cell.

solvent in the case of solutions. The two cells were mounted on a carriage sliding on ways perpendicularly to the direction of the light beam so that first one and then the other was in the path. With the exception of chloropicrin, $CH(NO_2)_3$, all the nonionizing solvents used had a practically uniform transmission of 85 percent to 100 percent in the region of HCl absorption.

Solvents were distilled into the absorption cell from an efficient rectifying column in an all-glass apparatus. Purity was checked by boiling point, and refractive index determinations. Special attention was paid to preventing the entrance of traces of water to the solution. Hydrogen chloride was prepared by dropping concentrated sulphuric acid on hydrochloric acid and drying the gas.

The concentration of HCl in solutions in non-hydrolyzing solvents was measured by direct titration; in other cases the concentration has been estimated from the amount of infrared absorption. All results reported have been checked at least twice, and most of them more often. The maxima of absorption in the solution are flatter than those of HCl gas lines, in whose wave-lengths the limit of reproducibility is set by the reproducibility of grating settings; we judge the maxima reported for the solution spectra correct to within 2 cm^{-1}.

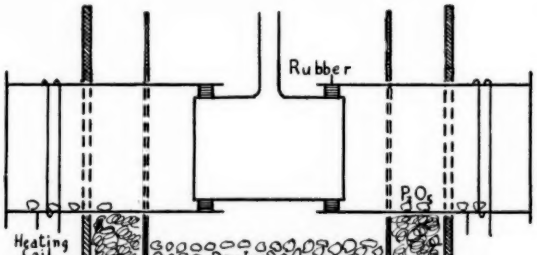

FIG. 2. Low temperature apparatus.

EXPERIMENTAL RESULTS

A glance at the diagrams (Figs. 3, 4, 5) shows the general nature of the absorption of HCl in nonionizing solvents. There is no sign of a structure analogous to the rotational structure of the gas. Except in carbon disulphide solution and in liquid hydrogen chloride two maxima of absorption are present, of which the low frequency one is the more intense. This latter band is of lower frequency, the other of higher than the origin of the gas band. (In the subsequent discussion of frequency differences between solution and gas absorption, these will be with reference to the gas band origin of HCl^{35}.) The interval between these maxima varies from solvent to solvent. In liquid hydrogen chloride, although only one maximum appears, the band is strongly asymmetrical, falling off much more rapidly in intensity towards the low frequencies from the maximum than towards the high frequencies. Compared with the gas absorption there is in solution a general shift to lower frequencies.

In the single case for which we have yet obtained data on both fundamental and harmonic, CCl_4 solutions, the appearance of the HCl absorption bands is similar in both regions and the separation between the two components almost the same.

EFFECT OF CONCENTRATION

The figures for CCl_4 solutions for the fundamental show no effect of concentration on the position of the maxima for a twofold change, and similarly, in the overtone in PCl_3 solution at $-67°$, a fivefold change in concentration is without effect.

Effect of Temperature

There is a distinct shifting of the absorption of HCl in PCl_3 solution to lower frequencies with diminishing temperature. Also, the short wave satellite maximum becomes less distinct. The interval between the two maxima does not change appreciably at low temperatures. The asymmetric appearance of the liquid HCl absorption band, observed at $-100°C$, along with the tendency of the short wave maximum to

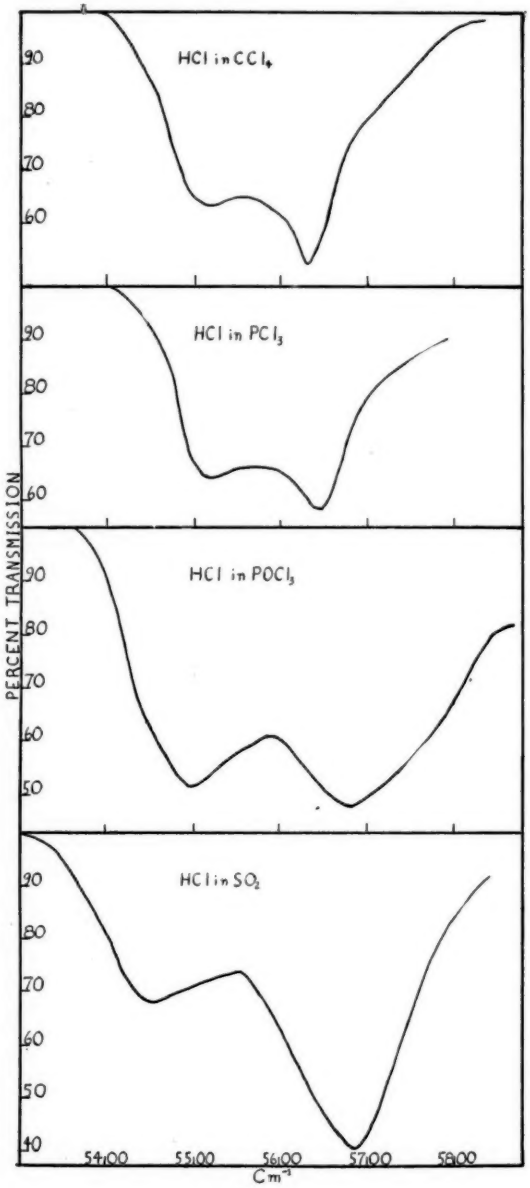

Fig. 3.

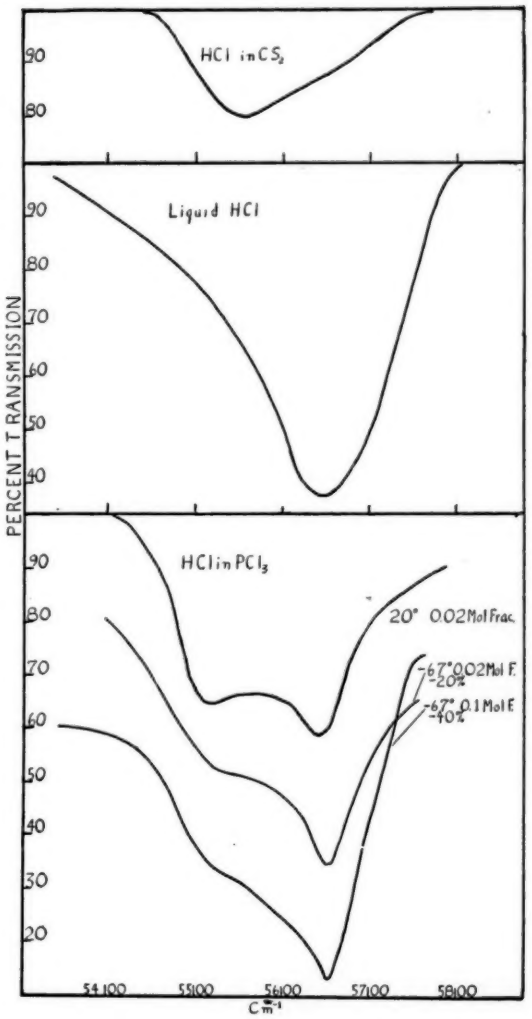

Fig. 4.

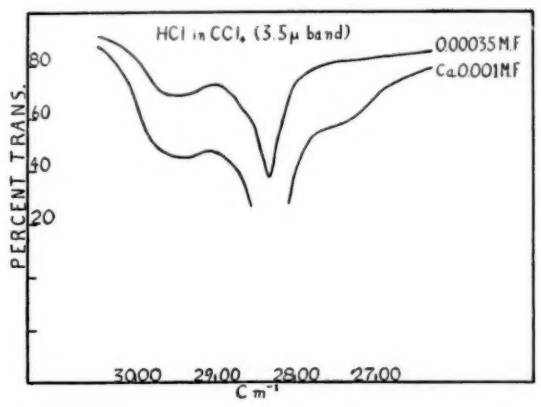

Fig. 5.

TABLE I. *0→1 vibration of HCl.*

SOLVENT	T°C	CONC. HCl (MOLE FRACTION)	ν_1	ν_2	$\nu_2-\nu_1$
HCl GAS			2886		
CCl_4	20°	0.00035	2833	2939	106
	20°	.0007	2833	2939	106
HCl LIQUID (HETTNER)	−100°		2780		

disappear in solution at low temperatures suggests that the liquid band may also be composite and that if it were observed at sufficiently high temperatures two maxima might appear.

RELATIVE INTENSITIES OF GAS AND SOLUTION ABSORPTION

In solution in the various nonionizing solvents examined the maximum absorption in the solution band at 1.7μ was approximately the same as the absorption of the most intense lines of the gas containing the same number of molecules in the light path. The total width of the overtone in the two cases is also about the same. At 3.5μ, in carbon tetrachloride solution, the number of HCl molecules in the light path required to produce a given absorption at the maximum was less than one-tenth of that required to produce the same absorption in the most intense gas lines. The ratio of intensities of first overtone to fundamental is thus considerably smaller in this solution than in the gas. A similar considerably greater apparent absorption of the HCl fundamental in benzene solution over that of the gas has been observed by Plyler and Williams.[4]

IONIZING SOLVENTS

In addition to the solutions in nonionizing solvents, we have investigated the absorption of the electrically conducting solutions of HCl in ether and ethyl alcohol in the neighborhood of wave-length 1.7μ. Thin layers (1 mm) of concentrated solutions were used; and, although the absorption bands of the solvents in this region, the first overtones of the C−H bands, were somewhat intensified and broadened by the HCl, no suggestion of an absorption maximum due to HCl molecules was observed, a result in accord with all published investigations of the absorption and Raman spectra of HCl in such solvents.

DISCUSSION OF RESULTS

While the lack of rotational structure in the solution bands was to be expected, the appearance of the solution bands, especially in sulphur dioxide and phosphorus oxychloride, at first sight, recalls the envelope of the P and R branches of the gas bands, such as would be observed if in solution the individual rotational lines of the branches were merged together but at the same time the significance of the branches as indicating negative and positive rotational transitions, respectively, were maintained. The separation between the two maxima in the solutions is in some solutions indeed comparable with that between the maxima of the P and R envelopes in the gas, nevertheless it seems very improbable that the two solution bands are to be interpreted in this way. 1. The high frequency band in solution is always of lower intensity than the other, in some cases, much lower, the opposite intensity relation to that for the R and P branches of a gas absorption band. As these intensity relations are determined practically by the statistical weights of the rotational levels and the Boltzmann distribution law, it is difficult to see how an inversion could take place in going from gas to solution. 2. Liquid HCl and HCl in CS_2 show only one band with a maximum of lower frequency than the origin of the gas band. Evidently these solvents are exceptional on any

TABLE II. *0→2 vibration of HCl.*

SOLVENT	T°C	CONC. HCl (MOLE FRACTION)	ν_1	ν_2	$\nu_2-\nu_1$
HCl GAS			5668		
CS_2*	20°	0.009	5644		
CCl_4	20°	.018	5570	5675	105
PCl_3	20°	.02	5556	5678	122
	−67°	.02	5534	5660	126
	−67°	.10	5534	5660	126
HCl LIQUID	−100°	1.00	5551		
$CH(NO_3)_2$	20°	.02	5541	5668	127
$POCl_3$	20°	.02	5518	5702	184
SO_2	−65°		5513	5744	231

* Since the anomalous behavior of the HCl absorption in CS_2 as compared with that of other solutions might be associated with the low concentration of the saturated solution at 20°, we attempted to increase the concentration by lowering the temperature to −65°C. The experiment was not completely satisfactory, as the solution became cloudy, but the nature of the absorption was the same as at 20°.

interpretation of the solution doublet, but an exception consisting of the absence of an R branch, if it is normally exhibited, is very difficult to understand. 3. Although the interval between the two solution bands is for a number of solutions comparable with the "doublet separation" in the gas (125 cm^{-1}) it varies a good deal with the solvent, from 105 cm^{-1} in CCl_4 to 231 cm^{-1} in SO_2. To interpret the bands as produced in the same way as the P and R branches of the gas would involves the conclusion that the moment of inertia of dissolved HCl is greater in CCl_4 than in SO_2 in the ratio of $(\Delta\nu_{SO_2}^2 \cdot T_{CCl_4})/(\Delta\nu_{CCl_4}^2 \cdot T_{SO_2})$, approximately 6.5, where $\Delta\nu$ is the frequency interval between the two components at an absolute temperature T; and this would mean, if the reduced masses were the same in the two solvents, that the equilibrium internuclear distance in CCl_4 was about $2\frac{1}{2}$ times greater than in SO_2, a most improbable conclusion. 4. Lowering the temperature from 20°C to −65° in PCl_3 solution makes the high frequency band relatively less intense, and no very accurate determination of its frequency can be made, but definitely the separation between the two bands at the lower temperature is not more than a few cm^{-1} different from that at 20°. If the two bands had been P and R branches, the separation would have diminished from 122 to 102 cm^{-1} at the lower temperature, which is certainly not true.

Our conclusion, therefore, is that the appearance of two maxima of absorption in the regions of the fundamental and first overtone vibrational bands of these solutions does not represent the liquid phase analog of the two branches of the gas absorption bands. How they do originate is a problem which is not unambiguously answered by our present data, but the high intensity of the long wave band and the fact that in certain solutions it alone is present suggest that it is the band originating in the internuclear vibration of the dissolved HCl molecule; and it is true that the relative displacement of the maximum of this solution band from the origin of the gas band agrees with the corresponding displacement of the Raman band. As only one internal vibration can exist in a hydrogen chloride molecule, the short wave satellite to the main band seems to originate in some other kind of motion not existing in the gas and called up in solution. Arguments have recently been advanced from studies both of the spectral and dielectric properties of liquids that polar molecules in the liquid state undergo more or less regular torsional oscillations about relatively slowly moving positions of equilibrium.[7] Thus, liquid water has frequencies of 500 cm^{-1} and 167 cm^{-1} which are absent in the vapor, and which have been attributed by Cartwright to a torsional oscillation of the water molecule and an intermolecular vibration respectively, and Ellis[8] had previously suggested as explanation of some features of the water spectrum peculiar to the liquid that they were combination bands between intramolecular vibrations and a low frequency vibration of about 500 cm^{-1}. It is perhaps possible that an HCl molecule in a solvent medium may be disposed in such a way as to carry out similar oscillations, and we tentatively make the suggestion that the short wave component of the near infrared absorption bands of HCl in solutions is a combination frequency between the intramolecular nuclear vibration which gives rise to the long wave component and a torsional vibration of the HCl molecule or perhaps some other kind of intermolecular solute-solvent vibration of frequency varying between 100 cm^{-1} and 230 cm^{-1} according to the solvent. The approximate identity of the frequency difference between the two components in the fundamental and first overtone of HCl in CCl_4, which, on the hypothesis advanced, is equal to the slow intermolecular vibration, is in accord with this explanation; and such a motion would also depend on the nature of the force field due to the solvent molecules acting on the solute and lead to a different frequency in different solvents. Fig. 6 shows indeed that the interval between the two components of the first overtone of HCl is approximately directly proportional to the dielectric constant of the solvent.

---

[7] M. Magat, J. de phys. et rad. **5**, 347 (1934), which see, for reference to previous work by Segrè and by Bolla, J. D. Bernal and G. Tamm, Nature **135**, 229 (1935); P. Debye, Zeits. f. Physik **36**, 100 (1935); J. H. Cartwright, Phys. Rev. **49**, 470 (1936).

[8] J. W. Ellis, Phys. Rev. **38**, 693 (1931).

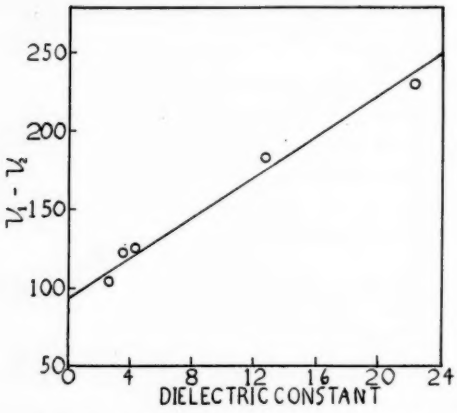

FIG. 6. Separation of maxima as a function of dielectric constant.

FREQUENCY SHIFT

It is evident that if the stronger maximum is taken to represent the internuclear H−Cl vibration in the dissolved molecules it is displaced from the origin of the gas band in the same way as the Raman frequencies. Table III, in which $(\Delta\nu/\nu)_{01}$ represents the relative displacement of the fundamental in solution, from Raman data, except for CCl_4, and $(\Delta\nu/\nu)_{02}$ of the first overtone shows that the relative displacements of the two bands are about the same. The figures of Jung and Gude[9] show a similar approximate constancy in the relative displacement of the frequency of the 4th, 5th and 6th harmonics of 22 normal aqueous ammonia solution.

A very general treatment of the changes in vibrational frequency suffered by molecules in dispersive media has been made by G. Breit and E. O. Salant.[10] A displacement of the absorption frequency is found at high density of the dispersive medium, describable in terms of at least three effects; one analogous to the classical Lorentz-Lorenz pressure damping, one originating in electrostatic interaction of the molecule with its neighbors, due to its excitation, and one originating in overlapping of the electronic wave functions, an electronic "exchange effect." Beyond showing that the observed diminution in frequency produced by liquefying HCl and HBr was much too large to be ascribed to the Lorentz-Lorenz interaction, these authors made no attempt to evaluate the contributions of the various actions.

J. G. Kirkwood, using the model of a point dipole in a continuous dielectric he employed in his calculations of the chemical potential of ionic dipoles in dielectric media,[11] has deduced an expression for the change in vibrational frequency of a dipole caused by the change in energy consequent on the electrostatic interaction of medium and dipole, in a calculation to be offered by him for publication at a later date. The expression for the relative frequency shift is $(\Delta\nu/\nu)=C[(D-1)/(2D+1)]$, where C is a constant and D the dielectric constant of the medium. This function is seen to reproduce qualitatively the observed variation of frequency of HCl and HBr with dielectric constant of the solvent—it reaches a limiting value of $C/2$ at high dielectric constants, and in fact, practically at moderate values of D. Taking for HCl the empirical limiting value of 0.03 for $\Delta\nu/\nu$, we find $C=0.06$; in Fig. 7, the curve represents the function $0.06[(D-1)/(2D+1)]$ and the only experimental points seriously off the curve are for CS_2 and liquid HCl. The constant C depends on the details of the model; for a point dipole at the center of the sphere of radius b occupied by the molecule, it has the value α/b^3, where $\alpha=(10^{28}(\mu_1^2+2\mu_0\mu_2))/((2\pi\nu_0 c)^2 I)$, with μ_0 the electric moment of the dipole at the equilibrium position r_0, in units of 10^{-18} e.s.u.

$$\mu_1=[(\partial\mu)/(\partial r)]_{r_0}, \quad \mu_2=[(\partial^2\mu)/(\partial r^2)]_{r_0}$$

and I the moment of inertia in units of 10^{-40}. Substituting Bourgin's[12] value for the first derivative, 1.06, and Dunham's[13] smaller value, ap-

TABLE III. *Relative displacements of fundamental and first overtone frequencies HCl solution.*

SOLVENT	D	$(\Delta\nu/\nu)_{01}$	$(\Delta\nu/\nu)_{02}$
CS_2(20°)	2.64		0.0042
CCl_4(20°)	2.24	0.0187	.0173
PCl_3(20°)	3.43		.0198
PCl_3(−65°)	4.2	.022	.0236
$POCl_3$(20°)	12.7		.0264
SO_2(−65°)	22.4	.030	.0274
LIQUID HCl (−90°)	8.85	.030	.0206

[9] G. Jung and H. Gude, Zeits. f. physik. Chemie **B18**, 380 (1932).
[10] G. Breit and E. O. Salant, Phys. Rev. **36**, 871 (1930).
[11] J. G. Kirkwood, J. Chem. Phys. **2**, 351 (1934).
[12] D. G. Bourgin, Phys. Rev. **29**, 815 (1927).
[13] J. L. Dunham, Phys. Rev. **35**, 1347 (1930); J. E. Rosenthal, Proc. Nat. Acad. **21**, 281 (1935).

proximately zero, for the second, and using Zahn's value of the electric moment as μ_0 one finds $\alpha=0.0146$ and $b=0.62$A, to be compared with a reasonable value of about 2A. Kirkwood, however, argues that since the electrical center of the HCl molecule is probably displaced towards the proton, the point dipole in the model must be displaced a distance a from the center of the sphere of radius b, making

$$C=(\alpha/b^3)[(1+a^2/b^2)/(1-a^2/b^2)^3].$$

If a is assumed 1.27A, i.e., the point dipole, of moment equal to the observed, imagined to exist in the HCl molecule to account for its dielectric actions on its surroundings, is placed near the proton, the reasonable value of 1.7A for b will satisfy the observations.

This theory of Kirkwood's is also qualitatively correct in predicting the same relative shift for overtones as for the fundamental. It may also be pointed out that this relation between frequency and dielectric constant can account for the greater displacement of the HCl absorption in PCl_3 at lower temperatures, as the dielectric constant of this polar solvent increases considerably with diminishing temperature.

E. Cremer and M. Polanyi[14] have attempted to see in the diminution in frequency of HCl produced by liquefaction that loosening in binding, as a result chiefly of the electronic exchange interactions with other systems, which is a preliminary to chemical action between homopolar molecules, the third effect deduced by Breit and Salant as effective to the first order at high densities. The frequency shift thus calculated amounts to a diminution of a few per thousand, against the observed change of a few percent. The situation seems to be then that the electrostatic forces make the largest contribution to the energy charges when HCl and HBr are liquefied or dissolved in nonreactive solvents, and that Kirkwood's calculation of their magnitude is, in principle, correct. The Raman experimental data for SO_2 in solution, and also our knowledge of the electric moment derivatives are inadequate for a test of the theory, though there is a tendency of the shift to increase with dielectric constant of solvent, while for ammonia

[14] E. Cremer and M. Polanyi, Zeits. f. physik. Chemie, Bodenstein Festband, 770 (1931).

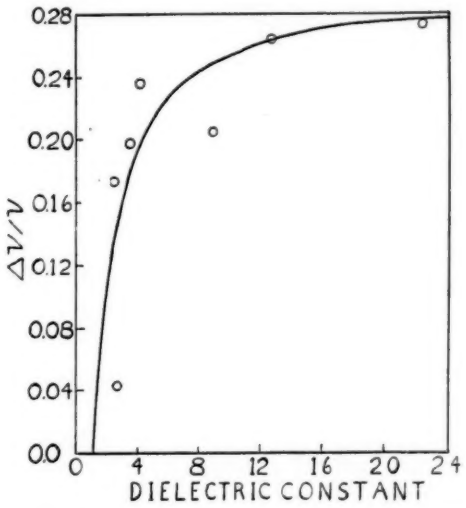

FIG. 7. Relative shift as a function of dielectric constant.

our Raman and Jung and Gude's absorption results cannot be accounted for by the electrostatic effect alone.

ANHARMONIC NATURE OF VIBRATION IN SOLUTIONS

If we apply the theory of the anharmonic oscillator to the maxima of absorption of the 0→1 and 0→2 bands of HCl dissolved in carbon tetrachloride, we find an $\omega_0 x$ factor of 48 cm^{-1}, not very different from the gas value of 52 cm^{-1}. The less accurate Raman values for the 0→1 vibration along with the absorption for the 0→2 in PCl_3 and SO_2 also lead to anharmonic factors near that of the gas. Hettner's figures for the absorption of the fundamental of liquid HCl with ours for the overtone give an anharmonic factor of 10 cm^{-1}, much smaller than that of the gas. It is apparent that in dilute solutions of HCl in the solvents we have examined, the potential energy function differs from harmonic in approximately the same way as in the gas. On the other hand, the considerable increase in the intensity of the 0→1 vibration of HCl in carbon tetrachloride, compared with that of the gas as estimated in the way indicated in the section on results, and the approximate equality of the absorption of the 0→2 vibration in the two phases point to rather considerable changes in the coefficients of the electric moment

as a function of internuclear distance.[15] In this connection it is perhaps interesting to recall the peculiar intensity relations in the harmonics of the liquid hydrogen halides.[2] Although gaseous HI absorbs very feebly in the fundamental and first overtone, the liquid absorbs as well as liquid HCl and HBr in the first overtone, and in fact, the 0→3 transition was found in HI at a thickness of absorbing layer at which this transition was unobservable in the other two halides. In these changes of intensity between the dilute gas and liquid and solution we are evidently dealing with effects of the medium on the electric moment-internuclear distance curve, which could take the forms of shifting the equilibrium distance on the curve and of altering its shape, from the investigation of which it may ultimately be possible to gain further insight into molecular interactions in the condensed state.

We are greatly indebted to Professor John G. Kirkwood of Cornell University for his discussing with us his theory of the frequency shifts, and to the Physics Department of Washington Square College for the use of much of the equipment employed.

[15] We can make no statement from our measurements as to the relative magnitudes of the true absolute intensities in gas and solution. The gas measurements being made with slit widths of 4–6 cm^{-1}, amply adequate to resolve the rotational structure and for calibration with sufficient accuracy for our purpose, but very large compared with the natural width of the lines, indicate an apparent absorption at the maxima of the lines much less than corresponds to the true absorption coefficient. In solution, on the other hand, rotational structure having disappeared, and the variation of absorption coefficient over the region covered by the slit being small, the apparent absorptions are much closer approximations to the true, and our measurements here should give a fairly accurate value of the mean transition probability for the 0→1 vibrational transition according to the method employed by E. Bartholomé (Zeits. f. physik. Chemie **B23**, 131 (1933)). But at present it does not seem profitable to discuss the absolute magnitude of the absorption intensity in solution until the difficulty presented by the serious discrepancy between the results of Bourgin and Dunham, on the one hand and of Bartholomé, on the other, has been resolved. See especially E. C. Kemble, J. Chem. Phys. **3**, 316 (1935).

JANUARY, 1937 JOURNAL OF CHEMICAL PHYSICS VOLUME 5

The Absorption Spectra of Salts of Ytterbium in Crystals and Solutions Compared with Those of Cerium

SIMON FREED AND RAYMOND J. MESIROW, *George Herbert Jones Laboratory, University of Chicago, Chicago, Illinois*

(Received August 3, 1936)

The absorption spectra of salts of ytterbium [the chloride $YbCl_3 \cdot 6H_2O$, the acetate $Yb(C_2H_3O_2)_3 \cdot 4H_2O$ and the ethylsulfate $Yb(C_2H_5SO_4)_3 \cdot 9H_2O$] were found to resemble those of cerium very closely, especially in their diffuseness even at low temperatures. This is in marked contrast with the sharp spectra of the other rare earths. The resemblance was anticipated on the supposition that the thirteen electrons in the 4*f* shell of Yb^{+++}, one short of the maximum the shell can hold, would give rise to but one term ^2F, the same term as the one electron of Ce^{+++} gives rise to. That is, activations aside from fine structure, are impossible when the thirteen electrons remain in the 4*f* shell. This prohibition is derived from the Pauli exclusion principle as it has been applied in gases. The lattice, however, may possibly modify the application of this principle. It was thought likely that the activated states of the ions in crystals would respond to any change in the application of the principle the lattice might impose. The spectra show that the principle holds for these ions in crystals in exactly the same way as it does in gases. Strong confirmation is obtained that the sharp spectra of the other rare earths consist of "forbidden transitions," arising from a change in coupling among the electrons of the 4*f* shell.

THIS work is concerned with whether the Pauli exclusion principle can be applied to spectra of ions in crystals and solutions in precisely the same way as it has been applied to ions in gases. Even if it be granted that the Pauli principle is valid for ions in crystals, there yet remains the uncertainty that the usual operation of the principle may be modified by the influences in the lattice which have no parallel in gases. Such influences if they exist are most likely to be revealed at present with ions of the rare earths in their activated states.

The basic electronic states of these ions, with possibly one or two exceptions, are known definitely[1] from their magnetic susceptibilities. The

[1] F. Hund, Zeits. f. Physik **33**, 855 (1926).

FIG. 1. The absorption spectrum of Yb $Cl_3 \cdot 6H_2O$ at the temperature of liquid nitrogen.

activated states, however, are not known except those of Ce^{+++} and these we have set out to study.

An immediate corollary of the Pauli principle for gaseous ions, a corollary we shall employ in a specific form, is that a shell containing but one electron gives rise to the same term as the shell when it is just one electron short of being full. Ce^{+++} is an example of an ion containing but one electron in its incomplete shell, the 4*f* shell, and Yb^{+++} is the ion conjugate to Ce^{+++} with thirteen electrons in the same shell, one short of the maximum number. Except for fine structure, both electronic configurations can give rise to but one and the same state (^2F) according to the Pauli principle. That is, no activated state is possible with these electronic configurations and hence absorption of radiation in the visible or ultraviolet regions is to be associated with a transition of a 4*f* electron to another shell.

The magnetic susceptibilities of Ce^{+++} and Yb^{+++} prove that their basic electronic states in crystals and in solutions are the same as that computed for the ions in the gaseous state (^2F). Furthermore it was shown[2] that the activated states of Ce^{+++} in crystals and solutions are due to transitions of a 4*f* electron to a virtual outer shell of Ce^{+++}, to the 5*d* shell or, possibly in addition, to the 6*s* shell. The 5*s* and 5*p* shells are already full. Such transitions in that they go to the outer part of the ion, regions close to the fluctuating perturbations of neighboring atoms, result in diffuse bands. And the bands remain diffuse even at low temperatures in contrast to the characteristic sharp spectra of the rare earths. The same kind of behavior might be expected with Yb^{+++} provided the lattice introduced no singular effects, that is, provided the Pauli principle would apply as in gases.

A close resemblance in the spectra of Ce^{+++} and Yb^{+++} in crystals was then to be looked for. The spectra of Yb^{+++} actually resembled those of Ce^{+++} so closely not only in the diffuseness of the bands but in their wave-lengths that it was of chief concern in the beginning whether our salts of ytterbium were contaminated with cerium. A more extended study, however, revealed differences in the spectra.

Professor B. S. Hopkins of the University of Illinois had generously put at our disposal some ytterbium oxide of extraordinary purity. In addition to the usual long processes of purification, the ytterbium had been separated from the other rare earths by electrolytic reduction. The possibility of being reduced singles out ytterbium from the rare earths which accompany it in the usual fractionations. When the uncertainty as to the purity of the ytterbium arose, Professor Hopkins was good enough to make an especial analysis with arc and spark spectra but found no lines due to cerium. In the meantime, we examined our substances employing a sensitive colorimetric test for cerium.[3] No trace of cerium was found even though one part in about 200,000 would have been detected.

Crystals of the chloride [Yb $Cl_3 \cdot 6H_2O$], the acetate [Yb $(C_2H_3O_2)_3 \cdot 4H_2O$] and the ethylsulfate [Yb $(C_2H_5SO_4)_3 \cdot 9H_2O$], all had the same absorption spectra both at 78°K (the temperature of liquid nitrogen) and at room temperature. They were completely transparent in the visible and also in the ultraviolet until about 2550A and then absorption set in and extended throughout the remainder of the (quartz) ultraviolet. An example of the chloride is given in Fig. 1.

Our thinner crystals, about $\frac{1}{2}$ to $\frac{3}{4}$ mm thick, transmitted to 2450A. The acetate and the ethylsulfate were somewhat more transparent than the chloride with the beginning of their absorption at about 100A further toward shorter wavelengths. Aqueous solutions of these salts possessed practically the same spectra as the crystals.

Virtually the same absorption spectra had been furnished by the corresponding salts of cerium.[2]

[2] S. Freed, Phys. Rev. **38**, 2122 (1931). This conclusion was independently arrived at by D. M. Bose and S. Datta, Nature **128**, 270 (1931) and confirmed by R. W. Roberts, L. A. Wallace and I. T. Pierce, Nature **132**, 782 (1933), from measurements on the Faraday effect.

[3] F. Feigl, *Qualitative Analyse mit Hilfe von Tupfelreaktionen* (Leipzig, 1931).

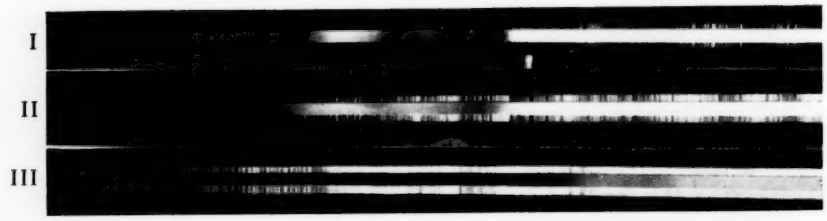

FIG. 2. Mixed crystal of lanthanum and cerium chloride. III. Room temperature: crystal grown from solution containing about ten times as much lanthanum as cerium. II. Room temperature: crystal grown from solution containing about 200 times as much lanthanum as cerium. I. Temperature of liquid hydrogen: crystal containing same concentration as II.

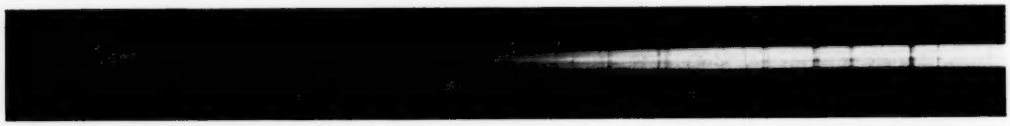

FIG. 3. Absorption spectrum of mixed crystals of Yb $Cl_3 \cdot 6H_2O$ and Sm $Cl_3 \cdot 6H_2O$ at the temperature of liquid nitrogen.

FIG. 4. Absorption spectra of a dilute solution of Yb $Cl_3 \cdot 6H_2O$ in water.

However, it had been found possible to resolve this continuous absorption into three bands by diluting the cerium in the homologous lanthanum salt with which it forms mixed crystals in all proportions. These bands may be seen in Fig. 2. The pure lanthanum salt was completely transparent. The same sort of dilution was carried out with Yb^{+++} by forming mixed crystals with the salts of yttrium (Y^{+++}). Y^{+++} has practically the same radius as Yb^{+++} in terms of x-ray measurements,[4] and these two are found almost always together in nature in the form of mixed crystals. (Ytterbium is one of the elements of the so-called yttrium earths.) Y^{+++} having a rare gas configuration would in all probability be transparent as La^{+++} had been found to be. A mixed crystal of ytterbium and yttrium chloride grown from a solution roughly equimolar in these salts yielded a rather faint absorption band 150A wide with its center at about 2750A and continuous absorption from about 2500A to the limit of the quartz spectrograph. The band remained diffuse at 78°K and the continuum beginning at about 2500A remained unchanged. However, a close study showed a very faint band in our "pure" yttrium and hence it was decided to seek confirmation by diluting ytterbium chloride in the very pure samarium chloride (Sm $Cl_3 \cdot 6H_2O$) we had available. This samarium had been sent to us also by Professor Hopkins to make possible another investigation. Many spectra had confirmed its high purity. Pure Sm $Cl_3 \cdot 6H_2O$ has a rather sharp absorption spectrum which refines remarkably at low temperatures. A mixed crystal of ytterbium and samarium would then offer the opportunity of comparing from the same crystal the spectrum of Yb^{+++} with that of a true rare earth, true in the sense that both its initial and final states are sharp. Mixed crystals were grown from a solution of the chloride containing 1.3 moles samarium per mole ytterbium. The band which had appeared at about 2750A appeared in this mixed crystal also, with center more nearly at 2725A but still diffuse and the continuum began at about 2450A. Again the band remained diffuse at 78°K and it is reproduced in Fig. 3, where the sharp absorption due to Sm^{+++} can be seen.[5]

[4] V. Goldschmidt cited in v. Hevesy, *Die Seltener Erden* (Berlin, 1927), p. 111.

[5] The photograph reproduced here was obtained with several small crystals rather than one, since the band was

The peculiar behavior of a band which appears to pass through a maximum of intensity as the dilution is increased had also been observed with Ce^{+++} at 3020A.[6] Attempts to decompose the continuous absorption in Yb^{+++} beginning at about 2550A failed although the corresponding continuum in Ce^{+++} was resolved without much experimentation. Diluting an aqueous solution of $YbCl_3 \cdot 6H_2O$ also brought out the band at 2700A but it proved ineffectual in resolving the band beginning at 2500A. Such a spectrum is given in Fig. 4.

In still another particular did the spectra differ. There was an enormous disparity in the intensities of their absorptions, Ce^{+++} absorbing much more than Yb^{+++}. The high intensity of the absorption bands of Ce^{+++} had been used to establish that the transition was from a ^2F term (electron in $4f$ shell) to ^2D term (electron in $5D$ shell). This is a dipole transition and is of high probability. The transitions to the same shells in Yb^{+++}, on the other hand, would be expected to be multipole transitions or other transitions of feeble intensity.[7] There is a possibility that the continuum beginning at about 2500A is really to be interpreted as an electronic dissociation of Yb^{+++} in the lattice. If such were the case, in addition to the internal photoelectric effect to be expected, there would be a considerable probability that Yb^{4+} can be made to occur in chemical compounds.

The other rare earths which have their $4f$ shells partially filled may, without violating the Pauli principle, enter into activated states merely by a change in the coupling among the electrons in the shell. In that case, the protection which both the initial and final states are offered by the closed $5s$ and $5p$ shells against perturbation from the lattice would permit the spectra to remain sharp. This explanation has often been advanced to account for the well known sharp spectra of the rare earths.[8] The present work furnishes strong evidence for this explanation since when there is no choice as in Ce^{+++} and in Yb^{+++} but that transitions end in the outer virtual shells, the entire spectra are diffuse.

The transitions within the $4f$ shell do not comply with the selection rules for electric dipole radiation; the sharp spectra consist then of "forbidden transitions."

found somewhat intensified in this way. A single crystal, however, showed the same spectrum clearly. The smaller crystals were obtained by the slow evaporation of a solution of the chlorides of Yb^{+++} and Sm^{+++} in the molal ratio of 1 : 1.3. The crystals grew on the bottom and remained on the bottom of a small quartz beaker which was put in a horizontal position in a quartz dewar vessel and continuous radiation was sent through in the usual manner.

[6] See reference 2. The quantitative dependence of intensity upon dilution was not investigated.

[7] In their basic states the configurations of these ions arranged according to atomic number are the following: A few other ions are added for the easy orientation of the reader.

	$1s$	$4d$	$4f$	$5s5p$	$6s$
La^{+++}	full		0	full	0
Ce^{+++}	"		1	"	0
Yb^{+++}	"		13	"	0
Lu^{+++}	"		14 (full)	"	0.

Upon activation the single electron in the $4f$ shell of Ce^{+++} which had determined the basic state as ^2F had gone to the $5d$ shell resulting in a ^2D state. This corresponds to a dipole transition $\Delta L = -1$, $\Delta J = -1$. The $5f$ and $5g$ shells are extremely unstable compared with the $5d$ shell as there appears to be no atom, no matter how high its atomic number, which stabilizes an electron in these shells. (H. E. White, *Introduction to Atomic Spectra* (New York, 1934), p. 83.) The stability of the $5d$ shell is supported by the known basic state in lanthanum *atom* which has a $5d$ electron in its configuration. The same electronic assignment holds for lutecium and presumably for all the other rare earths. A transition of a $4f$ electron in Yb^{+++} to the $5d$ shell or $6s$ would produce a ^4K or ^4H term, respectively, if Russel-Saunders' coupling holds. Such a transition with $\Delta L > 1$ is not a dipole transition. If $j-j$ coupling exists, both multipole and dipole transitions are possibilities. However, if the final state is simply inverted as the basic state is $\Delta J > 1$ implying a transition of low probability. The presence of electric fields in the lattice would somewhat invalidate the use of the quantum numbers which are customary for computations on gases. The qualitative conclusions appear to us of value, nevertheless.

[8] However, diffuse bonds are possible from these rare earths also when a transition to an outer virtual shell occurs and indeed they have been found (S. Freed, reference 2) further in the ultraviolet than the usual sharp spectra.

The Absorption Spectra of Samarium Tungstate and of Samarium Molybdate at Low Temperatures

SIMON FREED AND EDWARD L. HAENISCH, *George Herbert Jones Laboratory, University of Chicago, Chicago, Illinois*

(Received August 31, 1936)

As a preliminary to a study of the relation between the fluorescence and the absorption spectra of crystals, we photographed the absorption spectra of single crystals of $Sm_2(WO_4)_3$ and of $Sm_2(MoO_4)_3$ at 78°K, 113°K, 169°K, and 298°K. Evidence was found that an activated state 76 cm^{-1} from the basic state exists in the tungstate. The general patterns of the spectra of the tungstate and of the molybdate are not the same, indicating that the crystals do not belong to the same space group, an inference likely to be made from crystallographic data. There is also evidence for a dissociation, perhaps an incipient dissociation in the lattice, as if the tungstate and especially the molybdate dissociated into the basic and acidic oxides within the single crystal.

THIS work, somewhat preliminary in its nature, is the first step in our study of the relation between the emission and the absorption spectra of crystals. The emission spectra are to be obtained from a crystal whose absorption spectra are also available and the spectra are to be identified with a single rare earth at a time. Rare earths are known to fluoresce strongly in native calcium tungstate, scheelite, and in calcium molybdate, powellite, giving their characteristically sharp line spectra.[1]

Zambonini[2] has studied the miscibility of the crystals of the rare earth tungstates in the alkaline earth tungstates as well as the miscibility of the corresponding molybdates. The effect on the axial ratios of the pure substances was found to be:

$CaWO_4$	tetragonal c = 1.530
$CaWO_4$ with 10.3% $Ce_2(WO_4)_3$	tetragonal c = 1.532
$CaMoO_4$	tetragonal c = 1.551
$CaMoO_4$ with 39% $De_2(MoO_4)_3$	tetragonal c = 1.542
$CaMoO_4$ with 21% $Ce_2(MoO_4)_3$ 24.7% $\frac{1}{2}(MoO_4)_3$	tetragonal c = 1.544

A few percent of a rare earth are ample for obtaining absorption spectra from single crystals of such size as may be grown in the laboratory.

A similar example is fluorite, calcium fluoride, from which the very word fluorescence is derived. The emission spectra of fluorite as excited by light or cathode rays are rich in sharp lines which have been identified by Urbain[3] and others as due to the rare earth fluorides in solid solution.

As examples of the mixed crystals of these fluorides in calcium fluoride, the following may be taken:[4]

Yttrofluorite regular crystal contains about 15 percent fluorides of the rare earths.

Yttrocerite, presumably regular, contains about 25 percent rare earth fluorides.

Yttrocalcite hexagonal contains about 50 percent rare earth fluorides.

The hexagonal symmetry is characteristic of yttrium fluoride (tysonite) at room temperature.

We selected samarium as the rare earth in the hope of making contact with the recorded spectra of a number of its hydrated salts and with the energy levels which have been derived from them.

This communication deals with pure samarium tungstate $Sm_2(WO_4)_3$ and with pure samarium molybdate $Sm_2(MoO_4)_3$. Both of these salts were prepared from pure samarium oxide which Professor B. S. Hopkins of the University of Illinois was kind enough to supply us. The oxide was converted into the chloride by adding hydrochloric acid and evaporating to dryness. The chloride was dissolved in water and filtered through a sintered glass disk to remove dust and any other particles which might subsequently reduce the tungstate (or molybdate). The solution was diluted to a large volume and the percipitating agent (sodium tungstate or sodium molybdate) was added drop by drop and with constant stirring to minimize occlusion. The precipitates were white to a very pale yellow and very gelatinous. They were separated from the supernatant liquid by centrifuging and washed with water five to eight times by the

[1] Ch. de Rohden, Ann. de Chimie IX **3**, 338 (1916).
[2] F. Zambonini, Bull. Soc. Fr. Min. **38**, 206 (1915), cited by A. N. Winchell in *Microscopic Characters of Artificial Minerals* (John Wiley and Sons, New York, 1931).
[3] G. Urbain, Comptes rendus **143**, 825 (1906).
[4] Doelter's *Handbuch der Mineralchemie*, Vol. 4.

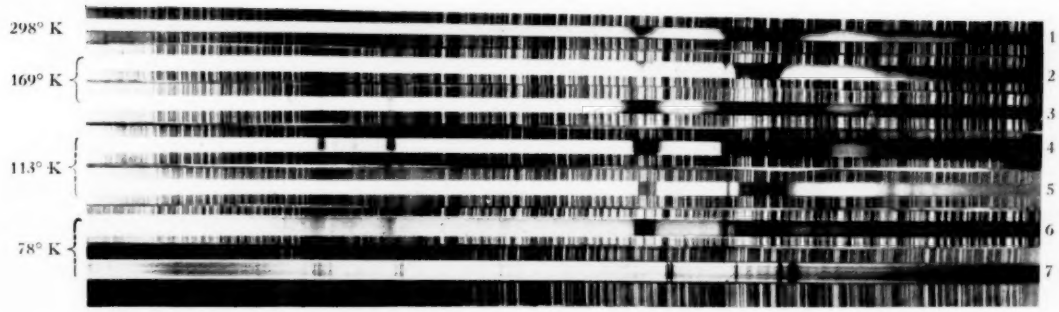

FIG. 1. Absorption lines and bands of samarium tungstate. 1 to 6 inclusive are spectra of the tungstate at the temperatures marked at the left. 3 and 4 are prints which were overexposed in the blue to bring out the very faint structure in the red region. 7 is the absorption spectrum of hydrated samarium chloride at liquid nitrogen temperature.

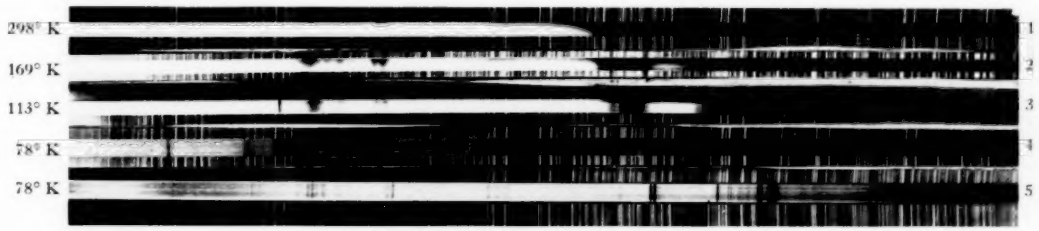

FIG. 2. Absorption bands of samarium moybdate. 1, 2, 3 and 4 are the absorption spectra of the salt at the temperatures noted at the left. 5 is the absorption spectrum of hydrated samarium chloride at liquid nitrogen temperatures.

FIG. 3. B. Spectrum of samarium tungstate at the temperature of liquid nitrogen. A. Spectrum of samarium molybdate at the temperature of liquid nitrogen.

same method. The final filtrations were carried out through a sintered glass plate.

An enormous shrinkage in volume occurred when these hydrated solids were heated to dull redness. They were therefore "pre-shrunk" by heating for several hours at 900°C in an atmosphere of oxygen before they were put into the large furnace in which the crystal was to be grown. During this heating the color changed to a deeper yellow.

The furnace consisted of an alundum core wound with molybdenum wire. However, within this core a nonporous mullite cylinder closed at the bottom served to keep the hydrogen gas (which constituted the atmosphere surrounding the molybdenum heating element) from diffusing into the region where the tungstate (molybdate) was being melted and crystallized. As a further precaution a stream of oxygen was directed just over the tungstate (molybdate) to insure that the salt remain in the oxidized state.

The crystals were grown from the molten state (1200° to 1300°C) by the method described by Kyropolous.[5]

The spectra were complicated by a phenomenon which may perhaps be thought of as a dissociation within the lattice, as a sort of dissociation of the salt into its basic and acidic oxides. This phenomenon showed itself more pronouncedly in the molybdate in that the color of the molybdate, a light yellow, darkened upon

[5] S. Kyropolous, Zeits. f. Physik **63**, 849 (1930).

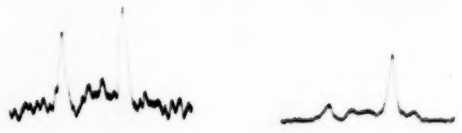

FIG. 4. Microphotometer curves of the 4520A multiplet in $Sm_2(WO_4)_3$. Left, liquid N_2; right, liquid CH_4.

heating into a tan and on cooling the color paled again but not to such a degree as to end in the original yellow. The resulting heterogeneity within the lattice was brought out in the general diffuseness of the spectra of the molybdate as compared with sharper spectra of the tungstate and with the especially sharp spectra of the hydrated chloride. It was to be expected that any departure from regularity within the lattice would impress such a diffuseness on the spectrum of Sm^{+++} ions. The ions would not be in exactly equivalent situations in the lattice, the electrical fields to which an ion would be exposed would differ from ion to ion and correspondingly the energy levels or frequences would also differ slightly and since the spectrum registers the absorption of all the ions traversed by the beam of light it would show closely neighboring frequencies, i.e., diffuse bands. We have not investigated this "dissociation" further. However, Jander[6] had come to consider the possibility of such a phenomenon in connection with the electrical conductivity of powders consisting of tungstates and also of molybdates of the alkaline earths. The fact that scheelite and powellite are known to contain more than the stoichiometrical amount of molybdic oxide confirms in some measure this point of view.

We shall postpone the detailed discussion of these spectra until we have studied the spectra by emission. For the moment, it may be pointed out again that the spectra of the tungstate, Fig. 1, are much sharper than those of the molybdate, Fig. 2. Fig. 3 permits the comparison of these spectra to be made more easily. Both spectra arising from crystals at 78°K are here reproduced. The tungstate ion and the molybdate ion begin with their own continuous absorption

[6] W. Jander, Zeits. f. anorg. allgem. Chemie **192**, 286, 295 (1930).

TABLE I. *Absorption lines and bands of samarium tungstate at 78°K. Intensity was estimated on a rough scale of 10 with very faint lines considered as 0. S (sharp), d (diffuse), b (broad) and vb (very broad) are used to indicate the character of the lines and edges. Primed values are band edges.*

WAVE-LENGTH	WAVE NUMBER	INTENSITY	WAVE-LENGTH	WAVE NUMBER	INTENSITY	WAVE-LENGTH	WAVE NUMBER	INTENSITY
5645.6	17,708.0	0s	4751.4	21,040.6	1vb*	4096.8	24,402.4	4s
5636.7	17,736.0	1s	4743.5	21,075.6	1vb*	4093.0	24,425.1	1sd
5311.6	18,821.5	1s	4736.3	21,107.5′	2d	4091.4	24,434.6	6s
5306.3	18,840.3	2s	4721.2	21,172.2′	2d	4090.1	24,442.4	6s
5020.6	19,912.4	5s	4715.5	21,200	0vb	4088.2	24,353.7	2d
5014.9	19,935.0	1sd	4657	21,467′	0d	4083.8	24,480.1	3s
5007.4	19,964.9	1sd	4652	21,490	0vb	4078.6	24,511.3	2vb
4992.3	20,025.3	0d	4639.6	21,547.5	5vb	4075.6	24,529.4′	4d
4984.9	20,055.0	0d	4630.5	21,590′	1d	4072.5	24,548′	2d
4920.7	20,316.7	2d	4530.4	22,066.9	5s	4064	24,599′	2vd
4913.9	20,344.8	3s	4524.9	22,093.8	0s	4027	24,825′	0vd
4909.8	20,361.8	3s	4520.8	22,113.8	0s	4019	24,875	0d**
4899.3	20,405.4	4sd	4514.8	22,143.2	3s	3998	25,005	0d
4891.7	20,437.1	4sd	4456.1	22,434.9	0b*	3994	25,031	0d
4885	20,465	0b	4417	22,633	vfvd*	3991.5	25,045′	0d
4876.5	20,502	0b*	4411.5	22,662	vfvd*	3988	25,068′	0d
4865.3	20,549.0	0vb	4405	22,690	vfvd*	3986	25,081′	0d
4855.4	20,589.9	0b	4401	22,716	vfvd*	3980	25,118′	0d
4842.2	20,646.0	0b	4206.5	23,766′	10sd	3935	25,406	0d
4829	20,702	1b	4201.8	23,792.6′	10sd	3931	25,430	0d
4821.6	20,734.2	4b	4200	23,803′	8sd	3914	25,540	0d
4814.5	20,764.8	1b	4197	23,820′	5sd	3911	25,559	0d
4806	20,801	2b	4195.6	23,827.8′	5sd	3907	25,587	0d
4782	20,906	1vb*	4189.5	23,862.5′	2d	3905	25,600	1d
4774.5	20,938	1vb*	4186.9	23,877.3	3vd	3897	25,648	0d
4766	20,976	1vb*	4184	23,894′	2d	3799	26,310	***
4758.5	21,009	1vb*	4180.2	23,917′	10sd			

* May be 2–3*A* wide.
** Region from this point to the blue is very faint and difficult to discern.
*** Transmission ceases.

TABLE II. *Absorption lines and bands of samarium tungstate at 113°K. Intensity was estimated on a rough scale of 10 with very faint lines considered as 0. (Some rather doubtful lines indicated by 00.) S (sharp), d (diffuse), b (broad), vb (very broad) are used to indicate the character of the lines and edges. Primed values are band edges.*

Wave-Length	Wave Number	Intensity	Wave-Length	Wave Number	Intensity	Wave-Length	Wave Number	Intensity
5646.3	17,705.8	00s	4805.1	20,805.4	2d	4199.9	23,803.4′	8s
5637.3	17,734.1	00s	4783.4	20,899.8′	2s	4197.6	23,816.5′	5s
5312.8	18,817.2	00s	4779.2	20,918.2′	2s	4196.0	23,825′	2s
5308.1	18,833.9	00s	4767	20,973	vbvf	4190.2	23,858.5′	2d
5020.6	19,912.4	1d	4751	21,042	vbvf	4187.3	23,875.0	0vd
4992.8	20,022.9	00d	4743	21,077	vbvf	4184.3	23,892.1′	2d
4984.1	20,058.2	00d	4736.0	21,109.0′	1d	4181.0	23,911.0′	7s
4921.1	20,315.0	00d	4720.3	21,179.2′	1d	4097.3	24,399.4′	5d
4914.0	20,344.4	3d	4715.5	21,201	0vd	4095.0	24,413.2′	5d
4910.2	20,360.1	2d	4657.2	21,466.1′	2d	4092.9	24,425.7′	8s
4899.5	20,404.6	1d	4649.2	21,503.1′	2d	4091.2	24,435.8′	3d
4892.0	20,435.8	1d	4645.1	21,522.1	2d	4090.8	24,438.2′	2d
4876	20,503	vbvf	4641.5	21,538.7′	3d	4089.6	24,445.4′	2d
4866	20,545	vbvf	4636.4	21,562.4′	5d	4089	24,450′	0d
4857	20,593	vbvf	4530.5	22,065.9	5s	4087.3	24,459.1′	8s
4843	20,643	vbvf	4524.9	22,093.7	0sd	4084.7	24,475.2′	5d
4831	20,690′	2d	4520.7	22,114.3	0sd	4082.2	24,489.7′	2d
4827	20,711′	2d	4514.9	22,142.7	1s	4079.8	24,504.1′	1d
4823.2	20,726.5′	2d	4419	22,623′	0d	4077.5	24,518′	0d
4820.4	20,739.4′	2d	4400	22,720′	0d	4076.8	24,522′	0d
4816.7	20,755.3′	2d	4207.2	23,762.1′	10s	4023.5	24,847′	0d
4811.1	20,779.0′	2d	4201.7	23,793.2′	8s	3998	25,007	vfvd

TABLE III. *Absorption bands of samarium molybdate at 78°K. Intensity was estimated on a rough scale of 10 with very faint lines considered as 0. S (sharp) and d (diffuse) are used to indicate the character of the edges.*

Wave-Length	Wave Number	Intensity	Wave-Length	Wave Number	Intensity	Wave-Length	Wave Number	Intensity
5635.8	17,739	2d	4913.3	20,347	8s	4656.6	21,460	0d
5624.9	17,773	2d	4904.8	20,382	8s	4645.9	21,518	0d
5304.4	18,847	3d	4822.0	20,733	0d	4634.2	21,573	1d
5292.5	18,889	3d	4792.7	20,859	0d	4622.6	21,627	1d
5019.7	19,916	1d	4773.1	20,945	1d	4523.1	22,103	*
5013.6	19,940	1d	4765.4	20,979	1d	4219.5	23,693	0d
5005.5	19,972	0d	4753.7	21,030	0d	4161.5	24,023	0d
5000.0	19,994	0d	4726.9	21,150	0d	4093.1	24,424	**

* The region around this value is very diffuse.
** Transmission ceases.

at about 3800A and 4100A, respectively. The two salts do not exhibit spectra of the same pattern although the supposed isomorphism of their crystals would lead to a close parallelism in their spectra. The spectra indicate then definitely that the molybdate and tungstate do not belong to the same crystallographic space group.

The tungstate gives evidence that a thermally excited state exists 76 cm^{-1} removed from the basic state. Fig. 4 shows the relative intensities of two lines associated with this interval. The component of this pair toward smaller wavelengths becomes more intense as the temperature is lowered, a behavior in keeping with the presence of activated ions. To establish these activations beyond question, we plan on measuring the absorption spectrum at the temperature of liquid hydrogen. The long wave component should practically disappear since the number present in such an activated state at this temperature would be negligibly small.

The Free Energy of Hydrogen Cyanide from Spectroscopic Data

A. R. GORDON, *Chemistry Department, University of Toronto, Toronto, Canada*

(Received October 30, 1936)

The free energy and heat content of gaseous hydrogen cyanide are computed from spectroscopic data, and the equilibrium constant for the reaction involving the formation of the gas from its elements is tabulated. The results are in good agreement with the experimental value for the free energy of formation obtained by Lewis and his associates, but are in definite disagreement with the results of Badger. The equilibrium constant for the exchange reaction with deuterium is also tabulated. From the spectroscopic entropy for the gas and the most recent density data, the entropy of liquid hydrogen cyanide is estimated.

THE determination of the free energy of hydrogen cyanide has been a problem that has concerned physical chemists for many years. Von Wartenberg[1] attempted to measure the equilibrium constant for the reaction involving the formation of the gas from its elements, but his data provide little more than an order of magnitude, while the more recent results of Lewis and his associates[2] and of Badger[3] are not in as close agreement as one could wish. Badger and Woo[4] have computed from spectroscopic data $S°_{298.1}$ for the gas, and from this, the other known entropies, and the heat of formation given in *International Critical Tables*, Yost and Stone[5] have calculated $\Delta F°_{298.1}$ for the formation of the gas from its elements. Recently, as an example of the use of approximation methods,[6] I computed the rotational-vibrational contribution to F/T for 1500°K, and the present paper gives the results of similar calculations of the free energy and heat content for the temperature-range of greatest experimental interest.

The spectroscopic constants[7] are: $\epsilon_V = 2037.0v_1 + 52.0v_1^2 + 712.1v_2 - 2.9v_2^2 + 3364.2v_3 - 51.3v_3^2 + 3.1l^2 - 0.2v_1v_2 - 15.1v_1v_3 - 19.6v_2v_3$; $B_v = 1.47890 \times (1 - 0.00625v_1 - 0.00726v_3)$; $D = -3.63 \times 10^{-6}$. The rotational-vibrational interaction term for ν_2 has not been determined, but from Choi and Barker's work it is evidently small. The resulting $(F°-E_0°)/T$ and $(H°-E_0°)$ are listed in Table I;[8] the reader is referred to example 2 of reference 6, for details of the calculation.

There has been no recent determination of the heat of combustion of hydrogen cyanide; Thomsen[9] gives 158,600 cal. Von Wartenberg and Schütza[10] have recently pointed out in connection with their measurement of the heat of combustion of cyanogen, that about three and a half percent of the nitrogen is converted to nitric oxide; if a correction be made for this, Thomsen's value for cyanogen is raised by 1500 cal. to 261,100 cal., in excellent agreement with their result 261,300 cal. Since Thomsen carried out his

TABLE I. $K_1 = (P_{HCN})/(P_{H_2})^{\frac{1}{2}}(P_{N_2})^{\frac{1}{2}}$; $K_2 = (P_{HCN})(P_{HD})/(P_{DCN})(P_{H_2})$.

T°K	$-(F°-E_0°)/T$ cal./deg.	$(H°-E_0°)$ kcal.	$-\log K_1$	K_2
250	39.537	1.807	—	0.65
298.1	40.824	2.210	20.91	0.84
300	40.871	2.225	20.76	0.84
350	42.029	2.666	17.54	1.01
400	43.060	3.127	15.12	1.15
500	44.846	4.099	11.74	1.36
600	46.371	5.125	9.49	1.52
700	47.712	6.199	7.89	1.63
800	48.913	7.314	6.68	1.71
900	50.005	8.469	5.75	1.77
1000	51.010	9.658	5.01	1.81
1200	52.811	12.12	3.90	1.87
1400	54.399	14.69	3.10	1.91
1600	55.823	17.34	2.51	1.93
1800	57.117	20.06	2.06	1.95
2000	58.306	22.83	1.69	1.96
$S°_{298.1}$	48.238			

[1] Von Wartenberg, Zeits. f. anorg. allgem. Chemie **52**, 299 (1907).
[2] Lewis and Randall, *Thermodynamics* (1923), p. 584 et seq.
[3] Badger, J. Am. Chem. Soc. **46**, 2166 (1924).
[4] Badger and Woo, J. Am. Chem. Soc. **54**, 3523 (1932).
[5] Yost and Stone, J. Am. Chem. Soc. **55**, 1889 (1933).
[6] Gordon, J. Chem. Phys. **3**, 260 (1935).
[7] Choi and Barker, Phys. Rev. **42**, 777 (1932); Herzberg and Spinks, Proc. Roy. Soc. **A147**, 434 (1934); Adel and Barker, Phys. Rev. **45**, 277 (1934).
[8] The natural constants used were: $hc/k = 1.4324$, $R = 1.9869$, additive constant for the translational free energy $= -7.267$. None of the entries in Table I includes the nuclear-spin contribution.
[9] Thomsen, *Thermisch-chemische Untersuchungen*, Vol. II, p. 387.
[10] Von Wartenberg and Schütza, Zeits. f. physik. Chemie **A164**, 386 (1933).

hydrogen cyanide and cyanogen combustions under comparable conditions, it is evident that his hydrogen cyanide value should be increased by roughly half the correction for cyanogen, giving a heat of combustion of 159,400 cal. per mole. Combining this with the heats of combusion of graphite[11] and hydrogen,[12] 94,240 and 68,313 cal., respectively, ΔH_{298} for the reaction $C_{\beta\text{graph.}}+\frac{1}{2}N_2+\frac{1}{2}H_2=HCN(g)$ is 31,000 cal. From this and the thermodynamic data for graphite,[13] hydrogen[14] and nitrogen,[15] $\Delta F^\circ_{298.1}$ for the reaction is 28.510 cal. and ΔE_0° is 31,090 cal. The resulting $\log K_1=\log (P_{HCN})/(P_{H_2})^{\frac{1}{2}}(P_{N_2})^{\frac{1}{2}}$ are listed in the fourth column of the table.

A repetition of Lewis and Randall's calculation[2] for the free energy of hydrogen cyanide but using spectroscopic free energies of formation for water, carbon monoxide, carbon dioxide and ammonia[16] leads to a standard free energy of formation at 298.1° of 28,520 cal., some 350 cal. less than the result they obtained by using the older free energy data, and in fortuitously close agreement with the value obtained in this paper. Badger[3] used the equilibrium $NH_3+C=HCN+H_2$, and found for 800°, $K=5.8\times10^{-6}$, leading to a ΔF°_{800} of 19,200 cal.; from a slight extrapolation of Haber's data,[17] the standard free energy of formation of ammonia at this temperature is 9200 cal., so that the free energy of formation of hydrogen cyanide at 800° would be 28,400 cal., nearly 4000 cal. greater than the result from Table I, *viz.* 24,470 cal. The discrepancy is most puzzling, as Badger approached equilibrium from both sides, and his apparent experimental error is much less than 4000 cal. Von Wartenberg's averaged result for $\log K_1$ at 2000° (quoted by Lewis and Randall), $\log K_1=-1.24$, probably agrees as closely as can be expected with the value in the table.

Recently Bartunek and Barker[18] have determined the moment of inertia and fundamental frequencies of DCN, $I=22.92\times10^{-40}$; $\omega_1=1897$, $\omega_2=569.1$, $\omega_3=2630$ cm^{-1}. The second- and third-order terms in the expression for the energy levels are not known, but to a good approximation the difference between the rotational-vibrational contributions for HCN and DCN may be obtained by using the harmonic oscillator-rigid rotator approximation for both molecules, i.e., for HCN, $I=18.72\times10^{-40}$; $\omega_1=2089$, $\omega_2=712.1$, $\omega_3=3313$ cm^{-1}. The respective zero-point energies for the two molecules (one-half unit of vibrational energy for the valence frequencies ν_1 and ν_3, and one unit[19] for the degenerate deformation frequency ν_2) are 9718 and 8062 cal. per mole, respectively; thus from Johnston and Long's data[20] for HD and Giauque's for H_2, ΔE_0° for the reaction $H_2+DCN=HD+HCN$ is 837 cal. The resulting $K_2=(P_{HCN})\times(P_{HD})/(P_{DCN})(P_{H_2})$ for the exchange reaction are listed in the last column of Table I.

While the calculation of $S^\circ_{298.1}$ for $HCN(g)$ is perfectly straightforward, the calculation of the entropy of $HCN(l)$ is a matter of some uncertainty. Perry and Porter's measurements of the vapor pressure[21] can be represented by the equation

$$\log p_{mm}=7.44558-(1453.063/T)+2.1052\times10^{-3}T-3.716\times10^{-6}T^2 \quad (1)$$

[11] Roth and Naeser, Zeits. f. Elektrochem. **31**, 461 (1925), as corrected by Clayton and Giauque, reference 13.

[12] Rossini, Nat. Bur. Stand. J. Research **6**, 1 (1931).

[13] Clayton and Giauque, J. Am. Chem. Soc. **54**, 2610 (1932). Their table of $(F^\circ-E_0^\circ)/T$ and the calculations of this paper both are based on the assumption that there is no zero-point entropy for graphite. It has been pointed out by the author (J. Chem. Phys. **1**, 308 (1933)) and by Kassel (J. Am. Chem. Soc. **56**, 1838 (1934)) that there is some evidence from the experimental results for the producer gas equilibrium that there may be a zero-point entropy for graphite of 0.5 cal./deg. Had such a zero-point entropy been assumed, the standard free energy of formation at 298° would have been 28,660 cal., and all the entries in the fourth column of Table I would have been increased numerically by 0.11.

[14] Giauque, J. Am. Chem. Soc. **52**, 4816 (1930).

[15] Giauque and Clayton, J. Am. Chem. Soc. **55**, 4875 (1933).

[16] For water, −56,690 cal. (Gordon, J. Chem. Phys. **2**, 65 (1934)); for CO, −33,000 cal. (Clayton and Giauque, reference 13); for CO_2, −94,440 cal. (Kassel, J. Am. Chem. Soc. **56**, 1838 (1934)); for NH_3, −3935 cal. The value for ammonia was obtained from Haber's direct measurement of the heat of formation at room temperature (reference 17), −11,075 cal. at 298°, and the entropies of hydrogen, 31.23 (reference 14), of nitrogen, 45.79 (reference 15), and of ammonia, 45.79 (Kassel, Chem. Rev. **18**, 277 (1936)).

[17] Haber, Zeits. f. Elektrochem. **20**, 597 (1914).

[18] Bartunek and Barker, Phys. Rev. **48**, 516 (1935).

[19] Dennison, Rev. Mod. Phys. **3**, 280 (1931).

[20] Johnston and Long, J. Chem. Phys. **2**, 389 (1934). There are obviously some serious misprints in their approximation equations which are intended to represent the entries in their Table IV between 1000° and 3000°. The following equations agree with their tabulated values for this range within ±0.001 cal./deg. For HD,

$$-(F^\circ-E_0^\circ)/T=-8.597+3.5R\ln T-R\ln[1-\exp(-5199.1/T)]-1.25\times10^{-5}T+1.15\times10^{-8}T^2.$$

For D_2,

$$-(F^\circ-E_0^\circ)/T=-7.541+3.5R\ln T-R\ln[1-\exp(-4288.7/T)]+1.00\times10^{-6}T+1.10\times10^{-8}T^2.$$

[21] Perry and Porter, J. Am. Chem. Soc. **48**, 299 (1926).

which fits their experimental results somewhat more closely than does the equation they employ. If hydrogen cyanide were a perfect gas, this would correspond to a heat of vaporization at 298.1°K of 6603 cal. Actually, as Usherwood[22] and Felsing and Drake[23] have shown, the gas deviates very markedly from ideality. Felsing and Drake find for $P=1$ atm. that the ratio (density of actual gas)/(density of ideal gas) is 1.0705 at 30°C, 1.0301 at 70°C and 1.0170 at 110°C, results which are in agreement with Usherwood's less precise measurements. Bredig and Teichmann[24] find that the critical pressure and temperature are 53.2 atm. and 456.7°K, respectively, which would correspond (assuming a Berthelot equation) to a density ratio of 1.025 at 30°C and 1 atm.; thus there must be considerable association. Even in the absence of complete $P-V-T$ data, however, it is still possible to make a plausible estimate of the necessary corrections to the calculated thermodynamic quantities.

Assume that the actual gas consists of unassociated molecules obeying the Berthelot equation (partial pressure P') and of double molecules which behave ideally (partial pressure P''). Then if α be the degree of association,

$$PV=(P'+P'')V=RT[1-\alpha/2+\beta(1-\alpha)], \quad (2)$$

where β is the Berthelot term $(9p_r/128t_r).(1-6/t_r^2)$, $t_r=T/T_c$, $p_r=P'/P_c$, and T_c and P_c are the critical temperature and pressure, respectively. Eq. (2) can then be solved for P' at Felsing and Drake's three temperatures, giving $P'=0.953$, 0.987 and 0.995 atm., respectively, with corresponding fugacities for the single molecules of 0.930, 0.970 and 0.983 atm. The fugacity of the double molecules is equal to their partial pressure, so that log K_a for the reaction $(HCN)_2=2\,HCN$ is 1.263 at 303.2°, 1.850 at 343.2° and 2.278 at 383.2°K. When these values of log K_a are graphed against $1/T$, they lie quite closely on a line whose slope corresponds to a heat of association, ΔH_a, of 6780 cal. per mole $(HCN)_2$. To a good enough approximation P' can be replaced by P in the definition of β in Eq. (2) and α can be replaced by $2P/(K_a+4P)$, since even with these simplifying assumptions Eq. (2) (with the values of K_a obtained above) predicts densities which agree with Felsing and Drake's data within their limit of error. V can thus be written explicitly as a function of T, P and K_a, and thus by means of the relation $(\partial S/\partial P)_T=-(\partial V/\partial T)_P$, an expression for the entropy of the nonideal saturated vapor can be obtained by conventional methods:

$$S_{\text{actual gas}}=S_{\text{ideal gas}}+(R/4).\ln(K_a+4P)/K_a - R\beta'-P.\Delta H_a/T(K_a+4P) + (P/K_a).(R\beta'-\beta.\Delta H_a/T), \quad (3)$$

where $R\beta'$ is the Berthelot correction to the entropy $R(27p_r/32t_r^3)$ and $\Delta H_a=6780$ cal. Eq. (1) predicts for 298.1° a vapor pressure of 738.8 mm,[25] so that the entropy of the saturated vapor as an ideal gas is 48.294; from the value of K_a at 303.2° and the heat of association, K_a at 298.1° is 15.1, so that the entropy of the actual saturated vapor is 47.17 cal./deg. From Eq. (2), the density ratio at this temperature is 1.080 for the saturated vapor so that the heat of vaporization is 6112 cal. and the ΔS of vaporization 20.50 cal./deg. Thus $S^\circ_{298.1}$ for $HCN(l)$ is 26.67 cal./deg.; had ideality of the gas been assumed throughout, the result would have been 26.14 cal./deg. One would expect, however, that the third law entropy of liquid hydrogen cyanide would be definitely less that 26.67 in view of the results that have been obtained for other unsymmetrical molecules such as nitric oxide,[26] carbon monoxide[13] and nitrous oxide.[27]

[22] Usherwood, J. Chem. Soc. **121**, 1604 (1922).
[23] Felsing and Drake, J. Am. Chem. Soc. **58**, 1714 (1936).
[24] Bredig and Teichmann, Zeits. f. Elektrochem. **31**, 449 (1925).
[25] The normal boiling point according to Eq. (1) is 298.86°K.
[26] Johnston and Giauque, J. Am. Chem. Soc. **51**, 3194 (1929).
[27] Blue and Giauque, J. Am. Chem. Soc. **57**, 991 (1935).

The Line Absorption Spectrum of Gadolinium Ion in Crystals

G. C. NUTTING[1] AND F. H. SPEDDING,[2] *Department of Chemistry, University of California, Berkeley, California*

(Received August 8, 1936)

With a view to determining the dependence upon crystal symmetry and chemical composition of the energy levels in a solid, the absorption spectrum of Gd^{+++} in a number of different synthetic crystals has been photographed at temperatures between 300° and 20°K. Using the external crystallographic symmetry as an indication of the probable degree of symmetry about the gadolinium ion in the lattice, it is established that the important factor in determining the splitting of the multiplets or the excited levels is the lattice symmetry and not the negative ion except insofar as the negative ion influences the crystal structure, for the spectra of monoclinic gadolinium chloride, bromide, sulfate and selenate are almost identical, but are very different from the spectra of the hexagonal formate, bromate and ethylsulfate. Gadolinium propionate and butyrate evidently have somewhat different internal symmetry from that of the other monoclinic crystals since their spectra resemble much more the spectrum of triclinic gadolinium acetate. The group of compounds including gadolinium trichloracetate, propionate, butyrate, isobutyrate and trichlorbutyrate is similar in that the spectra of all are weak, diffuse, and little resolved even at the temperature of liquid hydrogen. The presence or absence of water of crystallization affects the spectra only slightly. The positions of the multiplets, and the positions of the lines within the multiplets of anhydrous gadolinium formate are much the same as in the ethylsulfate and bromate enneahydrates. The phenomenon of highly discrete selective reflection in the ultraviolet region by three compounds has been observed. A discussion of the nature of the excited states of the gadolinium ion in crystals is presented.

IN a previous paper[3] the absorption spectrum of gadolinium ion in six compounds was reported on. It was shown that through studies of the discrete absorption of salts of the rare earth elements intimate knowledge of the energy states arising from various configurations of electrons in the outer regions of atoms in crystals (hence of most immediate interest to chemists) can most readily be gained. Compounds of gadolinium are especially suitable for this purpose for their spectra are simple, and, since the basic states are single, the absorption lines present in effect energy level diagrams of the excited states. Changes attending alteration of lattice structure and changes of chemical composition are easily followed and may be exactly measured. There are three major difficulties in using gadolinium for such a study. In seeking to interpret the spectra of ions in the solid state analyses of the spectra of the gaseous ions are of immense value, and such analyses are lacking for all but one of the triply ionized rare earth atoms. That one is cerium. Gadolinium is also unfortunate in that its spectrum lies in the ultraviolet, with the chief multiplets near 2700A. A regrettably large number of anions absorb in this region, so salts of gadolinium with them, although they may be interesting chemically and crystallographically, cannot be studied. There is, furthermore, no powerful source of ultraviolet light, and thus spectrograms obtained by transmission through conglomerates of small crystals or by diffuse reflection from powders of microcrystalline substances cannot be obtained with an instrument of high dispersion in a reasonable length of time. It seems to be a fact, moreover, that the rare earth compounds which crystallize in the tetragonal and isometric systems, and are of most theoretical interest, are uniformly insoluble, and hence may be obtained with an ordinary expenditure of effort only as powders.

In the present paper new data are given on the absorption spectra of the Gd^{+++} ion in hexagonal crystals of $Gd(COOH)_3$, $Gd(BrO_3)_3 \cdot 9H_2O$ and $Gd(C_2H_5SO_4)_3 \cdot 9H_2O$; in monoclinic crystals of

$$Gd_2(SO_4)_3 \cdot 8H_2O, \quad Gd_2(SeO_4)_3 \cdot 8H_2O, \quad Gd(C_2H_5COO)_3 \cdot 3H_2O$$

and $Gd(C_3H_7COO)_3 \cdot 2H_2O$; in triclinic crystals of $Gd(CH_3COO)_3 \cdot 4H_2O$; and in

$$Gd(CCl_3COO)_3 \cdot 3H_2O; \quad Gd(CCl_3CH_2CH_2COO)_3 \cdot 10H_2O$$

and Gd(iso $C_3H_7COO)_3 \cdot 6H_2O$. Crystallographic

[1] DuPont Fellow in Chemistry, 1932–33. Shell Research Fellow in Chemistry, 1933–34.

[2] This writer wishes to express his appreciation to the John Simon Guggenheim Memorial Foundation for making it possible for him to visit many European laboratories where work in closely allied fields is being carried on.

[3] F. H. Spedding and G. C. Nutting, J. Am. Chem. Soc. 55, 496 (1933).

measurements on most of the compounds have been made for us by Professor Adolf Pabst[4] of the geology department of the University of California, and we are glad to acknowledge his aid. There are no crystallographic data on gadolinium chloracetate, chlorbutyrate and isobutyrate.

Experimental Part

With the exceptions of the bromate and ethylsulfate, which were obtained by double decomposition between barium bromate and ethylsulfate and gadolinium sulfate, the compounds were prepared by dissolving gadolinium oxide in the appropriate acids. When it was possible to obtain them, only perfect single crystals were photographed, but in the case of the formate, selenate, chlorbutyrate and isobutyrate conglomerate pictures were found necessary. The thickness of the crystals ranged from 0.4 to 2.5 mm. In establishing the composition of the compounds, molecular weight determinations, carried out by converting weighed quantities of salts into gadolinium oxide, were made. Wolff[5] has reported only three molecules of water of crystallization in cerous isobutyrate while we have found six molecules in the gadolinium compound.

In order to take advantage of the increased sharpness and increased resolution of the absorption lines obtained at low temperatures, whenever feasible the spectra were photographed at 78°K, and in several instances at 20°K. The crystals were immersed directly in the cooling bath of liquid air, liquid nitrogen or liquid hydrogen contained in a large Dewar flask with a quartz extension at the bottom. The background of continuous ultraviolet light was provided by a hydrogen discharge tube. Photographs were made with a quartz three meter Littrow spectrograph (Hilger E185) giving dispersion of 3A per mm at 3100A, 2.1A per mm at 2750A and 1.5A per mm at 2500A. Since many exposures were long (the times varied from three minutes to a week) the temperature of the room was kept constant within 0.1°C. Positions of the absorption lines were measured with reference to the iron spectrum.

[4] A. Pabst, Am. J. Sci. **22**, 426 (1931); **26**, 73 (1933).
[5] H. Wolff, Zeits. f. anorg. allgem. Chemie **45**, 89 (1905).

Repeated attempts to secure satisfactory spectra of gadolinium nitrate and bromate in the 2700A region failed. Regardless of the purity of the salts, the ultraviolet light brought about decomposition whose products showed continuous absorption, although potassium nitrate and potassium bromate (both anhydrous salts, incidentally) transmit well as far as 2700A, particularly at low temperatures. The difficulty was partially overcome in the case of gadolinium bromate by using very thin crystals, but no spectra of the hydrated nitrate below 3100A were ever obtained.

Observations

The Gd IV absorption spectrum consists of nine principal multiplets, which, since they arise from a single lower level, constitute an energy level diagram of the excited states. Besides these multiplets there are scattered through the spectrum numbers of much fainter lines, sometimes sharp, sometimes diffuse, sometimes gathered into groups, sometimes appearing as widely separated individuals. Slight overexposure frequently masks them altogether. Their intensity is greatly enhanced at low temperatures and they appear most prominently in the sulfate, chloride and acetate spectra. Since it may be that many of them are due to other rare earths than gadolinium, we shall not consider them further.[6]

[6] These lines are of the same general type as the faint lines reported in the visible by S. Freed and F. H. Spedding, (Phys. Rev. **34**, 945 (1929), and J. Am. Chem. Soc. **52**, 3747 (1930)). While the Gd salt was some of atomic weight purity, kindly sent us by Professor Hopkins, this does not mean that it was entirely free from traces of other rare earths. These traces will have a negligible effect on any atomic weight determinations since the differences in the atomic weights of the rare earths are small but in absorption spectra they may become important. Since the above papers were published we have definitely found that some of those weak lines were due to other rare earths. We therefore think it advisable in this paper to omit all lines below a certain level of intensity as at present we have no way of knowing which of the lines (if any) come from the gadolinium and which from traces of other rare earth impurities. If these lines should prove to be due to impurities it would appear that the hexagonal lattice is less tolerant of other rare earth ions than the monoclinic. Therefore in the fractional crystallization of the rare earths, if one picked out large single crystals free from mother liquor a more rapid separation might be effected. It is interesting in this connection to observe that the bromate and ethylsulphate, both hexagonal crystals, are two of the best salts for rapid fractionation of the Gd group of rare earths.

It is found that the gross features of the spectra are independent of the nature of the negative radical and the presence or absence of water of crystallization. Dilution through hydration brings shifts of the multiplets a few angstroms toward shorter wave-lengths, and the multiplets of the metal organic compounds lie almost invariably slightly to the red of the multiplets of wholly inorganic compounds. Much greater differences are noted in the spectra of compounds having different crystallographic symmetry. It appears that the multiplets would in gaseous ions degenerate into single levels, or at any rate into simpler structures, and that the complicated patterns actually observed have arisen from the various action on the simple levels of the force fields existing between the gadolinium ions and their definitely and regularly oriented neighbors in the crystal lattice. If this is true, since vibrational coupling between the positive and negative constituents of the compound in most cases is clearly absent, it might be expected that the structure of the multiplets is largely determined by the symmetry of the lattice, and the higher the symmetry type the simpler the spectrum. Just what the symmetry is, is to be decided from x-ray patterns, and x-ray data on rare earth compounds are at present and probably will be for some time to come very meager. At least it is likely that the internal symmetry is reflected in some measure in the external form of the crystal, and that it is probably of higher order in a hexagonal than in a monoclinic or triclinic crystal. The gadolinium spectra support this view, for spectra of varied compounds which crystallize in the monoclinic system are very similar, yet unlike the spectra of hexagonal crystals, which among themselves are also similar.

The usual result of cooling the crystals is marked sharpening of the absorption lines. Lessening the thermal motion in the lattice decreases the Doppler broadening and in addition doubtless decreases the natural width of the lines. A third reason is perhaps most important of all. The approach and recession of an ion or a dipole adjacent to a gadolinium ion is attended by a continuously varying Stark field which shifts the position of the gadolinium energy levels by a small amount. The total effect produced upon the multitude of atoms contributing to the absorption is the pronounced widening of the absorption lines. At low temperatures the shift of the levels is small and the absorption lines are correspondingly sharp. It is also true that the multiplets widen slightly with decreasing temperature and the lines in general shift to the red. The shift is small and takes place principally between room and liquid-air temperatures. Sometimes on further cooling to 20°, a few of the lines are displaced once more to the violet, but only by about 1 cm^{-1} from the position they occupy at 78°. The amount of the shift appears to depend largely upon the symmetry of the crystal, being greatest (from 8 to 10 cm^{-1}) in the spectra of the hexagonal bromate and ethylsulfate, intermediate (4 to 7 cm^{-1}) in the monoclinic chloride and sulfate, and least (1 to 3 cm^{-1}) in the triclinic acetate. The shifts are probably to be accounted for in the main by the contraction of the lattice. This brings the adjacent atoms closer to the gadolinium, thus increases the strength of the electric fields acting on the gadolinium and increases the amount of the splitting of its energy levels.

Gadolinium propionate, butyrate, isobutyrate, trichloracetate and trichlorbutyrate show strange behavior, for the lines in their spectra are always very wide and very fuzzy, in decided contradistinction to the lines of gadolinium sulfate and bromate, and even formate and acetate. The apparent intensity of absorption is very low, too, but this is understandable in view of the unusual width of the lines. Lowering the temperature brings some narrowing and resolution, but even at the temperature of liquid hydrogen the absorption lines are much wider than those of an inorganic gadolinium compound at room temperature.

The phenomenon of strong selective reflection in the λ3100 multiplet found by Spedding and Bear[7] in gadolinium chloride has been observed also in gadolinium ethylsulfate and isobutyrate. Although a reflection phenomenon, we have usually observed it in spectra photographed by transmission through either a badly cracked single crystal or a conglomerate of small crystals, in which the surfaces necessary for multiple

[7] F. H. Spedding and R. S. Bear, Phys. Rev. **39**, 948 (1932).

reflection are abundant. Absorption spectra of conglomerates of gadolinium fluoride, sulfite, selenate, iodate, trichloracetate, formate, propionate, butyrate and malonate have been photographed and all showed the normal absorption lines. It is to be regarded as a chance occurrence that in a mass of tiny crystals the facets should be so oriented that on the average the light of wave-lengths represented in the λ3100 band is reflected from them instead of passing through the surfaces and being absorbed in the body of the crystals. It seems likely that if it were possible to obtain large single crystals of these gadolinium salts, successive reflection from certain of their surfaces would in all cases bring about isolation of the frequencies of the λ3100 lines. Selective reflection from crystals is common enough, but gadolinium is absolutely unique in the narrowness of its reflection bands, which at 20° in the ethylsulfate are considerably less than one angstrom in width, and are quite comparable with the selective reflection of the 2537A line of mercury in the vapor state described by Wood.[8] Since the reflectivity of a substance for a given wave-length depends on both the index of refraction and the extinction coefficient, it is probably fortuitous that it should reach the observed high value in the λ3100 multiplet rather than in any of the others. The relative intensities of the lines are usually very different from the intensities of the corresponding absorption lines. One chloride plate showed λ3118, 3115 and 3112 in reflection and λ3110 faintly in absorption. Another chloride conglomerate, photographed by reflection, showed the four 3110A lines strongly in reflection, the 3050A lines entirely absent and the 2700A lines extremely faintly in absorption. An ethylsulfate spectrum showed the 3110 and 3109 lines in reflection and 3108 in absorption. Careful comparison of plates made at 300°K has demonstrated that for both gadolinium chloride and ethylsulfate the positions of the lines absorbed and selectively reflected are identical. It is noteworthy that the λ3050 and 3110 multiplets were never obtained from sulfate conglomerates at 300°, despite many attempts to do so, yet they invariably showed up perfectly in the photographs of single crystals at all temperatures and of conglomerates at 85°. It was presumably because the sulfate crystals were immersed in liquid air (a medium of very different refractive index from gaseous air) that the absorption lines appeared in this last case. Perhaps it should be mentioned that selective reflection was observed when the interfaces through which the incident light entered the various crystals were of quartz, air, liquid air, liquid nitrogen and liquid hydrogen. For a given substance the intensity of reflection in each of these cases would probably be different because of the differences in indices of refraction, but we have not attempted to secure data on this point.

In the paragraphs which follow are set forth some of the details of the spectra. We shall consider the multiplets in turn.

3110 and 3050A multiplets

The spectra of the chloride, bromide and sulfate single crystals are practically identical—the position, width and intensity of the lines for a given temperature are the same. The spacing of the lines in the spectrum of the selenate conglomerate is much like that of the other wholly inorganic monoclinic crystals, but the multiplet spreads are distinctly greater. The lines are unusually wide, unusually intense and unusually fuzzy.

Monoclinic crystals of gadolinium propionate and butyrate give lines which are wide and very much blurred. The 3110A lines in both are practically not resolved at all at room temperature. The 3050A group is somewhat better, distinctly so in the case of the butyrate. The 3118 line of the propionate is missing at 300° but shows up faintly at 78°. At 78° the propionate spectrum at 3110A sharpens markedly, but still the lines are very much less sharp than in one of the inorganic compounds. At 78° the 3050A lines of the propionate are stronger but about as fuzzy as at 300°, and are spread out over about one and one-half times the distance. Upon cooling propionate crystals to 20°, it is found that the absorption lines are about as diffuse as they are at 78°. There is no resolution, no change in relative intensities and no change in relative position. On the other hand the butyrate lines are appreciably narrower at 20° than at 78°, and one line resolves into two components. The multiplets of gadolinium isobutyrate are at room temperature two very faint, ill-defined, structureless, unmeasurable bands. At the temperature of liquid air the absorption is more intense and the bands become narrower and resolve, showing five lines in the λ3110 and four lines in the λ3050 multiplets. The lines are wider and the multiplets are wider and situated farther toward the red than in the butyrate spectrum.

The lines of the nitrate are stronger and wider than those of the chloride and are less spread out, but have about the same limit on the violet side. They do not become narrower or less diffuse at the temperature of liquid air. The lines of the acetate resemble the lines of the chloride very much in width, spacing and intensity. They are, however, displaced somewhat to the red, and the multiplet spread is two-thirds

[8] R. W. Wood, *Physical Optics*, third edition, p. 534.

or less that of the chloride. In the spectrum of the trichloracetate the lines are faint, diffuse and unresolved. The multiplets are slightly wider than the multiplets of the acetate and are shifted several angstroms to the violet. At 85° the 3110A multiplet which, for most salts, is composed of either three or four lines shows ten, distributed irregularly, all of them fuzzy and faint and spread over twice the distance of the acetate multiplet. The 3050A group has the normal number of three lines.

The spectra of the bromate, formate and ethylsulfate resemble one another closely and are radically different from the spectra of salts crystallizing in other systems. The resemblance between the ethylsulfate and formate is particularly close. There are only three λ3110 lines in the ethylsulfate at room temperature, and no resolution takes place on cooling. At room-temperature there are two 3050A lines in the ethylsulfate, the violet one of which splits at 78°. At 20° the absorption lines of gadolinium ethylsulfate and bromate are as sharp as the finest of the emission lines of gaseous iron which served as the comparison spectrum. The 3110A lines of the bromate are four in number at 300°, the violet two being a close doublet. At 78° the multiplet is spread somewhat, and the separation of the two violet lines is quite noticeably increased. In addition, the red components increase their intensity markedly. At 20° the λ3110 lines of the bromate become six, spreading toward the red but beginning at about the same wave-length on the violet side. There are three lines in the 3050A group at all temperatures. The violet two are by themselves and appear to be the close doublet of the ethylsulfate enormously separated. The overall multiplet spreads of the hexagonal crystals are about one-third those of the monoclinic. The ethylsulfate spectrum is shifted farthest to the violet of any salt, while the bromate is next, and the centers of gravity of the formate multiplets are slightly to the violet of those of the chloride.

2700A multiplets

The bromide and chloride spectra are practically completely identical, even to distribution of intensities. The sulfate spectrum also resembles that of the chloride very closely, but shows somewhat more resolution, and the intensities are a bit different. All the sulfate multiplets are shifted slightly to the violet, but within the multiplets the position of corresponding lines is nearly the same. The selenate spectrum resembles that of the sulfate closely in its gross appearance. All the 2700A multiplets have the same overall spread as the sulfate multiplets, thus contrasting them with the λ3100 bands. Owing to the continuous absorption by the selenate ion and to the fact that a conglomerate of crystals were used, detail, especially in the violet groups, is lacking. Within the 2720–2760A multiplets the general appearance of the fine structure resembles that of the sulfate multiplets, but the resemblance is not nearly so close as in the case of the sulfate, bromide and chloride.

The 2700A groups of the propionate and butyrate are so pulled in that the spectra mirror that of the triclinic acetate more than they do the spectra of the other monoclinic salts. As in the 3100A multiplets, the lines are extremely hazy and the resolution extremely bad. The widths of the multiplets of the propionate and butyrate are nearly identical at room temperature. The grouping of the lines within the multiplets appears to be somewhat closer in the butyrate, and in the butyrate the lines are slightly narrower. At 78° the spectra of gadolinium propionate and butyrate are alike. The multiplets are wider than at room temperature and the lines are fuzzier and broader. It looks as if, without exception, each of the 2700A lines is about to split into two lines. This seeming resolution does not proceed further, however, and the spectra of both salts appear much the same at 20° as at 78°. A few lines sharpen, while the majority remain as diffuse as at the higher temperature. The gadolinium isobutyrate spectrum is distinguished by possessing a few sharp lines at room temperature, while most are very diffuse and all are very faint. All the multiplets are much wider than those of the butyrate and lie several angstroms to the red, in fact farthest to the red of any of the salts investigated. A single photograph of gadolinium trichlorbutyrate made at room temperature with a Hilger E3 spectrograph indicates that the line groups are intermediate in position between those of the isobutyrate and trichloracetate, and are wider and slightly better defined than the butyrate multiplets.

In the acetate spectrum the red edges of the multiplets lie at nearly the same positions as those of the chloride, but the spread of the multiplets is only three-fourths as great. The consequent crowding of the lines gives an impression of haziness at room temperature, while actually the lines are only slightly less sharp than the lines of the chloride. There is practically line for line correspondence within the multiplets. The trichloracetate lines are even fuzzier and less resolved than those of gadolinium butyrate; the detail is scarcely better than in spectra of solutions containing gadolinium ion, where, owing to the relatively great freedom of motion and the indefinite composition of the clouds of water molecules surrounding the positive ions, blurring is to be expected .Except in their extreme haziness, the spectra of solutions and chloracetate crystals have little in common. The 2790A multiplet of the chloracetate, which at 300° consists of two very wide lines, becomes at 85° nine lines of which two are almost surely double. The rest of the multiplets both at 85° and at 20° show little resolution and are wider and are spaced differently from the propionate multiplets at the same temperatures.

The multiplets of the hexagonal crystals are only one-fourth to one-half as wide as those of the chloride, and there are fewer lines within the multiplets. All are displaced to the violet, the ethylsulfate and bromate appearing at about the same places, the farthest to the violet of any of the compounds used. The formate lines are wide and blurred and resolution is incomplete. The ethylsulfate and bromate spectra resemble one another more than they do the formate spectrum. At liquid nitrogen temperature the lines and multiplets of the bromate widen and give evidence of impending further resolution. Spedding and Bear[9] have observed the same phenomenon in the spectrum of samarium bromate.

[9] F. H. Spedding and R. S. Bear, Phys. Rev. **44**, 287 (1933).

TABLE I. *Frequencies of the absorption lines of gadolinium compounds.* Intensities (Int.) have been visually estimated on the scale 0–10. *D* indicates a double line, *T* a triple line, *M* a multiple line of unknown number of components. The letters *w*, *d* and *vd* indicate lines which are wide, diffuse and very diffuse. Primed frequency numbers represent band edges; *c*, band centers.

$Gd_2(SO_4)_3 \cdot 8H_2O$							$Gd_2(SeO_4)_3 \cdot 8H_2O$	
20°			78°		300°		300°	
λ	ν	Int.	ν	Int.	ν	Int.	ν	Int.
3116.47	32078.3	5	32078.6	6	32083.8	5	32061	10*wd*
3113.64	32107.5	5	32106.2	7	32110.6	7	32101	10*wd*
3110.87	32136.1	6	32135.8	9	32136.4	9	32131	10*wd*
3108.27	32162.9	5	32162.2	8	32159.9	9	32166	10*wd*
3065.2	32615	0						
3059.24	32678.4	7	32678.7	7	32683.3	7	32665	10*wd*
3055.60	32717.3	7	32717.0	7	32719.0	7	32709	10*wd*
3052.44	32751.2	7	32750.6	8	32748.8	7	32752	10*wd*
3049.1	32787	0						
3029.8	32996	0						
2792.35	35801.6	5	35801.2	5	35808.0	4	35797	8*wd*
2789.63	35836.5	5	35836.5	5	35839.3	3	35832	10*wd*
2788.13	35855.8	7	35856.4	7	35858.5	7	35851	10*wd*
2786.13	35881.5	5	35880.9	4	35883.2	1	35873	4*wd*
2765.63	36148.8	10	36149.4	10	36155.6	10	36141	10*d*
2763.33	36177.6	10	36178.0	8	36181.6	8	36170	10*w*
2762.07	36194.1	10	36194.1	9	36195.6	9	36198	10*dD*?
2761.10	36206.8	10	36207.0	9	36209.4	8	36215	6*d*
2759.92	36222.3	6	36222.5	7	36227.8	9	36225	6*d*
2759.48	36228.0	6	36227.9	7	36236.8	6	36236	6*d*
2759.08	36233.3	5	36233.4	5				
2758.56	36240.1	5	36240.3	5	36243.3	6	36242	6*d*
2757.99	36247.6	6	36247.7	6	36250.4	6	36248′	
2757.60	36252.7	6	36254.4	10*D*	36254.3	6		
2757.36	36255.9	6						
2757.02	36260.4	5	36260.3	6	36258.8	10*M*	36259*c*	10
2756.43	36268.2	9	36268.4	8				
2756.11	36272.3	7	36272.5	8	36271.5	10*M*	36271′	
2744.68	36423.4	10	36423.9	10	36430.3	9*D*	36417	8*dD*
2742.59	36451.1	10	36451.7	8	36455.5	8	36443	7*wd*
2741.41	36466.8	10	36467.1	10	36471.4	10*D*	36462	7*dD*
2741.05	36471.6	10	36472.4	10			36482	7*dM*
2739.42	36493.3	9	36493.4	8	36495.4	8	36503	6*wd*
2738.38	36507.2	8	36506.9	7	36507.8	8	36542	7*wd*
2735.52	36545.3	9	36545.9	9	36551.2	10	36556	5*wd*
2734.32	36561.4	8	36561.6	7	36567.0	7	36567′	
2733.42	36573.4	9						
2732.97	36579.4	9*D*	36578.0	10*D*	36581.0	10*M*		
2732.17	36590.1	9	36590.1	9	36593.6	8		
2731.28	36602.1	8*D*	36599.9	7	36605.1	10	36607*c*	5
			36604.1	7	36621.2	10*M*		
2730.01	36619.1	10*M*	36618.9	8*T*				
2728.81	36635.2	10	36635.2	10	36638.9	10*D*	36649′	
2728.37	36641.1	10*D*	36640.8	10				
2727.24	36656.3	10	36656.4	10	36661.7	10*D*	36664	5*dD*
2726.52	36666.0	10	36665.7	10				
2725.6	36678	1						
2725.2	36684	0						
2528.85	39531.8	8	39532.9	6	39523	5		
2528.11	39543.4	8	39544.8	6	39546.5	6		
2525.54	39583.6	9	39584.5	5	39585.9	5		
2523.52	39615.3	10	39616.5	7	39619.2	6		
2521.62	39645.1	10*d*	39645.6	6*d*	39645.4	5		
2462.44	40597.8	4	40608.7	10				
2462.1	40604	4	40604.9	10	40602	8*D*		
2461.60	40611.7	7*D*	40610.9	10	40613	8*D*		
			40613.6	10				
2453.3	40748	0	40747	2*d*				
2452.8	40757	0						
2445.6	40878	0	40879	3*d*	40884	1*d*		
2443.4	40914	0	40916	3*d*	40921	1*d*		
2440.7	40959	0	40963	3*d*	40968	1*d*		

TABLE I.—*Continued.*

$Gd(C_2H_3COO)_3 \cdot 3H_2O$						$Gd\,Cl_3 \cdot 6H_2O$ solution.	
20°		78°		300°		300°	
ν	Int.	ν	Int.	ν	Int.	ν	Int.
32054	0*d*	32057.6	4*wd*	32067	4*wvd*	32088′	
32079	0*d*	32081.2	6*wd*	32082	4*wvd*	32092*c*	3
32096	0*d*	32094.3	6*wd*	32098	4*wvd*	32097′	
32104	0*d*	32105.0	6*wd*			32111′	
						32116*c*	3
32655	0*d*	32654.5	5*wd*	32660.7	6*wd*	32121′	
32678	0*d*	32681.3	6*wd*	32676	6*wd*	32138′	
						32157*c*	6*D*
32697	0*d*	32696.6	6*wd*	32686	6*wd*	32174′	
35782	1*wd*	35783.7	10*wd*	35785.3	4*d*	32684′	
						32689*c*	4
35809	1*wd*	35810.8	5*wd*	35810	2*d*	32696′	
35823	1*d*	35823.4	6*wd*	35823	1*d*		
						32721′	
35843	1*dD*	35843.2	7*dD*	35841.3	3*wd*	32726*c*	6
						32732′	
36136	2*dM*	36141.9	10*dM*	36136.8	7*d*		
						32750′	
36148	2*d*			36146.6	7*d*	32757*c*	6
36161	1*d*	36162	7*wd*	36161	3*d*	32762′	
36171	1*d*	36174.2	7*wd*	36171	3*d*		
36184	1*wd*	36182.4	7*wd*	36183.2	4*d*		
		36189.2	4*wd*				
		36203′		36208	6*dM*?	35819′	
36211	2*d*	36219*c*	8	36219	5	35823*c*	0
36228	3*wd*	36236′		36227.8	10*D*?	35826′	
36247	2*dD*	36248.1	10*D*	36244	10	35841′	
36410	1*wd*	36407′		36417	8*d*	35849*c*	2
		36420*c*	10			35852′	
36427	3*wd*	36434′		36426.8	10*dD*?	35860′	
36439′						35866*c*	2
36446*c*	1*d*	36448	8*dM*	36446	7*wd*	35874′	
36452′		36464	7*dD*	36462	7*d*	35889′	
36464	1*wd*					35895*c*	1
36527	1*wd*	36523′		36529.7	7*wd*	35904′	
36538	1*wd*			36540.8	9*wd*	36167′	
36551	2*wd*			36552.4	9*wd*	36173*c*	1
36562′		36570*c*	6*d*	36566′		36178′	
36572*c*	3*d*			36574.5*c*	10*d*	36187′	
36583′				36584′		36195*c*	10
36592	2*d*			36594.0	8*wd*	36205′	
36599′				36607	8*wd*	36219′	
36606*c*	1*d*						
36614′		36617′				36224*c*	1
36630	1*dM*	36630	7*dM*	36625	9*wd*	36229′	
				39501	7	36245′	
				39515	6	36270*c*	10
				39536	9	36294′	
				39567	6	36303′	
				39580.8	7	36309*c*	10
				40552′		36316′	
				40566*c*	7*d*	36442′	
				40584′		36446*c*	1
				40844	1*wd*	36449′	
				40884	1*wd*		
						36460′	
						36475*c*	10
						36490′	
						36510′	
						36519*c*	8
						36529′	
						36577′	
						36628*c*	10
						36692′	

TABLE I.—*Continued.*

$Gd(C_3H_7COO)_3 \cdot 2H_2O$				$Gd(\text{iso } C_3H_7COO)_3 \cdot 6H_2O$			
78°		300°		78°		300°	
ν	Int.	ν	Int.	ν	Int.	ν	Int.
32066	1*d*	32069	5*vd*	32041	1*wd*		
32079	3*d*	32080	5*vd*	32069	1*wd*		
32092	2*d*	32090	5*vd*	32089	1*d*	Too faint	
32103	2*d*	32103	5*vd*	32124	0*d*	to	
32662	2*d*	32661	5*wd*	32139	0*d*	measure	
32678	3*d*	32678	5*wd*	32650	1*wd*		
32697	3*d*	32691	5*wd*	32672	1*wd*		
35789	5*d*	35788	4*d*	32703	1*wd*		
35809	2*d*	35813	1*vd*	32768	0*d*		
35820	2*d*	35824	1*vd*	35757	2*d*	35757	1*d*
35842	3*d*	35841	2*d*	35777	0*d*	35788	0*d*
36137′		36144	8*dD*?	35801	1*d*	35802	0*d*
36144*c*	8*d*			35830	1*d*	35820	0*d*
36152′		36158	2*d*	35856	0*d*		
36160	3*d*			35869	0*d*		
36171	4*wd*	36170	3*d*	36110	2*dM*	36111	1*d*
36186	5*wd*	36181	4*d*	36126	2*wd*	36123	1*d*
36203′		36207	6*wvdM*?	36169	2*wd*		
36219*c*	8*d*	36219	4*d*	36181′		36192	2*d*
36233′		36228	10*w*	36203*c*	2*d*	36213	2*d*
				36224′			
36244	7*wd*	36241	9*w*	36245	0*wd*	36247	1*d*
36414′		36417′		36259	0*wd*		
36423*c*	8*d*	36424*c*	10*d*	36272	2*wd*	36272	1*d*
36432′		36431′		36379′		36390	1*d*
36443	3*d*	36442	3*d*	36398*c*	2*d*	36399′	
36452	2*d*	36450	1*d*	36418′		36407*c*	1*wd*
36464	4*wd*	36460	5*d*			36414′	
36528′		36528′		36431′		36438′	
36544*c*	6*d*	36543*c*	7*d*	36442*c*	1*d*	36443*c*	2*wd*
36559′		36558′		36451′		36450′	
36564′		36567′		36468	1*d*	36468	0*d*
		36575*c*	10*d*	36490′		36536	1*wd*
36584*c*	6*d*	36583′		36548*c*	1*d*	36554′	
		36590′				36562*c*	1*d*
		36596*c*	8*d*			36570′	
36606′		36602′				36590′	
36613	1*d*	36625	7*w*			36598*c*	1*d*
36621′		39501	2*d*			36607′	
36627*c*	5*d*	39515	2*d*	36606′		36627	1*d*
36634′		39534	2*d*	36626	0*wd*	36658	1*d*
		39564	2*d*	36661	1*d*		
		39580	2*d*				
		40561′					
		40567*c*	7*vd*				
		40575′					

$Gd(CH_3COO)_3 \cdot 4H_2O$				$Gd(CCl_3COO)_3 \cdot 3H_2O$			
78°		300°		78°		300°	
ν	Int.	ν	Int.	ν	Int.	ν	Int.
32059.8	10	32062.5	7	32077	0*wd*		
32070.9	10	32073.6	7	32088	0*d*		
32087.4	10	32087.9	7	32096	2*d*	32093	0*d*
32099.7	10	32098.2	7	32106′			
32643.9	10	32648.7	7	32112*c*	1*d*	32115	0*d*
32673.2	10	32673.6	7	32118′			
32698.4	10	32696.1	7	32124	0*d*		
35788.3	8	35792.0	8	32135	1*d*	32134	0*d*
35810.4	3	35813.4	3	32147	1*d*		
35824.4	8	35826.7	8	32152	1*d*		
35839.3	4	35840.5	4	32671	2*d*	32683	0*d*
36139.6	10	36143.4	10	32699	2*d*	32699	0*d*
36148.0	10	36151.1	10	32738	1*d*	32721	0*d*
36160.7	7	36162.8	7	35773	0*d*		
36171.8	9	36174.9	9	35797	1*d*		
36183.8	8	36185.0	7	35805	1*d*	35802′	
36205.5	7	36208.0	8	35812	4*d*	35810*c*	3*d*
36209.4	7	36212.2	8	35818	3*d*	35819′	
36215.2	7*D*	36217.3	8*M*	35828	1*d*	35837′	

TABLE I.—*Continued.*

$Gd(CH_3COO)_3 \cdot 4H_2O$				$Gd(CCl_3COO)_3 \cdot 3H_2O$			
78°		300°		78°		300°	
ν	Int.	ν	Int.	ν	Int.	ν	Int.
36220.0	7			35833	1*d*	35842′	3*d*
36223.7	7	36223.0	8	35842	4*wd*	35846′	
36228.8	7	36230.7	8	35868	1*d*		
36233.9	8	36237.4	8*D*	36133	1*d*		
36238.9	8			36148	3*d*	36148′	
36415.8	10*w*			36157	3*wd*	36153*c*	4*d*
36425.5	10*w*	36419.9	10*wd*	36165	3*wd*	36160′	
36432.3	10*w*	36431.7	10*D*	36173	3*wd*	36173	3*wd*
36440.9	10	36443.3	8	36182	1*d*		
36454.3	10	36456.6	9	36188	1*d*		
36464.2	10	36465.0	9*d*	36195	6*wd*	36192	3*wd*
36536.1	10*D*?	36539.4	8*wD*?	36208	1*d*		
36546.8	10*D*?	36549.9	8*wD*?	36212	1*d*		
36554.2	10	36559.0	8	36215′		36220′	
36566.4	10	36565.6′		36240*c*	6*d*	36241*c*	5*d*
36569.7′				36263′		36262′	
36582.8*c*	9	36582.2*c*	10	36407	1*d*		
36596.4′		36597.8′		36422	4*wd*	36420′	
36604.9	8	36605.5	8	36432′			
36616.7	8*w*			36440*c*	6*d*	36441*c*	3*d*
36623.1	8*w*	36620.8	10*D*	36448′			
39504.9	10*w*	39507.0	8	36458	6*wd*	36462′	
39517.3	10*w*	39518.2	8	36467	0*d*	36474′	
39538.4	10*w*	39538.2	8	36478	3*wd*	36486*c*	1*d*
39561.3	10*w*	39562.3	7*d*	36496	1*wd*	36496′	
39590.2	10*w*	39589.6	7*d*	36535	4*d*	36535′	
40468	3*D*	40562′		36544′			
40573	3	40573*c*	5*d*	36587*c*	5*d*	36595*c*	4*d*
		40580′		36630′			
40848	1*wd*	40851	3*wd*	36638	3*d*		
40874	1*wd*	40877	3*wd*	36646	3*d*		
40895	1*wd*	40898	3*wd*	36654	3*d*	36655′	
				36659	3*d*		

$Gd(COOH)_3$				$Gd(BrO_3)_3 \cdot 9H_2O$			
78°		300°		78°		300°	
ν	Int.	ν	Int.	ν	Int.	ν	Int.
32108.6	4	32106.4	7	32126.1	10	32132.2	5
32121.6	4	32119.7	4	32140.1	10	32145.7	6
32133.9	5	32133.5	8	32146.0	7	32152.6	8
32704.3	4	32702.6	5	32153.7	6	32157.3	8
32725.0	5	32723.1	6	32702.4	8	32708.7	8
35841.4	4	35843.3	3	32743.9	8	32749.1	7
35858.9	3	35861.3	3	32757.8	9	32761.0	7
35873.7	6	35873.0	4	35878.8	10*D*	35883.7	10
36186.3	4	36187.5	4	35888.2	4	35892	2
36200.1	3	36203.0	4	35898.8	6	35899.8	3
36215.7	7*wD*?	36216.2	6*wdD*?	36222.3′		36227.8	6
36259.0	6*w*	36261.1	7	36229.3*c*	10	36232.1	10
36264.7	1			36236.6′		36237.1	6
36269.3	1	36270.3	1	36244.2	6	36246.8	4
36278.6	4	36279.0	5	36284.4′		36290.2	7
36282.9	4	36283.0	5	36292.5*c*	5	36296.6	8
36463.0	3	36465.2	4	36300.4′		36300.2	7
36472.5	4	36475.9	5	36306.4	5	36305.9	5
36491.3	5*w*	36492.0	6*wD*?	36498′			
36500.2	1*w*	36500.7	1	36505*c*	3	36502	6
36583.7	4	36587.3	6	36511′		36511	7*D*?
36601.0	2	36603.5	3	36516	2	36519	7*D*?
36609.4	7*D*	36611.8	8*M*	36526	2	36527	3
36625.6	3	36627.5	6	36612′		36619′	
36643.8	7*D*	36645.4	8*D*	36621*c*	1	36627*c*	5
36653.6	1			36630′		36635′	
36656.8	1			36640	1*M*	36643	3*D*?
				36650′		36655	2
				36667*c*	1	36660′	
				36685′		36666*c*	3
						36672′	
						36681	1*D*?

TABLE I.—*Continued.*

$Gd(BrO_3)_3 \cdot 9H_2O$ 20°		$Gd(C_2H_5SO_4)_3 \cdot 9H_2O$ 20°					
ν	Int.	ν	Int.	ν	Int.	ν	Int.
32119.6	3	32135.3	1	35900.7	3	36516.5	5
32128.0	4	32153.2	3	36216.1	8	36519.8	5
32137.9	6	32163.0	8	36229.0	10	36528.5	4
32145.1	4	32714	0	36236.4	5	36608.8	7
32151.5	1	32727.2	4	36238.8	5	36618.9	7
32155.4	3	32758.5	4	36249.3	4	36628.2	7*M*
32702.8	6	32761.0	4	36291.7	10*wD*?	36641.5	7
32743.4	4	35873.9	4	36297.4	9	36646.9	8*wD*?
32758.5	4	35881.0	4	36491.0	8	36657.5	7
		35897.4	3	36508.2	10*wD*?	36668	6*wD*?
						36671.9	6
						36679.7	6
						36682.9	5

2500A multiplets

The lines of the chloride and sulfate are almost identical in spacing, spread, intensity and width, while the lines of the propionate and butyrate, though fuzzy, are nevertheless far sharper than the lines at 2700 and 3100A. The multiplet spread in the propionate and butyrate spectra is the same as that of the acetate—about three-fourths that of the chloride. The acetate lines are wider and more blurred than the lines of the chloride. Numerous attempts to obtain absorption bands in this region from gadolinium ethylsulfate have resulted in finding a single weak, wide, blurred line, which appears at 300° at 2458A.

Table I presents new data on the positions and intensities of the absorption lines and bands in the spectra of the various gadolinium compounds discussed, while in Figs. 1, 2 and 3, a number of the spectra are reproduced.

DISCUSSION

While the normal state of the Gd^{+++} ion in crystals is indubitably the virtually unperturbed $^8S_{7/2}$ term[10] the nature of the excited states is not known. They may arise through transitions in which all the 4*f* electrons remain within the completed 5*s*, 5*p* shells. In other words all the electrons are 4*f* electrons both in the initial and final states, and in any transitions between the states there is violation of Laporte's rule ($\Delta\Sigma l = 0$) which holds rather rigorously for dipole radiation by gaseous atoms. The rule can be violated if the atoms are strongly perturbed by an electric field not possessing a center of symmetry. Violation in the case of Gd^{+++} is unlikely because in a number of its salts, whose spectra have all the multiplets we are considering, there is definitely octahedral arrangement of the atoms closest to the Gd^{+++} ion, and with such an arrangement there is associated a cubic, centro-symmetric field.[11] By Pauli's principle the only octet term permitted Gd^{+++}, with its seven 4*f* electrons half completing the 4*f* shell, is the lowest one, $^8S_{7/2}$. All transitions involving only 4*f* electrons then require reversal of one or more of the electron spins. The possible terms resulting from such intercombination transitions are again limited by Pauli's principle to ^6P, ^6D, ^6F, ^6G, ^6H, ^6I, a larger number of quartets and a still larger

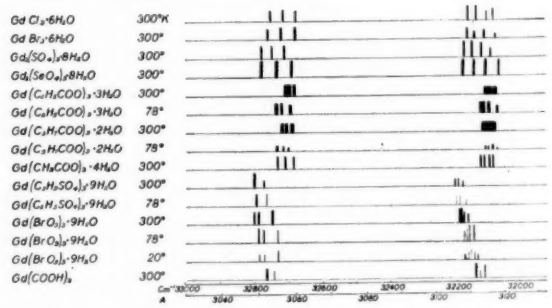

FIG. 1. The 3100A multiplets of the absorption spectra of gadolinium compounds.

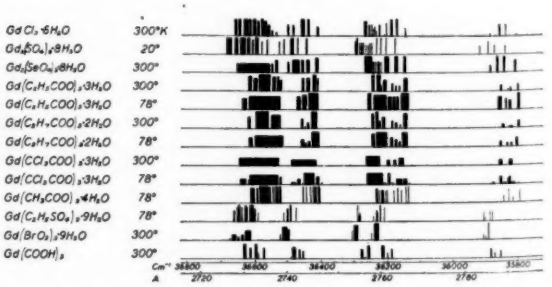

FIG. 2. The 2700A multiplets of the absorption spectra of gadolinium compounds.

[10] W. F. Giauque, J. Am. Chem. Soc. **49**, 1870 (1927).

[11] Phys. Rev. **50**, 574 (1936).

FIG. 3. Photographs of the spectra of gadolinium compounds. (a) Absorption and selective reflection in the 3000A multiplets of gadolinium ethylsulfate; (b) and (c) the 3000A multiplets of gadolinium chloride hexahydrate crystals and solution, respectively; (d) and (e) the 2700A multiplets of gadolinium chloride hexahydrate crystals and solution.

number of doublets. If the absorption multiplets of Gd^{+++} may be assigned to the jumps ${}^8S \rightarrow {}^6P$, ${}^8S \rightarrow {}^6D$, etc. (with the multiplet fine structure determined for the most part by the manner of crystal splitting of the upper state) then to account for the entire number of well-separated multiplets one must probably concede the likelihood of the breakdown of the selection rule $\Delta L = \pm 1$, or the reversal of two or three spins, producing octet-quartet and octet-doublet transitions, or both. Absorption in the principal multiplets is of comparable intensity and if one assumes octet-quartet jumps to explain their number one must make the unattractive premise that the frequency of occurrence of octet-sextet and octet-quartet transitions is about the same. To sum up, dipole radiation by Gd^{+++} requires violation of the three selection rules $\Delta \Sigma l = 0$, $\Delta S = 0$, $\Delta L = \pm 1$, and therefore is improbable. In quadrupole radiation the selections rules for $\Delta \Sigma l$, ΔS and ΔL are different, but the intensity of radiation is weak, perhaps too weak to account for the observed absorption by rare earth ions in crystals.

The upper states of Gd^{+++} may also arise from electron configurations in which one $4f$ electron has jumped through the complete shells to the $5d$, $5f$, $5g$ or higher orbits. The supposition often made that all the states outside $5s$, $5p$ are necessarily diffuse seems unwarranted. Sharp line spectra of a number of chromium and manganese salts have been observed.[12] The spectra arise from jumps of $3d$ electrons, which are outside completed shells and are presumably exposed to forces very similar to those acting on a $5d$ electron of a rare earth ion. Since sharp quantization is possible in both the upper and lower states of Cr^{+++} and Mn^{++}, it is reasonable that it should be possible also in the upper state of a rare earth ion, which may be closely analogous to the lower state of Cr^{+++} and Mn^{++}.

Magnetic evidence at present favors the idea that the transitions in Gd^{+++} are of the type $4f \rightarrow 5x$ for the g factors of the upper states are all either 0 or 2, again resembling Cr^{+++} and indicating that only the electron's spin moment orients in a magnetic field.[13] It is difficult to understand how the g is 0 or 2 for all the upper states if they originate in a $4f$ configuration, because the upper states should then be shielded to about the same extent as the normal state and should express their individualities by showing a

[12] F. H. Spedding and G. C. Nutting, J. Chem. Phys. **2**, 421 (1934), and unpublished data; J. Gielessen, Ann. d. Physik **22**, 537 (1935).

[13] In continuing the magnetic researches reported in the preliminary paper (F. H. Spedding, J. Chem. Phys. **1**, 144 (1933)) we have greatly improved the experimental technique so that polarized spectra could be studied. We have found that with a light path parallel to any principal axis the g factor of the upper state is either 2 or 0 (usually 2). While the second-order Zeeman effect is small in monoclinic crystals, it is fairly large in the hexagonal ones. Thus gadolinium salts behave like chromium salts (F. H. Spedding and G. C. Nutting, J. Chem. Phys. **3**, 369 (1935)) in that the orbital moments are not so tightly frozen if the crystals have a hexagonal axis of symmetry.

wide variety of g values. However, the g's of the sextet states are presumably very different from those calculated by Landé's equation for pure L–S coupling since the multiplets are very narrow. Ideally the multiplet width of the sextet terms of gadolinium would be zero since the $4f$ shell is just half completed.

We feel that at present the evidence for the various proposals as to the nature of the absorption process is inconclusive, with some points supporting the view that absorption is to be attributed to quadrupole radiation involving only $4f$ electrons, while others suggest jumps outside the $5p$ orbit. It appears highly probable from the experimental results which we have presented that all the lines of the multiplets of the inorganic salts and most of the lines of the organic salts arise from a crystal Stark splitting of lines in the spectrum of gaseous Gd^{+++} ion. If they originate in the superposition of intramolecular or lattice frequencies on electronic frequencies, one would expect some correlation between the masses of the ions and molecules associated with the gadolinium ions and the separations in the gadolinium absorption spectrum, yet none is observed. All the compounds which we have studied are either highly hydrated or else contain carboxyl groups, so it is likely that each gadolinium ion in the crystals has as its nearest neighbors a group of oxygen atoms. It may be argued that the presence of a shell of oxygen atoms would tend to mask the mass effect, but it should be pointed out that the oxygen atoms themselves are joined to various other atoms and that in some compounds this coupling is known from chemical evidence to be stronger, even, than the gadolinium—oxygen binding.

If the separations of the multiplet lines are identified with vibrations somewhere in the lattice most of the vibrational energies are of the order of a few tens of wave numbers. Harmonics and constant frequency differences between lines of different multiplets might well be expected (but are not found) and there should almost certainly be notable intensity changes with changing temperature. New absorption lines corresponding to jumps from higher and higher vibrational states should appear as the temperature is raised and the population of molecular groups in the higher states increases, but none are observed within the range 20° to 300°.

We have not yet been able to account satisfactorily for the excessive diffuseness of the spectra of all but the simplest of the organic compounds of gadolinium. Crystals of the substances are soft but are usually perfectly formed, and show no very obvious indication of possessing a vitreous or semivitreous structure. If they were glass-like the randomness of the atomic arrangement would presumably be expressed in the unusual breadth and lack of sharpness of the absorption lines of the rare earth ion. Diffuseness of the lines of a perfect crystal of a salt such as gadolinium butyrate would result if, as a result of oscillation or rotation somewhere in the alkyl group, the carboxyl oxygens which join the alkyl group to the gadolinium atom undergo a small, periodic displacement. The magnitude of the displacement would be much greater than that experienced by the oxygen of the water molecules in contact with the metal ion in highly solvated $GdCl_3 \cdot 6H_2O$, for example. We have shown that the fuzziness of the absorption of gadolinium propionate and butyrate persist in large measure even to temperatures as low as 20°K, so that if its origin is in motion of some part of the alkyl radical the energy producing that motion cannot be thermal. It might, however, be abstracted from the ultraviolet continuum with which the crystals were illuminated. None of the lower members of the series of fatty acids absorb in the region of the principal bands of gadolinium but all show absorption below 2500A. The intensity of absorption is greater in propionic and butyric than in formic and acetic acids. The principal part of the light energy absorbed probably goes to excite electrons of carbon, but associated with the electron jumps may be vibration of carbon against carbon, carbon against hydrogen, and so on. In a series of experiments lately completed we have photographed the absorption spectrum of perfect crystals of $Gd(C_2H_5COO)_3 \cdot 3H_2O$ using as source of light regions about 100A broad selected from the hydrogen continuum by means of a quartz monochromator. The temperature of the crystals was about 25°C. The line groups between 2700 and 2800A and at 3050 and 3100A were observed yet there was no sharpening of the lines over that

previously recorded when the light incident on the crystals contained all wave-lengths transmitted by quartz. When a Wollaston prism was placed between the crystal and the spectrograph, the lines were slightly sharper than before.

It has been known for a long time from Werner's work on complex salts and from transference experiments that the coordinated water molecules in the first shell about an ion in solution are probably fixed in number and position with respect to the central ion. Fig. 3, which shows spectra of a crystal and a solution of gadolinium chloride, gives further confirmation of this. The fact that in dilute solutions the multiplets are resolved into lines indicates that a field of definite symmetry is acting on the central ion. This means that the water molecules in the first shell about the central ion must be fixed in number and approximately in position, for if they were not and a condition of randomness existed, some atoms would have one type of splitting, other atoms another and the net result would be a blurred band, instead of discrete lines.

That the general order in solution is not as perfect as in solids is demonstrated by the fact that the lines are from two to seven times as broad as the corresponding lines in the solid crystalline salts which were used in preparing the solutions. The field about the ion in dilute solution is almost certainly determined by the closest water molecules, which probably are situated at the corners of an octahedron. This octahedron for a given atom is distorted more or less depending on the position of the water molecules in the second shell, and that considerable variation in distortion is present can be seen from the great width of the lines. Most of the distortion is probably due to the lack of order in the outer shells of the water envelope but some of it is undoubtedly due to thermal motion. At present we have no way of separating these factors.

It is interesting to note that the solution spectrum resembles the monoclinic type of crystal spectrum more than it does the hexagonal. Furthermore, in solution the negative ion does not approach very close to the gadolinium ion, since we could detect no deviation from Beer's law even for saturated solutions of the very soluble gadolinium chloride.

JANUARY, 1937 JOURNAL OF CHEMICAL PHYSICS VOLUME 5

Carbon Dioxide. The Heat Capacity and Vapor Pressure of the Solid. The Heat of Sublimation. Thermodynamic and Spectroscopic Values of the Entropy

W. F. GIAUQUE AND C. J. EGAN, *Department of Chemistry, University of California, Berkeley, California*

(Received October 17, 1936)

An apparatus for low temperature calorimetric and vapor pressure measurements on condensed gases is described. The heat capacity of solid carbon dioxide has been measured from 15 to 195°K. The heat of vaporization at the sublimation point, 194.67°K, was found to be 6030 cal./mole. The vapor pressure has been measured and the observations are closely represented by the equation: Solid carbon dioxide, 154−196°K; $\log_{10} P(\text{int. cm Hg}) = -(1354.210/T)+8.69903+0.0015880T-4.5107\times10^{-6}T^2$. The entropy of carbon dioxide gas has been calculated from the calorimetric data and the third law of thermodynamics to be 51.11 cal./deg. per mole at 298.1°K. This value is in excellent agreement with the value 51.07 cal./deg. per mole obtained from band spectrum data.

BECAUSE of the importance of carbon dioxide, it seems desirable that its thermodynamic properties should be investigated as accurately as possible. The fact that its band spectrum has been measured and very satisfactorily interpreted by several investigators offers an unusually good opportunity to compare the entropy obtained from the third law of thermodynamics with that obtained with the assistance of the spectroscopic data. The molecule is known to be of the linear symmetrical type. Thus there should be no possibility of encountering false equilibrium of the end for end random orientation type such as occurs in solid carbon monoxide, nitric oxide and nitrous oxide. Kelley[1] has shown that the available low

[1] Kelley, Bureau of Mines Bulletin, (a) **350**, 20 (1932); (b) **383**, 35 (1935).

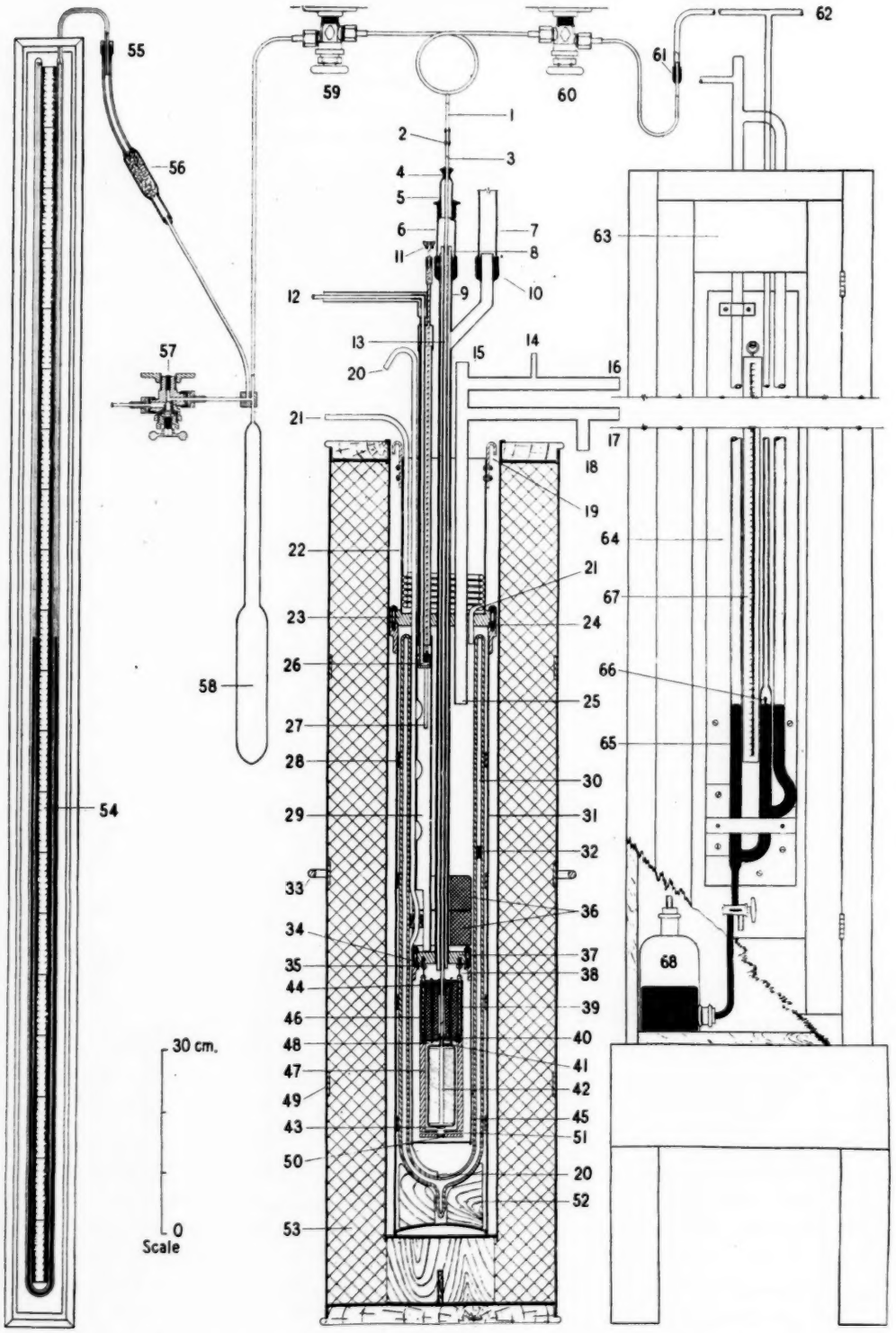

FIG. 1. Apparatus for low temperature calorimetry and vapor pressures of condensed gases.

DESCRIPTION OF FIG. 1. Apparatus for low temperature calorimetry and vapor pressures of condensed gases. 1. copper tubing; 2. cobalt glass seal; 3. soda glass tube; 4. De Khotinsky joint; 5. and 6. glass tubes; 7. glass line to vacuum system; 8. glass tubes containing heater leads and thermocouples; 9. German silver tube; 10. De Khotinsky joint; 11. valve handle; 12. vacuum jacketed transfer tube; 13. top of calorimeter tube heater; 14. tube for taking out thermocouple from bottom of container; 15. extra opening; 16. connection for rubber safety valve; 17. to vacuum pumps; 18. to low pressure hydrogen system; 19. hooks for raising apparatus; 20. tube for removing liquid in Dewar; 21. tube for introducing and precooling hydrogen gas; 22. monel cup for liquid air; 23. stainless steel disk; 24. ball-v type joint; 25. outlet tube; 26. valve in transfer tube; 27. end of transfer tube 12; 28. steel supporting rings in monel case; 29. fluted tube; 30. silvered, Pyrex Dewar; 31. monel case; 32. asbestos plug in Dewar; 33. handle on outer kapok case; 34. ball-v type joint; 35. hooks in upper part of container; 36. lead blocks; 37. upper part of container; 38. suspension cords for protective cylinder; 39. suspension pins screwed into lower part of protective cylinder; 40. cobalt glass seal; 41. platinum tube; 42. calorimeter; 43. thermocouple well; platinum tube filled with Rose metal; 44. Woods metal; 45. lower part of container; 46. upper half of protective cylinder; 47. lower half of protective cylinder; 48. calorimeter heater terminals; 49. reinforcing rings in outer case; 50. removable plug in protective cylinder; 51. holes through protective cylinder; 52. balsa wood block; 53. outer kapok filled case; 54. high pressure manometer; 55. De Khotinsky joint; 56. tube containing copper foil; 57. valve to preparation line; 58. steel bomb; 59. and 60. McKay valves; 61. De Khotinsky joint; 62. tube to vacuum system; 63. manometer case; 64. manometer for vapor pressure measurements; 65. tube used for leveling purposes; 66. manometer tube containing fixed point; 67. standard meter bar; 68. mercury reservoir.

temperature calorimetric data for carbon dioxide lead to a third law entropy value which is about one entropy unit larger than the value known from spectroscopic data. There was no evident reason for this discrepancy other than inaccuracies in the available data.

The apparatus used in this investigation is similar to that employed in the large number of published and as yet unpublished researches on condensed gases which have been completed in this laboratory. The apparatus has not previously been adequately described and we will therefore include a full description in this paper.

Four calorimeters, which either have been or are to be referred to in the literature as Gold Calorimeters I,[2a] II,[2] III and IV, have been built. Gold Calorimeter I was used in preliminary investigations and has been dismantled. Gold Calorimeter II was rebuilt[3] in 1932. While the following description applies particularly to the carbon dioxide experiments using Gold Calorimeter III, the other gold calorimeters differ only in minor particulars.

[2] (a) Giauque and Wiebe, J. Am. Chem. Soc. **50**, 101 (1928); (b) Giauque and Johnston, ibid. **51**, 2300 (1929).
[3] Blue and Giauque, J. Am. Chem. Soc. **57**, 991 (1935).

APPARATUS

The apparatus is shown in Fig. 1. The calorimeter, of laboratory designation Gold Calorimeter III, is represented at 42 in the diagram. It weighs 438 grams. The wall thickness is 0.1 cm. The height is 13.3 cm and the outside diameter 4.04 cm. 12 radial vanes, 0.2 cm thick and of length 12.5 cm, are welded on the inside wall of the calorimeter in order to facilitate the conduction of heat to the condensed gas. The carbon dioxide was introduced through a soda glass tube, 3, of inside diameter 0.2 cm, which is connected by means of a cobalt glass seal, 40, to a short platinum tube, 41, extending from the top of the calorimeter. The glass inlet tube is closely wound from the point, 13, to within 1 cm of the cobalt seal with a double silk covered B. and S. gauge number 30 constantan wire heater, which is used to aid in the removal of any gas condensed in the tube. The heater was painted with Bakelite varnish. Copper lead wires are taken off the heater at 10 cm intervals. The several leads from the tube heater could be used as thermocouples.

With the exception of 0.5 cm at each end, the outside of the calorimeter is roughened and covered with thin lens paper and is wound with number 40 double silk covered gold wire, which serves as a resistance thermometer heater. Both the lens paper and wire were painted with Bakelite varnish, and the calorimeter was baked at 120° for about 15 hours. 0.175 percent of silver was added to the gold to increase its resistance at the lower temperatures, since in this region pure gold is unsatisfactory as a heater. At each end, and about the middle of the thermometer, a copper lead wire of size B. and S. number 30 is attached. Each lead wire is joined to a thermometer terminal, 48, by one inch of B. and S. number 40 copper wire. The amount of stretching of the calorimeter when subjected to a pressure of 100 lbs. per square inch was calculated to determine if the resistance thermometer would be appreciably strained. The change in the diameter was only 0.0006 cm, which would not injure the thermometer.

A copper-constantan thermocouple, of laboratory designation W-25, is attached to the calorimeter by inserting it in a platinum tube filled with Rose metal, 43. The platinum tube is welded to the bottom of the calorimeter. Another thermocouple of laboratory designation, W-28, is attached in the same way to the top. 63 cm of each thermocouple are below the top of a protective cylinder, 46. 50 cm are wrapped around the calorimeter. This serves to eliminate the possibility of thermal gradients near the junction.

The calorimeter is suspended by the glass tube, which is fastened to and brought into good thermal contact with the protective cylinder by means of Woods metal, 44. The protective cylinder is a massive block of metal which provides a constant temperature environment at any desired temperature. The upper half, 46, rests on the lower part, 47, by means of a ground, tapered copper joint, 1 cm in length and cut at an angle of 4° from the vertical. This type of connection assures good thermal contact at all temperatures. The lower part is suspended by the pins, 39, which are connected by means of stout cord, 38, to the hooks, 35, in the top of the container, 37. The upper part of the protective cylinder consists of 3700 g of lead and copper, the lower part, 2500 g of copper. Eight radial holes, 51, in the lower part of the protective cylinder, allow the space around the calorimeter to be evacuated. A plug, 50, in the bottom can be removed in order to center the calorimeter during the assembling of the apparatus. Both parts of the protective cylinder are wrapped with No. 30 B. and S. gauge double silk covered heater wire which is brought into good thermal contact by means of Bakelite lacquer. The heater is covered with a sheath of copper foil to reduce heat radiation between the protective cylinder and its surroundings. At room temperature, the resistance of the heater on the upper part of the cylinder is 216 ohms and the resistance of that on the lower part is 311 ohms. Two thermocouples, one on the upper part and one on the lower part, assure that the temperature of the protective cylinder is uniform.

The lower part of the container, 45, made from monel metal and stainless steel, is attached to the top of the container by means of a stainless steel ball-v type joint, 34, which can be made vacuum tight. The temperatures of the top, 37, and bottom, 45, of the container are obtained from two thermocouples.

The container, 37, is supported by means of a German silver tube, 9, attached to the upper part of a large stainless steel and monel Dewar case, 23 and 31. Inside this tube are three glass tubes, 8, containing the heater and thermocouple wires, which are taken out through De Khotinsky cement between the two glass tubes, 5 and 6. Similarly, the glass calorimeter tube and the leads from the tube heater are taken out at 4.

Two lead blocks, 36, are on the top of the container to increase the heat capacity. The space above is filled with narrow strips of copper foil, which act as a baffle to prevent the spraying of liquid hydrogen.

The apparatus is suspended inside a highly evacuated, silvered, Pyrex Dewar, 30, which is supported by a balsa wood block, 52, inside the lower part of the large monel case, 31. The upper part of the case consists of a monel cup, 22, and a stainless steel disk, 23, to which are soldered the various metal tubes entering the apparatus. The upper and lower parts are connected by another stainless steel ball-v type joint, 24. The point, 32, represents three asbestos plugs between the walls of the Dewar, while the point, 28, indicates steel supporting rings inside the monel case.

Liquid air or liquid hydrogen is introduced through the vacuum-jacketed, German silver transfer tube, 12. A fluted tube, 29, prevents splashing of the liquid air or liquid hydrogen entering at 27. A valve, 26, operated at 11, allows the cooling liquid to be admitted when there is reduced pressure inside the monel case.

The vaporized air or hydrogen leaves the apparatus through tube 25, the ends of which are connected as follows: 18 leads to the low pressure storage tank for hydrogen gas; 17 is connected to a high capacity pumping line for cooling the apparatus under reduced pressure; 16 is either open to the atmosphere or is closed off by a rubber safety valve; 14 is the exit for the thermocouple from the bottom of the container; 15, being an extra outlet, is closed by a clamped rubber tube.

Any cooling liquid in the apparatus can be forced out from the bottom of the Dewar through tube 20. It is important to be able to do this; for example, when the apparatus is to be cooled to the temperatures of liquid hydrogen, it is precooled with liquid air, which must be completely removed before the liquid hydrogen is introduced. Considerable economy in the use of liquid hydrogen can be obtained by cooling the apparatus to between 50 and 60°K by boiling liquid air under reduced pressure. Excess liquid air is then forced out through tube 20 by means of a small pressure of hydrogen gas. This hydrogen is precooled by passing it through a coil of copper tubing, 21, immersed in liquid air in the monel cup, 22.

The whole apparatus is inside a large air-tight jacket, 53, which is filled with kapok insulator. The hooks, 19, were attached to a lifting device when the apparatus was raised during assembly.

The glass tube from the calorimeter is connected just above the apparatus by means of a second cobalt glass to platinum seal, 2, to a copper tube, 1, thereby decreasing the amount of glass in the line. This was desirable when the apparatus was used for carbon dioxide since, as mentioned above, the gas was condensed at a pressure of about seven atmospheres.

One end of a T joint in the copper line leads through the valve, 59, to a 485 cc steel bomb, 58, and to a U-shaped, high pressure, mercury manometer, 54, which is sealed off on one side. The manometer is 200 cm high and is made of capillary glass tubing of 0.2 cm bore and 0.4 cm wall. The capillary tubing is connected to a steel tube at 55 with De Khotinsky cement. Copper foil was placed in the tube at 56 to prevent mercury vapor from reaching the gold calorimeter. The valve, 57, leads to the preparation line.

The other end of the copper line leads through valve 60 and the De Khotinsky joint, 61, to the manometer, 64, which was used for the vapor pressure measurements. The manometer tubing is 1.6 cm i.d. The standard meter bar, 67, is suspended between the glass tubes, 66 and 65, the latter being used as a leveling tube. The complete manometer is mounted in a case kept at uniform temperature by a stream of air.

Temperature Scale

Before the apparatus was assembled, thermocouple W-25 was compared with seven other thermocouples, including couple W-22, from 14 to 300°K in a comparison apparatus similar to that used by Giauque, Buffington and Schulze.[4] Couple W-22 was then put in the gas thermometer apparatus described in the above reference. The thermometer bulb was filled with helium gas and the measurements were made from 15 to 300°K in a manner similar to that of Giauque, Buffington and Schulze. The data of Henning[5] were used for correcting the helium scale to the thermodynamic scale. The temperature of the ice point on the thermodynamic scale was assumed to be 273.10°K, in conformity with the value given in the *International Critical Tables*.[6] Some of the other thermocouples have since been compared with hydrogen and oxygen vapor pressures under the same conditions of their calibration in the gas thermometer, and with the melting point of mercury and the transition point of sodium sulfate under somewhat different conditions. In all cases the agreement is within the limit of accuracy claimed, namely, 0.05°.

Preparation of Carbon Dioxide

The carbon dioxide was prepared from Merck's reagent quality sodium bicarbonate. The dry powder was heated to 200°C in a six-liter flask. All connections were made of glass, the preparation line being similar to that described by Meyers and Van Dusen.[7] The carbon dioxide was passed through a water-cooled condenser and then through 5 tubes, 30 cm long, the first two containing C.P. calcium chloride, and the last three phosphorus pentoxide to remove the last traces of water. The whole system was evacuated to a pressure of 0.01 mm of mercury and flushed for one hour with carbon dioxide. The gas was condensed in liquid air and sublimed from one bulb to another several times. After each transfer, any foreign gas which may have

[4] Giauque, Buffington and Schulze, J. Am. Chem. Soc. **49**, 2343 (1927).
[5] Henning, Zeits. f. ges. Kälte-Ind. **37**, 169 (1930).
[6] *International Critical Tables* (McGraw-Hill Book Co., New York, 1926), Vol. I.
[7] Meyers and Van Dusen, Nat. Bur. Stand. J. Research **10**, 381 (1933).

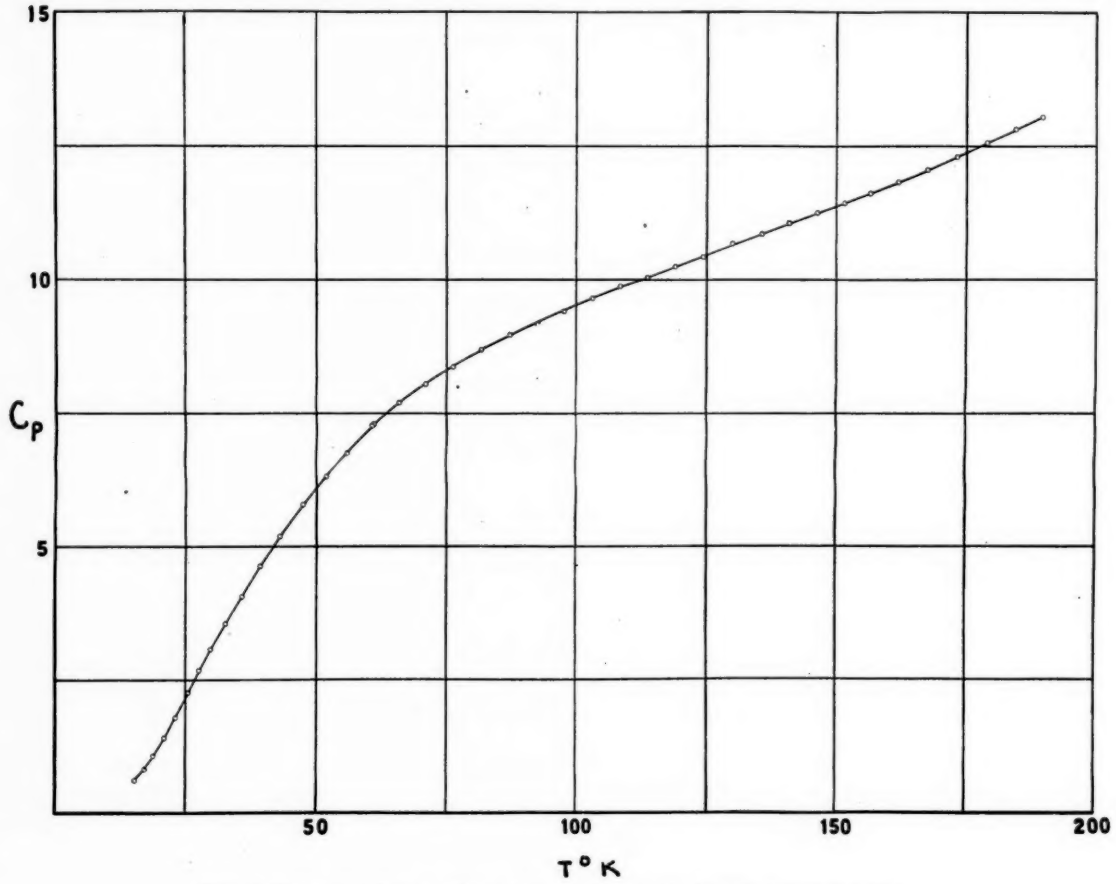

FIG. 2. Heat capacity of solid carbon dioxide in calories per degree per mole.

been previously occluded in the crystals was pumped out. The carbon dioxide was then sublimed into the bomb described previously.

By means of metal valves, the glass line could be shut off from the copper line. The carbon dioxide was allowed to melt in the bomb and the pressure was followed by reading the closed-end manometer. The liquid was frozen again and pumped to remove any gas which may have been previously occluded. The only probable impurity was a trace of air occluded in the sodium

TABLE I. *Vapor pressure of solid carbon dioxide (0°C=273.10°K).*

T, °K	P in cm Observed	P obs.− P calc.	T obs.− T calc.
154.196	1.132	−0.001	+0.006
158.403	1.940	− .002	+ .008
162.597	3.221	− .010	+ .025
166.704	5.186	− .002	+ .003
170.691	8.039	+ .004	− .004
174.688	12.220	+ .013	− .010
178.569	17.994	+ .002	− .001
182.333	25.785	− .007	+ .003
187.356	40.718	− .040	+ .010
192.663	64.336	− .028	+ .005
194.982	77.962	− .001	+ .000
195.831	83.530	+ .002	− .000

TABLE II. *Normal sublimation temperature of carbon dioxide (0°C=273.10°K).*

Observer	T, °K
Siemens[10] (1913)	194.65
Henning and Stock[9] (1921)	194.58
Heuse and Otto[11] (1931)	194.645
This Research	194.67

TABLE III. *Comparison of temperatures from vapor pressure equations of other observers.*

T, °K	$T_{\text{This Research}} - T_{\text{H. and S.}}$	$T_{\text{This Research}} - T_{\text{Siemens}}$
165	+0.10	+0.03
175	+ .12	+ .11
185	+ .09	+ .14
190	+ .09	+ .10
195	+ .09	+ .02

bicarbonate, and this should have been removed by the above procedure.

The copper line was then opened to the calorimeter, which was at 227°K, 10° above the triple point. The protective cylinder was 5° above the triple point, with one atmosphere pressure of air between the calorimeter and the protective cylinder in order to reduce the excess of pressure inside the calorimeter and to conduct away the heat of condensation. The carbon dioxide in the steel bomb was allowed to warm until the gas was liquefying in the calorimeter at a steady state with the pressure about seven atmospheres. Under these conditions, 15 hours were required to fill the calorimeter.

Vapor Pressure

The vapor pressure of the solid was measured by means of a Gaertner cathetometer, with a precision of 0.02 mm, used as a comparison instrument in connection with the standard meter mentioned above. The observations have been represented by the following equation: Solid carbon dioxide, 154 to 196°K;

$$\log_{10} P(\text{int. cm Hg}) = -(1354.210/T) + 8.69903 + 0.0015880T - 4.5107\times10^{-6}T^2. \quad (1)$$

The observed and calculated values are compared in Table I. The temperatures have been given to 0.001 degree because of the high relative accuracy. The absolute temperatures may be in error by several hundredths of a degree. The pressures are corrected to International cm of mercury by means of data given in the International Critical Tables.[6] The standard acceleration of gravity was taken as 980.665 cm/sec.^{2}. The gravitational acceleration, 979.973 cm/sec.^{2}, has been determined for this location.[8] From Eq. (1) the temperature of the normal sublimation point on the thermodynamic temperature scale was found to be 194.67±0.05°K (0°C = 273.10°K).

The previous vapor pressure measurements of carbon dioxide have been reviewed recently by Meyers and Van Dusen.[7] The more recent values of the normal sublimation temperature are given in Table II. Table III is a comparison of the temperatures calculated from the vapor pressure equations of this research, of Henning and Stock,[9] and of Siemens.[10] The different values used for the ice point on the Kelvin scale have been considered in preparing Tables II and III. The best value in Table II is probably that of Heuse and Otto.[11]

Heat Capacities

The heat capacities were measured by the method described in detail by Giauque, Wiebe

[8] Sternewarte, Landolt, Bornstein and Roth, *Physikalisch Chemische Tabellen* (Verlag Julius Springer, Berlin, 1923).
[9] Henning and Stock, Zeits. f. Physik **4**, 226 (1921).
[10] Siemens, Ann. d. Physik **42**, 871 (1913).
[11] Heuse and Otto, Ann. d. Physik **9**, 486 (1931); **14**, 181 (1932).

TABLE IV. *Heat capacity of solid carbon dioxide (molecular weight, 44.00) (0°C = 273.10°K).*

T, °K	Approx. ΔT	C_p cal./deg./mole	T, °K	Approx. ΔT	C_p cal./deg./mole
15.52	1.7	0.606	87.45	5.3	8.984
17.30	1.7	0.825	92.71	5.0	9.189
19.05	1.6	1.081	97.93	5.2	9.421
21.15	1.6	1.419	103.26	5.3	9.671
23.25	2.5	1.791	108.56	5.1	9.893
25.64	2.2	2.266	113.91	5.4	10.07
27.72	1.9	2.676	119.24	5.1	10.27
29.92	2.6	3.069	124.58	5.3	10.44
32.79	3.2	3.555	130.18	5.5	10.69
35.99	3.2	4.063	135.74	5.2	10.88
39.43	2.9	4.603	141.14	5.1	11.08
43.19	4.4	5.195	146.48	5.2	11.27
47.62	4.3	5.794	151.67	4.6	11.45
52.11	4.0	6.326	156.72	4.9	11.64
56.17	4.4	6.765	162.00	5.2	11.84
60.86	4.7	7.269	167.62	5.3	12.07
61.26	5.2	7.302	173.36	5.4	12.32
66.24	4.7	7.707	179.12	5.2	12.57
71.22	5.2	8.047	184.58	4.7	12.82
76.47	5.2	8.370	189.78	4.7	13.05
81.94	5.7	8.703			

TABLE V. *Heat capacity of solid carbon dioxide (molecular weight 44.00). Values taken from a smooth curve through observations.*

T, °K	C_p cal./deg./mole	DEVIATION E., E. AND H. − THIS RESEARCH, %	DEVIATION M. AND B. − THIS RESEARCH, %
15	0.540		
20	1.225	−3.0	
25	2.137	−3.7	
30	3.093	−2.0	
35	3.912	0.0	
40	4.690	2.7	
45	5.435	3.6	
50	6.095		
60	7.178		
70	7.972		
80	8.582	2.9	
90	9.105	3.2	
100	9.530	3.0	
110	9.915	4.1	
120	10.30	4.3	
130	10.67	4.1	
140	11.04	3.4	
150	11.39	2.8	
160	11.77	1.7	
170	12.17	0.3	1.6
180	12.61	−0.8	3.3
190	13.07	−1.5	5.8

and Johnston.[2] In calculating energy, 1.0004 absolute joules were taken equal to 1 International joule and 4.185 absolute joules were taken equal to 1 calorie (15°). The accuracy was ±0.2 percent from 35 to 195°K, ±1 percent at 20°K, and ±3 percent at 15°K. 2.3 cm pressure of helium was admitted to the calorimeter at 59°K before the measurements were made, in order to assure heat conduction at low temperatures.

The amount of carbon dioxide, 3.618 moles, was determined by measuring the increase in weight of an absorption bulb containing 40 percent potassium hydroxide solution.

The measured heat capacities are shown in Fig. 2 and in Tables IV and V. Table V shows values picked from a smooth curve through the observations. They are compared with those of Eucken,[12] Eucken and Hauck,[13] and Maas and Barnes.[14]

HEAT OF SUBLIMATION

During the measurement of the heat of sublimation, energy was introduced only by the lower half of the gold resistance thermometer-heater. Only a small portion of the total amount of carbon dioxide in the calorimeter was sublimed during the measurements. Thus the gas leaving the calorimeter was forced to pass along narrow channels between the upper portion of the solidified gas and the vanes or outer wall of the calorimeter. The above conditions insured that the amount of superheating of the gas did not decrease the accuracy of the measurements.

The method used in measuring heats of sublimation was similar to the method of measuring heats of vaporization used in this laboratory. The energy was started into the calorimeter, which was at the normal sublimation temperature, and a few seconds later a stopcock was opened which allowed the carbon dioxide to bubble through a mercury trap in the bottom of an absorption bulb containing 40 percent KOH solution. The bubbles were made to pass through a spiral tube as they moved upward in the solution. This tube increased the length of path and decreased the speed of the bubbles, thereby assuring complete absorption of the gas.

The thermocouple on the top of the calorimeter was compared with thermocouple W-25, on the bottom, before the measurements, and was read during the time of energy input to determine if the gas leaving the calorimeter was at the temperature of the solid carbon dioxide. Other experimenters have encountered difficulty in eliminating this superheating. Table VI shows the small temperature difference and also the correction applied to the heat of sublimation.

TABLE VI. *Corrections for superheating during measurements of heat of sublimation.*

MEASUREMENT NUMBER	TEMP. GAS − TEMP. SOLID	CORRECTION IN CAL./MOLE
1	0.02°	0.2
2	0.11°	0.9
3	0.20°	1.6

TABLE VII. *Heat of sublimation of carbon dioxide. Sublimation temp., 194.67°K.* (0°C = 273.10°K.)

NO. MOLES SUBLIMED	TIME OF ENERGY INPUT	ΔH AT 760 mm cal./mole
0.47154	200 MIN.	6028
0.23423	100 MIN.	6031
0.23466	100 MIN.	6032
		MEAN 6030±5

[12] Eucken, Verh. Deut. phys. Gesell. **18**, 4 (1916).
[13] Eucken and Hauck, Zeits. f. physik. Chemie **134**, 161 (1928).
[14] Maas and Barnes, Proc. Roy. Soc. London **A111**, 224 (1926).

TABLE VIII. *Calculation of normal heat of sublimation from the data of Eucken and Donath.*

	$T=140°K$	$T=170°K$
ΔH_T (SUBLIMATION) E. AND D.	6334	6190 cal./mole
$\int_{P_{\text{sublimation}}}^{P=0} (\partial H/\partial P)_T dP$	0.1	3.2
(Berthelot gas at $T_{\text{sublimation}}$)		
$\int_{T_{\text{sub.}}}^{T=194.67°K} (Cp_{\text{ideal gas}} - Cp_{\text{solid}})dT$	−256.5	−127.9
$\int_{P=0}^{P=1} (\partial H/\partial P)_T dP$	− 25.0	− 25.0
(Berthelot gas at 194.67°K)		
DATA OF EUCKEN AND DONATH CALCULATED TO 194.67°K	6053	6040 cal./mole

TABLE IX. *Heat of sublimation of carbon dioxide at 1 atmosphere.* ($T=194.67°K$.)

ΔH (at 760 mm Hg) in cal./mole	OBSERVERS	
6205	ANDREWS[16] (1925)	
6024	MAAS AND BARNES[14] (1926)	
6047	EUCKEN AND DONATH[15] (1926)	
6029	FROM VAPOR PRESSURES	THIS RESEARCH
6030±5	CALORIMETRIC	THIS RESEARCH

The results are summarized in Table VII. Table IX contains a summary of recent measurements of the heat of sublimation. The value given for Eucken and Donath[15] is based on their measurements at 140 and 170°K. Our calculation of the corresponding value at 194.67°K from their data is summarized in Table VIII. In the correction for gas imperfection the thermodynamic equation $(\partial H/\partial P)_T = V - T(\partial V/\partial T)_P$ has been combined with Berthelot's equation

$$PV = RT\left[1 + \frac{9PT_c}{128P_cT}\left(1 - 6\frac{T_c^2}{T^2}\right)\right],$$

$T_c = 304.1°K$,[6] $P_c = 72.8$ atmos.[6]

From which

$$\int_{P_1}^{P_2}\left(\frac{\partial H}{\partial P}\right)_T dP = \frac{9}{128}\frac{RT_c}{P_c}\left(1 - 18\frac{T_c^2}{T^2}\right)(P_2 - P_1).$$

The change of heat content of the ideal gas was obtained from spectroscopic constants to be given later.

The value of 6029 cal./mole for the heat of sublimation was obtained using vapor pressure Eq. (1) and Berthelot's equation. Although the agreement is excellent, the calculation using the vapor pressure data included a Berthelot gas imperfection correction of −127 cal./mole. Thus we can give this value no weight in comparison with the direct calorimetric observation.

[15] Eucken and Donath, Zeits. f. physik. Chemie **124**, 181 (1926).
[16] Andrews, J. Am. Chem. Soc. **47**, 1597 (1925).

TABLE X. *Entropy of carbon dioxide from calorimetric data.*

0–15°K, DEBYE EXTRAPOLATION ($h\nu/k$) = 140	0.190
15–194.67°K, GRAPHICAL	16.33
SUBLIMATION 6030/194.67	30.98
ENTROPY OF ACTUAL GAS AT NORMAL SUBLIMATION TEMPERATURE	47.50±0.10
CORRECTION FOR GAS IMPERFECTION	.09
ENTROPY OF IDEAL GAS AT 1 ATMOS. AND 194.67°K.	47.59 cal./deg. per mole

TABLE XI. *Entropy of carbon dioxide from spectroscopic data.*

	$T=194.67°K$	$T=298.10°K$
$S_{\text{trans.}} = 3/2\,R\ln M + 5/2\ln T - R\ln P - 2.300$	35.161	37.279
$S_{\text{rot.}} = R\ln IT - R\ln\sigma + 177.676$	12.215	13.062
$S_{\text{vib.}} = R\ln Q_{\text{vib.}} + RT\frac{d\ln Q_{\text{vib.}}}{dT}$	0.175	0.725
TOTAL ENTROPY IN cal./deg. per mole	47.55	51.07

TABLE XII. *Comparison of experimental and spectroscopic values for the entropy of carbon dioxide.*

T, °K	SPECTROSCOPIC	EXPERIMENTAL
194.67	47.55	47.59 cal./deg.
298.10	51.07	51.11

THE ENTROPY FROM CALORIMETRIC DATA

A summary of the entropy calculation from the calorimetric data is given in Table X. A small correction for gas imperfection was made by combining Berthelot's equation of state with the thermodynamic equation $(\partial S/\partial P)_T = -(\partial V/\partial T)_P$, giving

$$S_{\text{ideal}} - S_{\text{actual}} = (27RT_c^3P)/(32T^3P_c) = 0.09 \text{ cal./deg. per mole.}$$

Comparison of the Entropy Values from Calorimetric and Spectroscopic Data

The entropy of carbon dioxide gas was calculated from the available band spectrum data on this substance. Adel and Dennison[17] have given a classified summary of the observations. They have also derived equations for calculating the possible vibrational levels of the molecule. The moment of inertia in the normal state was taken to be 70.1×10^{-40} g cm^2.

The entropy calculation has been given in detail in Table XI. The symmetry number σ is 2. The vibrational entropy was calculated by means of the state sum, $Q_{\text{vib.}}=\sum_v p_v e^{-\epsilon_v/kT}$, where p_v and ϵ_v are the *a priori* weight and energy of the vth state. The values of all natural constants used here are those given in the I.C.T.[6]

The entropy at 298.1°K has also been calculated by Badger and Woo[18] and by Gordon and Barnes.[19] These authors obtain the values 51.07 and 51.09 cal./deg. mole, respectively.

The calorimetric and spectroscopic values of the entropy have been compared in Table XII. The experimental value given at 298.1°K was obtained by using the spectroscopic data to calculate the entropy change of the gas between 194.67 and 298.1°K.

It is evident from Table XII that the entropy obtained from the third law of thermodynamics and the experimental data is in excellent agreement with that calculated from statistics and band spectrum data.

[17] Adel and Dennison, Phys. Rev. **43**, 716 (1933); **44**, 99 (1933).

[18] Badger and Woo, J. Am. Chem. Soc. **54**, 3523 (1932).
[19] Gordon and Barnes, J. Chem. Phys. **1**, 308 (1933).

JANUARY, 1937 JOURNAL OF CHEMICAL PHYSICS VOLUME 5

The Transfer of Energy in Molecular Systems[1]

HAROLD GERSHINOWITZ, *Mallinckrodt Chemical Laboratory, Harvard University, Cambridge, Massachusetts*

(Received October 14, 1936)

A method of investigating problems of energy transfer, by means of potential energy surfaces, outlined in an earlier paper, has been extended to include a more general type of surface. The probability of energy transfer among atoms has been related with the rate of change of curvature of the equipotential lines. It has been shown that the relative reactivity of atoms depends on the degree of excitation of the system. An explanation has been suggested for the discrepancy existing between the data on the relative efficiencies of the inert gases as obtained from sound dispersion experiments and from reaction rate measurements.

I

IN a recent communication, hereafter called (I),[2] a technique was developed that seems to be applicable to the study of the transfer of energy. A complete calculation of the rate of combination of hydrogen atoms to form molecules was carried out by means of a potential energy surface. Since the problem is essentially one of energy transfer, the rate determining factor being the probability that some of the relative translational energy of two atoms will be removed by a third body before the atoms separate, it was possible to make some qualitative deductions concerning the more general problem of energy transfer. These were given only briefly in (I), since it was only indirectly concerned with this problem. This paper elaborates on them and gives some further extensions of the method.

It has long been obvious that classical mechanics alone can help us but little in the problem of calculating theoretically the mechanism and probability of the transfer of energy among the degrees of freedom of a system. The transfer of energy is essentially a quantum phenomenon, and the characteristics of molecules considered as hard spheres, or even as ensembles of classical oscillators, give little information about the

[1] Presented at the group symposium on Quantum Mechanics and Chemical Kinetics at the Pittsburgh meeting of the A. C. S.
[2] Eyring, Gershinowitz and Sun, J. Chem. Phys. **3**, 786 (1935).

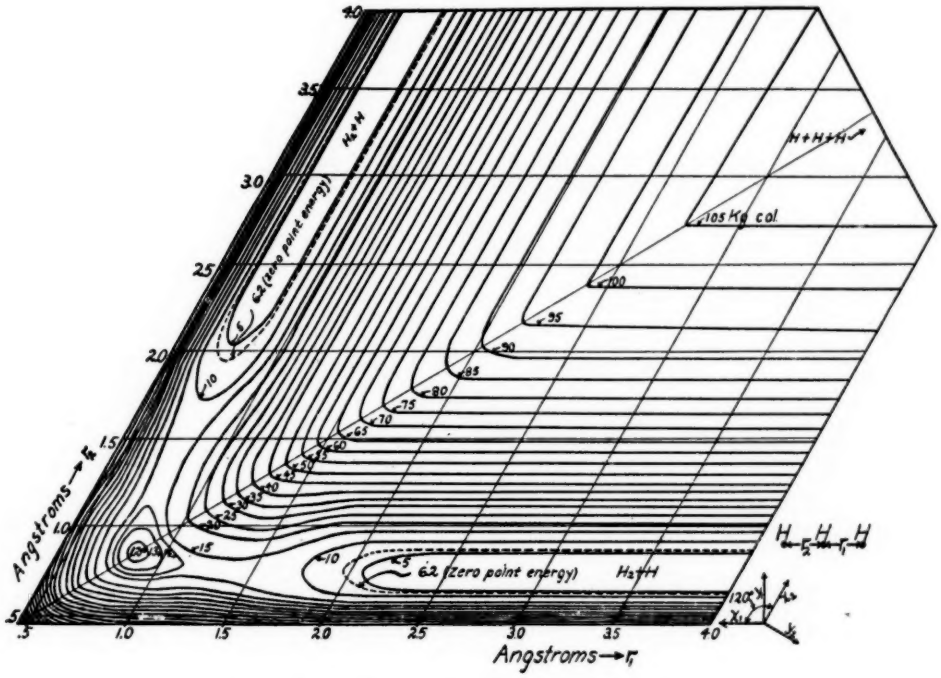

FIG. 1. Energy contour map of linear H_3 molecule.

behavior of actual molecules. It is possible, however, to use many of the laws of classical mechanics to good advantage in these problems, provided that we also take care of the quantized nature of the phenomena. A considerable amount of work has been done in the application of quantum mechanics to energy transfer, making use of the perturbation theory applied to the Schrödinger equation for the system.[3] This work has not been too successful, however. The difficulty is one that always arises when one attempts to apply rigorous quantum mechanics to chemical problems, i.e., the practical impossibility of solving the mathematical equations that one gets. Before any results are obtained it is necessary so to simplify the problem that it is doubtful that the conclusions apply to any actual experiments. But while the actual numerical results are of doubtful validity, the qualitative conclusions seem to be quite trustworthy, and have been of great value in the interpretation of experimental data. Because of the mathematical difficulties, it seems doubtful that many more valuable results can be obtained by these methods at the present time.

[3] (a) Zener, Phys. Rev. **37**, 556 (1931); (b) O. K. Rice, J. Am. Chem. Soc. **54**, 4558 (1932); (c) Rosen, J. Chem. Phys. **1**, 319 (1933).

In (I) it was shown that transfer of energy, and hence reaction, took place when the mass point that represented the system traveled across a ridge that separated the potential energy surface into two regions, in each of which a different set of coordinates was the normal set. The calculation of the probability of energy transfer then became a straightforward problem of statistical mechanics. This method of employing potential energy surfaces to represent the quantum character of the potential fields and then using classical mechanics to determine the motion of the nuclei in these fields affords a convenient semi-empirical approach to the problem of energy transfer.

In (I) it was shown that the greatest probability of reaction occurs when the three atoms involved lie on the same straight line; that the transverse vibrational degrees of freedom may be separated from the motions along the line to good approximation; and that the rotation of the system can be considered as adding another term to the expression for the potential energy of the system. In view of these results, in the following we shall concern ourselves only with the two degrees of freedom representing the relative motions of the three atoms along a straight line.

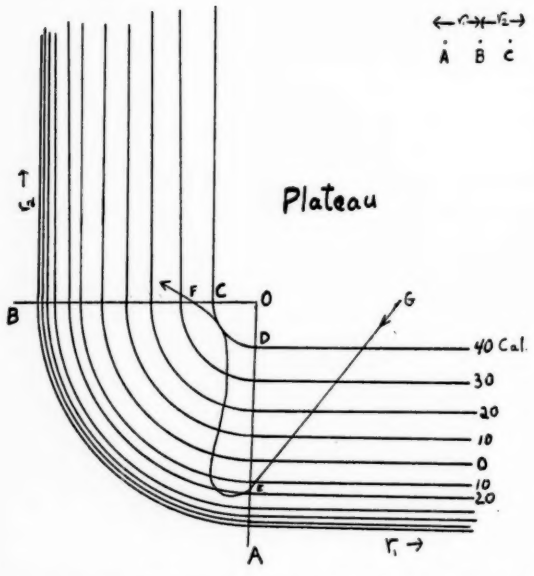

FIG. 2. Portion of potential energy surface for three collinear atoms.*

The results may be expected to hold for all cases except those for which the total and relative angular momenta are very large. Since most of the atoms concerned in the processes to be discussed have kinetic theory velocities, this exception is not of importance.

II

In the cases treated in (I), the ruled regions of the surface were separated by a straight line along a ridge (see Fig. 1). Since this represents a very special case, let us consider the situation in cases in which there is a curved region separating the parts of the surface which are ruled in terms of rectangular coordinates, assuming that the curve is the arc of a circle (Fig. 2). In such a region, in which the potential field is centrally symmetrical, the angular momentum $M=\mu r^2\dot{\theta}$ must be conserved, where μ is the reduced mass, r the distance from the center of curvature 0, and $\dot{\theta}$ is the angular velocity. Since the total energy must also be conserved, while the mass point remains in the curved region, energy will be transferred between the r and the θ directions. The amount of energy transferred will depend upon the phase relationships at the points at which the mass point that represents the system enters and leaves the curved region. These relationships will have to be determined individually for each specific case that is treated. We shall examine briefly a qualitative solution, in order to find out something about the determining factors.

Fig. 2 represents a portion of a potential energy surface for a hypothetical system of three atoms. r_1 is the distance between B and C, and r_2 the distance between atoms A and B. If r_1 and r_2 were used as the coordinates, they would not be perpendicular to each other, but at an angle determined by the masses of the atoms. K is a function of the masses which compensates for this fact by introducing a different scale for distances along the ordinate and abscissa, while permitting the use of rectangular coordinates.[4] As in Fig. 1, each of the two valleys represents the existence of a diatomic molecule and an atom, while the plateau to the north-east represents three separate atoms. The formation of a diatomic molecule corresponds to the passage of the mass point representing the triatomic system from the plateau into the valley without returning to the plateau. Any particle which leaves the plateau and does not enter the curved region must necessarily return to the plateau, since it is not possible for energy to be transferred between the directions normal to and along the valley. In the circular part of the valley, the angular momentum, $M=\mu r^2\dot{\theta}$, is conserved, as well as the total energy, so that the energy perpendicular to the direction of the radius vector, $M^2/2\mu r^2$, decreases as the square of the distance from the center of curvature, 0. If the particle enters the circular region at a point E, and emerges at a point F, and if it has not made exactly an even number of oscillations, energy will have been transferred between the directions normal to and along the valley. To increase the probability of staying in the valley, the transfer must of course be from the direction normal to the bottom of the valley to the direction along the bottom, i.e., if r_e is the radius at the point at which the mass point enters the curved region, and r_f the radius at the point at which it leaves (see Fig. 2) then $M^2/2\mu r_f^2 > M^2/2\mu r_e^2$, whence $r_e > r_f$. If at some point on the plateau G we represent the en-

* In Fig. 2 the coordinate r_2 should be replaced by Kr_2. In Fig. 3, r_2 should be replaced by Lr_2.

[4] (a) Eyring and Polanyi, Zeits. f. physik. Chemie **B12**, 279 (1931); (b) reference 1, p. 790.

ergy parallel to the bottom of the valley as $E_p = M^2/2\mu r_e^2$, and normal to it by E_n, then for this trajectory to lead to a stable molecule we must have $M^2/2\mu r_f^2 - M^2/2\mu r_e^2 > E_n$. Thus the four conditions that favor the formation of a diatomic molecule are that M and r_e be large and that E_n and r_f be small. In general, E_n will be of the order of $\frac{1}{2}kT$. For $E_n > 0$, there is no possibility of satisfying the above conditions if the trajectory enters the curved part of the valley by crossing the rim anywhere along the arc CD, since then r_f can never be less than r_e. Only trajectories that cross both AD and BC can give stable molecules. The smaller the radius of curvature, the greater the probability that r_e will be very much different from r_f, hence the greater the probability of energy transfer. Such a sharp curvature indicates a great reactivity, i.e., that the potential field is greatly disturbed by the presence of a third body in the compass of a very short distance.

It must not be imagined, however, that for energy to be transferred it is necessary for the mass point representing the system to pass completely through a curved region. It may be reflected back from a potential barrier and still transfer energy. If, for example, a high potential barrier were set up in the curved region of Fig. 2, so that the mass points would be reflected back into the valley whence they came, energy would still be transferred if they reentered the straight portion of the valley at a different point than they had left from. The type of potential energy surface that we have been considering in Figs. 1 and 2 is one that applies to the case in which all the particles involved can form valence bonds with each other. If the catalyzing particle repels the others at all distances (except for van der Waals forces), there will be only one deep valley in the potential energy surface with a hill closing off the end of this valley. If the potential field is such that this hill causes a curving of the equipotential lines of the surface, then energy will be transferred if the mass point goes partly up the hill at the end of the valley and then falls back in such a way that it reenters the valley at a different point.

Fig. 3 shows roughly the general nature of the potential energy surface for the interaction of an inert gas and a diatomic molecule. X represents

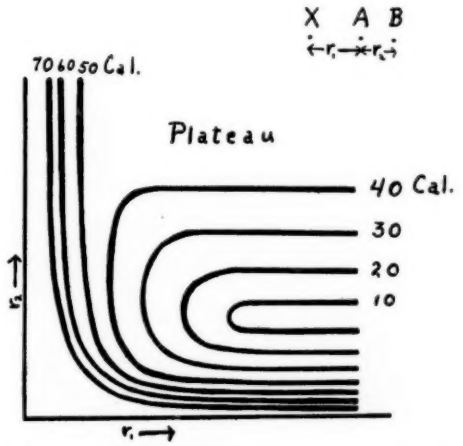

FIG. 3. Approximate potential energy surface for an inert gas atom (X) and a diatomic molecule (AB).

the inert gas and A and B the atoms of the diatomic molecule. (As shown, the molecule AB has a dissociation energy of about 40 Cal.) r_1 is the distance between X and A and r_2 the distance between A and B, the constant L being, as previously, a function of the masses. A collision between X and AB will be described by the motion of a mass point moving in the valley from right to left, towards the potential hill that represents the repulsive field of X. It can be seen that in the region at the bottom of the valley, i.e., for a diatomic molecule in an unexcited state, the nature of the surface can hardly be distinguished from that of Fig. 1. For high vibrational energies, however, the situation is entirely different from that in Fig. 1, and correspondingly, one would expect a much different probability for the transfer of energy. For the formation of a diatomic molecule, the mass point must move from the plateau into the region in which the equipotential lines are curved, so that there may be a transfer of energy between the two degrees of freedom.

III

It has long been fairly clear that in many cases the probability of energy transfer is related to the reactivity of the gases involved. Purely qualitative considerations have shown that strong intermolecular fields which perturb the energy should increase the probability of energy transfer. From this it has been concluded that those foreign gases will be most efficient in transferring energy which can react with the gas in

TABLE I. *Relative efficiencies of gases in transferring energy to Cl_2, N_2O and CO_2, from data on the dispersion of sound.*[5]

	Cl_2	N_2O	CO_2
Cl_2	1.0	—	—
N_2O	—	1.0	—
CO_2	—	1.1	1.0
N_2	0.88	—	—
A	1.1	—	1.0
He	33.3	3.3	33.3
D_2	—	12.5	—
H_2	50.0	9.1	125.0
CO	167	1.6	—
CH_4	200	6.7	25
HCl	200	—	500
NH_3	—	12.5	—
H_2O	—	100	2000

[5] Eucken, Oesterr. Chem. Ztg. (1935) 1.

question. This was the conclusion which was stated in (I). While this is true, it is very liable to misinterpretation. It is necessary to be careful in the definition of reactivity. We have shown above that, in the sense with which energy transfer is concerned, reactivity should be defined quantitatively in terms of the rate of change of curvature of the equipotential lines of the system. That is, reaction means the perturbation of the system so that a different set of normal coordinates must be used. The more a third body bends the equipotential lines of the system, the more reactive it is. This leads to the result that the relative reactivity depends on the region of the potential energy surface that is being considered. This can be seen by reference to Fig. 1, in which

TABLE II. *Relative efficiencies of gases in transferring energy in unimolecular reactions.*

	F_2O[6]	N_2O[7]	AZO-METHANE[8]
F_2O	1.00	—	—
N_2O	—	1.00	—
azomethane	—	—	1.00
O_2	1.13	.23	—
N_2	1.01	.24	.21
F_2	1.13	—	—
SiF_4	.88	—	—
He	.40	.66	.07
A	.52	.20	—
Ne	—	.47	—
Kr	—	.18	—
X	—	.16	—
H_2O	—	1.50	.46
CO_2	—	1.32	.25
CO	—	—	.13
CH_4	—	—	.20
D_2	—	—	.37

[6] Koblitz and Schuhmacher. Zeits. f. physik. Chemie **B25**, 283 (1936).
[7] Volmer and Frohlich, Zeits. f. physik. Chemie **B19**, 85 (1932); Volmer and Bogdan, ibid. **B21**, 257 (1933); Volmer and Briske, ibid. **B25**, 81 (1934).
[8] Sickman and Rice, J. Chem. Phys. **4**, 608 (1936).

it is very clear that reactivity of an H atom with respect to an H_2 molecule depends on whether the molecule is in the normal state or is highly excited, i.e., the bending of the equipotential lines and hence the probability of energy transfer, is different in the region $r_1 = 2.0$A, $r_2 = 0.74$A than it is in the region $r_1 = 2.0$A, $r_2 = 2.0$A. This affords an immediate explanation of the discrepancy that exists between the data on energy transfer obtained from experiments on the dispersion of sound and those obtained from reaction rates.

The most extensive investigations of transfer of energy among gases have been made in connection with the measurements of the rates of unimolecular and atomic reactions and of the dispersion of sound. Table I shows the results of some dispersion of sound experiments, giving the relative efficiencies of various foreign gases in transferring energy to Cl_2, N_2O and CO_2. There are no very noticeable regularities, but it can be seen that helium seems to be at least as effective as other molecules. Table II shows the relative efficiencies of various gases in the activation of fluorine oxide, nitrous oxide and azomethane. The inert gases are here noticeably less efficient than the others. Table III shows the relative efficiencies of various gases as third bodies in the recombination of Br_2 and I_2. Here also, it is apparent that the inert gases are less efficient than the others. Thus there is a discrepancy between the results of sound dispersion experiments and those of reaction kinetic experiments.

That there should be such a discrepancy is readily understood when one examines the nature of the potential energy surfaces. We are concerned with quite different regions of the surface in these two cases. In the case of the dispersion of sound, the experiments take place at low temperatures, when most of the molecules are in low energy states and are therefore represented by mass points moving along far down in the valley. In the reaction rate experiments the molecules

TABLE III. *Efficiency of gases in catalysing the recombination of halogen atoms.*[9]

	H_2	He	CH_4	N_2	O_2	A	CO_2
Br	2.2	.76	3.6	2.5	3.2	1.3	5.4
I	4.0	1.8	12	6.6	10.5	3.8	18

[9] Rabinowitsch and Wood, Trans. Faraday Soc. **32**, 907 (1936); ibid. **31**, 689 (1935); J. Chem. Phys. **4**, 497 (1936).

are highly excited and are represented by mass points moving across and high up on each side of the valley. The two situations are thus not analogous. In the case of dispersion of sound the energy transfer must take place in a comparatively small region of phase space at the bottom of the valley. In the case of reaction, the energy transfer may take place throughout a much larger region of phase space, in which the properties of the surface may be quite different from those of the limited region at the bottom of the valley. Translating into the older terminology of the kinetic theory, this means that in the two cases there will be different "collision diameters," referring to the spatial separation of the centers of gravity of the molecules when energy transfer takes place, different "steric factors," referring to the geometric orientation of the particles, and different transition probabilities.

With the aid of the two potential energy surfaces given in Fig. 1 and Fig. 3, it is possible to arrive at a more quantitative explanation of the fact that the inert gases are relatively more efficient in transferring energy to molecules in low energy states. An examination of these two surfaces shows that in the lower parts of the valley there will be a repulsive field even if the molecules involved are those which may react with each other. The inert gases, therefore, will have the same sort of effect as any other atoms. When large internuclear distances are involved, however, as in the case of dissociation, the attractive forces come into play, and change the nature of the surface, so that we should expect that atoms which may interact with valence forces should be more effective than those in which only van der Waals forces are present.

Since the surfaces referred to above are for triatomic systems, these arguments hold rigorously only for three atom processes. When polyatomic molecules are involved the situation is complicated by the presence of other degrees of freedom which may help in the transfer of energy. In general it may be expected that an increase in the number of degrees of freedom will increase the transition probabilities. Even though the number of degrees of freedom is increased, the situation will still be analogous to that of the three atom reaction. In the case in which reaction is taking place, there will be at least one degree of freedom in which large amplitude anharmonic vibrations will be taking place, while in the sound dispersion experiments all the degrees of freedom will be in low energy states. The essential characteristics of the problem therefore remain, and the conclusions reached with the aid of triatomic surfaces should be applicable. The interaction between the colliding particles depends on their state of excitation and the probability of energy transfer will be very different for different types of collision.

The above considerations apply to the transfer of vibrational and translational energy. It is easily seen that similar results would be obtained for transfer of other types of energy, such as rotational and electronic. The relative efficiencies of various molecules in transferring energy to a given molecule will depend on the type of process that is being considered and may well be different for different processes. There is no *a priori* reason why the relative efficiencies of gases in transferring energy in problems of heat conduction, sound dispersion, reaction rates, viscosity etc. should be the same. From the general principles that have been developed it is clear that the meaning of the term "collision" depends on the nature of the process that is being considered. The effective collision diameter will be different for the transfer of translational, vibrational or rotational energy. It will also depend on the nature of the molecules involved. For this reason one must be very careful in comparing data that are not strictly analogous. The term "collision" as it has been used in the classical kinetic theory is much too vague to be of any use when one considers that the particles involved have many internal degrees of freedom. Each of the problems of energy transfer will have its own peculiar set of conditions that will determine the relative probabilities of the configurations in which energy transfer may take place.

I wish to acknowledge my indebtedness to Professor Henry Eyring, with whom this work was begun.

The Activity Coefficient of Copper Sulphate in Aqueous Solution

F. E. W. WETMORE AND A. R. GORDON, *Chemistry Department, University of Toronto, Toronto, Canada*

(Received October 30, 1936)

The electromotive force of the cell Cu *two phase amalgam*/$CuSO_4$/Hg_2SO_4, Hg has been measured with solutions whose concentrations vary from 0.02 molal to saturation, and for temperatures from 15°C to 45°C. From these measurements and from freezing point and calorimetric heat of dilution data, activity coefficients have been calculated, and the value of $E°$ for the cell has been determined. The results are in reasonable agreement with those of Nielsen and Brown and of Getman, but are in definite disagreement with the results of Lebettre.

THE normal potential of the copper electrode and the activity coefficient of copper sulphate in aqueous solution have been the subject of numerous investigations dating back to the pioneer work of Lewis and Lacey.[1] The great difficulty has been the preparation of a reproducible electrode from a metal as stiff and as subject to surface strains as copper; to remove such strains, Lewis and Lacey used a spongy form of the metal, obtained by depositing it from solution with high current density, but most investigators have preferred a two phase copper amalgam.[2] A third type of electrode, the single copper crystal, has been used only by Getman. As reference electrode, the saturated mercury-mercurous sulphate electrode has usually been employed, although (owing to the appreciable solubility of mercurous sulphate) its use is restricted to fairly concentrated solutions (stronger than 0.02 molal, preferably 0.05 molal). Recently, Lebettre[3] has replaced the mercurous sulphate electrode by lead-lead sulphate in order to extend his measurements to the extremely dilute range, but his resulting activity coefficients are surprisingly small and are in complete disagreement with the freezing-point data.

We have been interested for some time in the effect of other sulphates on the thermodynamic potential of copper sulphate in aqueous solution, and in view of the considerable uncertainty that still exists as to the potential even in the absence of other salts, we have carried out the measurements recorded here on the cell Cu two phase amalgam/$CuSO_4$/Hg_2SO_4, Hg. We hope to extend this work by investigating the cell Cu amalgam/$CuSO_4+MSO_4$/$PbSO_4$, Pb.

The cells were H type of Pyrex glass; they were immersed in an oil bath electrically controlled to $\pm 0.02°$ and were shielded from light; two of the four electrode chambers served for amalgam electrodes and two for mercurous sulphate electrodes. The electromotive force was measured by means of a Leeds and Northrup type K potentiometer, a galvanometer of sensitivity 2×10^{-8} amp. per mm scale deflection, and a Weston standard cell with National Bureau of Standards certificate. Temperatures were measured by means of thermometers which had been calibrated against laboratory standards.

The mercury used was purified by spraying five times through 7 percent nitric acid, and then five times through distilled water; it was then dried, and thrice fractionally distilled at 30 mm pressure, the first and last fifth of each distillation being rejected. The copper was B.D.H. analytical reagent needles, while the copper sulphate was B.D.H. analytical reagent, recrystallized once from conductivity water slightly acidified with sulphuric acid, and once from neutral conductivity water. Mercurous sulphate was prepared by the method of Hulett[4] and was stored under twice molal sulphuric acid. The copper amalgam was prepared in a cell with an anode of copper needles, the electrolyte being 0.6 *m* $CuSO_4$ in aqueous solution slightly acidified with sulphuric acid; the cell was fitted with a Hulett type of stirrer operating at about

[1] Lewis and Lacey, J. Am. Chem. Soc. **36**, 804 (1914).
[2] Cohen, Chattaway and Tombrock, Zeits. f. physik. Chemie **60**, 706 (1907); Oholm, Medd. Vetenskapsakad. Nobelinst. **5** N:04, 1 (1919); Obata, Proc. Phys. Math. Soc. Japan [3] **2**, 223 (1920); Nielsen and Brown, J. Am. Chem. Soc. **49**, 2423 (1927); Getman, J. Phys. Chem. **34**, 1454 (1930); Quintin, Comptes rendus **196**, 473 and 538 (1933).
[3] Lebettre, J. de Chim. phys. **31**, 348 (1934); see also Quintin and Lebettre, Comptes rendus **198**, 1140 (1934).
[4] Hulett, Phys. Rev. **22**, 321 (1906).

TABLE I.

TIME	1.8	3.6	4.1	5.8	27.9
$A-1$	0.37248	0.37247	0.37249	0.37249	0.37245
$B-1$	.37247	.37244	.37244	.37243	.37240
$A-2$	.37246	.37246	.37248	.37251	.37252
$B-2$	.37246	.37244	.37244	.27245	.37247

TABLE II. $T=25.00°C$; $E°=0.2702$ volt.

m	E	$-\log \gamma$	m	E	$-\log \gamma$
0.02024	0.4011	0.520	0.1719	0.3728	0.970
0.02735	0.3968	0.577	0.3162	0.3651	1.104
0.03162	0.3945	0.601	0.3518	0.3640	1.132
0.05000	0.3876	0.684	0.5000	0.3596	1.210
0.0883	0.3802	0.806	0.9990	0.3518	1.379
0.0993	0.3787	0.831			

TABLE III. $T=25.00°C$.

$m^{1/2}$	$-\log \gamma$	$m^{1/2}$	$-\log \gamma$	$m^{1/2}$	$-\log \gamma$
0.100	0.390	0.25	0.730	0.6	1.135
.125	.468	.30	.808	.7	1.205
.150	.543	.35	.880	.8	1.263
.175	.598	.40	0.948	0.9	1.321
0.200	0.642	0.50	1.052	1.0	1.379

80 r.p.m., and the current density used in forming the amalgam was 3 amp./sq. dcm; after preparation, the product, containing 4 to 5 percent copper, was stored under the electrolyte. The copper sulphate solutions were made by gravimetric dilution of stock solutions (about 1 m in copper sulphate) which had been analyzed electrolytically for copper; a good grade of conductivity water was used in making all solutions. The nitrogen was purified by passing through a tower containing copper turnings in ammonia plus ammonium carbonate solution, then through water, then through sulphuric acid, and finally through a copper sulphate solution identical with that to be used in the cells.

In carrying out a measurement, the mercurous sulphate was washed five times with the electrolyte in a filtering crucible, and the copper amalgam was also washed thoroughly with the electrolyte and then dried with filter paper. The mercury, mercurous sulphate and amalgam were introduced into the cell, and the cell and the electrolyte in its reservoir in the thermostat were evacuated and flushed several times with nitrogen; the electrolyte was then forced over into the cell by nitrogen pressure.

In general a steady e.m.f. was obtained in a few hours, although this was not always the case (see below). Readings were made over a period of from 12 to 24 hours except in the high temperature runs, when the period was usually somewhat shorter. The history of one cell, 0.2176 m at 15.06°C, is summarized in Table I; A and B are the amalgam electrodes, and 1 and 2 are the mercurous sulphate electrodes. Times are in hours after the cell was formed. The mean value for the e.m.f. is thus 0.37246 ± 0.00006 volt. It is evident from the table that the mercurous sulphate electrodes (except for the last measurements) are in agreement within two-hundredths of a millivolt, and this was generally found to be the case; the deviation between the amalgam electrodes, on the other hand, is somewhat larger, and for this reason, the e.m.f. in Tables II and IV are recorded only to the nearest tenth of a millivolt, which is the reproducibility of the measurements.

While Table I is typical of the behavior of the great majority of the cells, occasionally a cell would behave somewhat erratically. For example, in one experiment with 0.9990 m solution at 25°, amalgam electrode B reached a steady state seven hours after the cell was formed, and showed an e.m.f. against either mercurous

TABLE IV.

(a) $T=15.06°C$				(b) $T=35.00°C$				(c) $T=44.95°C$			
m	E	$-\log \gamma$	$E°$	m	E	$-\log \gamma$	$E°$	m	E	$-\log \gamma$	$E°$
0.02850	0.3986	0.571	0.2776	0.02735	0.3943	0.593	0.2625	0.02735	0.3915	0.606	0.2546
0.0883	0.3823	0.786	(0.2769)	0.0878	0.3771	0.820	0.2624	0.2176	0.3623	1.054	(0.2540)
0.2176	0.3725	1.001	0.2774	0.2892	0.3628	1.104	0.2624	0.2892	0.3594	1.121	0.2546
0.2892	0.3694	1.066	0.2776	1.0000	0.3481	1.400	0.2625	0.7823	0.3467	1.349	0.2548
0.7823	0.3576	1.288	0.2778			Mean	0.2625	1.0000	0.3442	1.420	0.2546
1.0000	0.3551	1.356	0.2776							Mean	0.2546
		Mean	0.2776								

The Activity Coefficient of Copper Sulphate in Aqueous Solution

F. E. W. WETMORE AND A. R. GORDON, *Chemistry Department, University of Toronto, Toronto, Canada*

(Received October 30, 1936)

The electromotive force of the cell Cu *two phase amalgam*/$CuSO_4$/Hg_2SO_4, Hg has been measured with solutions whose concentrations vary from 0.02 molal to saturation, and for temperatures from 15°C to 45°C. From these measurements and from freezing point and calorimetric heat of dilution data, activity coefficients have been calculated, and the value of $E°$ for the cell has been determined. The results are in reasonable agreement with those of Nielsen and Brown and of Getman, but are in definite disagreement with the results of Lebettre.

THE normal potential of the copper electrode and the activity coefficient of copper sulphate in aqueous solution have been the subject of numerous investigations dating back to the pioneer work of Lewis and Lacey.[1] The great difficulty has been the preparation of a reproducible electrode from a metal as stiff and as subject to surface strains as copper; to remove such strains, Lewis and Lacey used a spongy form of the metal, obtained by depositing it from solution with high current density, but most investigators have preferred a two phase copper amalgam.[2] A third type of electrode, the single copper crystal, has been used only by Getman. As reference electrode, the saturated mercury-mercurous sulphate electrode has usually been employed, although (owing to the appreciable solubility of mercurous sulphate) its use is restricted to fairly concentrated solutions (stronger than 0.02 molal, preferably 0.05 molal). Recently, Lebettre[3] has replaced the mercurous sulphate electrode by lead-lead sulphate in order to extend his measurements to the extremely dilute range, but his resulting activity coefficients are surprisingly small and are in complete disagreement with the freezing-point data.

We have been interested for some time in the effect of other sulphates on the thermodynamic potential of copper sulphate in aqueous solution, and in view of the considerable uncertainty that still exists as to the potential even in the absence of other salts, we have carried out the measurements recorded here on the cell Cu two phase amalgam/$CuSO_4$/Hg_2SO_4, Hg. We hope to extend this work by investigating the cell Cu amalgam/$CuSO_4+MSO_4$/$PbSO_4$, Pb.

The cells were H type of Pyrex glass; they were immersed in an oil bath electrically controlled to $\pm 0.02°$ and were shielded from light; two of the four electrode chambers served for amalgam electrodes and two for mercurous sulphate electrodes. The electromotive force was measured by means of a Leeds and Northrup type K potentiometer, a galvanometer of sensitivity 2×10^{-8} amp. per mm scale deflection, and a Weston standard cell with National Bureau of Standards certificate. Temperatures were measured by means of thermometers which had been calibrated against laboratory standards.

The mercury used was purified by spraying five times through 7 percent nitric acid, and then five times through distilled water; it was then dried, and thrice fractionally distilled at 30 mm pressure, the first and last fifth of each distillation being rejected. The copper was B.D.H. analytical reagent needles, while the copper sulphate was B.D.H. analytical reagent, recrystallized once from conductivity water slightly acidified with sulphuric acid, and once from neutral conductivity water. Mercurous sulphate was prepared by the method of Hulett[4] and was stored under twice molal sulphuric acid. The copper amalgam was prepared in a cell with an anode of copper needles, the electrolyte being 0.6 *m* $CuSO_4$ in aqueous solution slightly acidified with sulphuric acid; the cell was fitted with a Hulett type of stirrer operating at about

[1] Lewis and Lacey, J. Am. Chem. Soc. **36**, 804 (1914).
[2] Cohen, Chattaway and Tombrock, Zeits. f. physik. Chemie **60**, 706 (1907); Oholm, Medd. Vetenskapsakad. Nobelinst. **5** N:04, 1 (1919); Obata, Proc. Phys. Math. Soc. Japan [3] **2**, 223 (1920); Nielsen and Brown, J. Am. Chem. Soc. **49**, 2423 (1927); Getman, J. Phys. Chem. **34**, 1454 (1930); Quintin, Comptes rendus **196**, 473 and 538 (1933).
[3] Lebettre, J. de Chim. phys. **31**, 348 (1934); see also Quintin and Lebettre, Comptes rendus **198**, 1140 (1934).
[4] Hulett, Phys. Rev. **22**, 321 (1906).

TABLE I.

TIME	1.8	3.6	4.1	5.8	27.9
$A-1$	0.37248	0.37247	0.37249	0.37249	0.37245
$B-1$	.37247	.37244	.37244	.37243	.37240
$A-2$	.37246	.37246	.37248	.37251	.37252
$B-2$	.37246	.37244	.37244	.27245	.37247

TABLE II. $T=25.00°C$; $E°=0.2702$ volt.

m	E	$-\log \gamma$	m	E	$-\log \gamma$
0.02024	0.4011	0.520	0.1719	0.3728	0.970
0.02735	0.3968	0.577	0.3162	0.3651	1.104
0.03162	0.3945	0.601	0.3518	0.3640	1.132
0.05000	0.3876	0.684	0.5000	0.3596	1.210
0.0883	0.3802	0.806	0.9990	0.3518	1.379
0.0993	0.3787	0.831			

TABLE III. $T=25.00°C$.

$m^{1/2}$	$-\log \gamma$	$m^{1/2}$	$-\log \gamma$	$m^{1/2}$	$-\log \gamma$
0.100	0.390	0.25	0.730	0.6	1.135
.125	.468	.30	.808	.7	1.205
.150	.543	.35	.880	.8	1.263
.175	.598	.40	0.948	0.9	1.321
0.200	0.642	0.50	1.052	1.0	1.379

80 r.p.m., and the current density used in forming the amalgam was 3 amp./sq. dcm; after preparation, the product, containing 4 to 5 percent copper, was stored under the electrolyte. The copper sulphate solutions were made by gravimetric dilution of stock solutions (about 1 m in copper sulphate) which had been analyzed electrolytically for copper; a good grade of conductivity water was used in making all solutions. The nitrogen was purified by passing through a tower containing copper turnings in ammonia plus ammonium carbonate solution, then through water, then through sulphuric acid, and finally through a copper sulphate solution identical with that to be used in the cells.

In carrying out a measurement, the mercurous sulphate was washed five times with the electrolyte in a filtering crucible, and the copper amalgam was also washed thoroughly with the electrolyte and then dried with filter paper. The mercury, mercurous sulphate and amalgam were introduced into the cell, and the cell and the electrolyte in its reservoir in the thermostat were evacuated and flushed several times with nitrogen; the electrolyte was then forced over into the cell by nitrogen pressure.

In general a steady e.m.f. was obtained in a few hours, although this was not always the case (see below). Readings were made over a period of from 12 to 24 hours except in the high temperature runs, when the period was usually somewhat shorter. The history of one cell, 0.2176 m at 15.06°C, is summarized in Table I; A and B are the amalgam electrodes, and 1 and 2 are the mercurous sulphate electrodes. Times are in hours after the cell was formed. The mean value for the e.m.f. is thus 0.37246 ± 0.00006 volt. It is evident from the table that the mercurous sulphate electrodes (except for the last measurements) are in agreement within two-hundredths of a millivolt, and this was generally found to be the case; the deviation between the amalgam electrodes, on the other hand, is somewhat larger, and for this reason, the e.m.f. in Tables II and IV are recorded only to the nearest tenth of a millivolt, which is the reproducibility of the measurements.

While Table I is typical of the behavior of the great majority of the cells, occasionally a cell would behave somewhat erratically. For example, in one experiment with 0.9990 m solution at 25°, amalgam electrode B reached a steady state seven hours after the cell was formed, and showed an e.m.f. against either mercurous

TABLE IV.

(a) $T=15.06°C$				(b) $T=35.00°C$				(c) $T=44.95°C$			
m	E	$-\log \gamma$	$E°$	m	E	$-\log \gamma$	$E°$	m	E	$-\log \gamma$	$E°$
0.02850	0.3986	0.571	0.2776	0.02735	0.3943	0.593	0.2625	0.02735	0.3915	0.606	0.2546
0.0883	0.3823	0.786	(0.2769)	0.0878	0.3771	0.820	0.2624	0.2176	0.3623	1.054	(0.2540)
0.2176	0.3725	1.001	0.2774	0.2892	0.3628	1.104	0.2624	0.2892	0.3594	1.121	0.2546
0.2892	0.3694	1.066	0.2776	1.0000	0.3481	1.400	0.2625	0.7823	0.3467	1.349	0.2548
0.7823	0.3576	1.288	0.2778			Mean	0.2625	1.0000	0.3442	1.420	0.2546
1.0000	0.3551	1.356	0.2776							Mean	0.2546
		Mean	0.2776								

sulphate electrode of 0.35183±0.00003 volt for over five days, a result that agreed within a few hundredths of a millivolt with the result of a previous experiment with the same solution. Amalgam electrode *A*, however, after seven hours, maintained a steady e.m.f. of 0.35165 ±0.00004 volt for the next 30 hours; then, in the next 12 hours, the e.m.f. rose and remained steady at 0.35187±0.00004 volt for the remainder of the run.

The measurements at 25.00°C are recorded in Table II, the first column giving the molality, and the second the observed e.m.f. At the lowest concentration of the table, the correction due to the solubility of the mercurous sulphate is probably not greater than 0.1 mv, which is the limit of error of the measurements, and so can be disregarded.

Hovorka and Rodebush[5] have determined the freezing point of dilute solutions of copper sulphate, and their measurements for 0.001, 0.005 and 0.01 molal can be represented within their limits of error by means of a Lewis and Randall[6] *j*-function with $j=1.718\,m^{0.423}$; this gives for these concentrations at the freezing point, log $\gamma=\bar{1}.865$, $\bar{1}.733$ and $\bar{1}.642$, respectively. If it be assumed that this *j*-equation is also valid for 0.02024 *m* solution, log γ for the weakest solution of Table II, at the freezing point, will be $\bar{1}.518$. Lange, Monheim and Robinson[7] have determined calorimetrically $\bar{L}_2$ for copper sulphate solutions, and since $(\bar{C}_{P_2}-\bar{C}_{P_2}^{\circ})$ is negligibly small,[8] log γ for these solutions at 298.2°K may be obtained at once. The resulting values for Hovorka and Rodebush's three solutions ($\bar{L}_2=448$, 813 and 965 cal., respectively) are $\bar{1}.850$, $\bar{1}.706$ and $\bar{1}.610$. The corresponding log γ for 0.02024 *m* ($\bar{L}_2=1127$ cal.) is $\bar{1}.480$, the uppermost entry in the third column of Table II. E°, defined by $E=E^{\circ}-(2RT/nF)\cdot\ln\gamma m$, is thus 0.2702 volt; this corresponds to a normal potential for the copper amalgam electrode of −0.3450 volt if the normal potential of the mercury-mercurous sulphate electrode[9] be taken as −0.6152 volt. The other entries in the third column follow at once from the observed e.m.f. and the value just obtained for E°.

TABLE V. *Cell Cu amalgam/CuSO₄ sat./Hg₂SO₄, Hg.*

T°C	15.06	25.0	35.00	44.95
E	0.3530	0.3468	0.3399	0.3329

From a large scale plot of the entries in the third column, values of the logarithm of the activity coefficient for rounded values of $m^{\frac{1}{2}}$ were obtained, and are entered in Table III; interpolation in this table yields values of log γ agreeing in general with those in Table II within ±0.002. The entries in Table III and the corresponding E° are of course uncertain to the extent of a small additive constant owing to the extrapolation of the freezing point equation from 0.01 *m* to 0.02 *m*, but they can be revised if necessary without difficulty when further data for more dilute solutions appear.

Table IV gives the results of measurements at other temperatures; the first column gives the molality, the second the observed e.m.f., the third the value of log γ obtained from Table II and Lange, Monheim and Robinson's values of $\bar{L}_2$, the fourth the resulting E°; bracketed values were not used in obtaining the final mean. It is evident from the table that $\partial E^{\circ}/\partial T$ at 25°C is about -7.6×10^{-5} volt per degree. Table V gives for the various temperatures the results for the cell Cu amalgam/$CuSO_4$ sat./Hg_2SO_4, Hg.

It is of interest to compare our results with those of other investigators who have used the same cell. Nielsen and Brown[2] with 0.05, 0.1, 0.2 and 0.5 molal solutions obtained at 25°C 0.3874, 0.3784, 0.3697 and 0.3592 volt, respectively; if our value of E° and the data of Table III (log $\gamma=\bar{1}.315$, $\bar{1}.168$, $\bar{2}.999$ and $\bar{2}.791$ for their concentrations) be assumed, the calculated values of *E* would be 0.3877, 0.3786, 0.3707 and 0.3595 volt, respectively, which with one exception are about 0.3 mv greater than their results. Getman[2] found for 25°C and $m=0.02098$, 0.04193, 0.10488 and 0.20984, $E=0.4007$, 0.3905, 0.3785 and 0.3701 volt, respectively; the values calculated from Table III with $E^{\circ}=0.2702$, are 0.4007, 0.3902, 0.3780 and 0.3702 volt. Thus Nielsen and Brown's results lie somewhat below

[5] Hovorka and Rodebush, J. Am. Chem. Soc. **47**, 1614 (1925).
[6] Lewis and Randall, *Thermodynamics*, p. 286 (1923).
[7] Lange, Monheim and Robinson, J. Am. Chem. Soc. **55**, 4733 (1933).
[8] *International Critical Tables*, Vol. V, p. 122.
[9] Harned and Hamer, J. Am. Chem. Soc. **57**, 27 (1935).

ours and Getman's on the whole somewhat above. Quintin's measurements, on the other hand, show a definite drift when compared with our data, her e.m.f. being smaller at lower concentrations and greater at high concentrations. The entry for 25°C in Table V is in agreement with the mean of the previous results for the saturated cell.

As we have mentioned above, Lebettre[3] on the basis of his results for the cell Cu amalgam/$CuSO_4$/$PbSO_4$, Pb, has computed activity coefficients from measurements extending down to solutions as dilute as 0.001 molal; his coefficients are in complete disagreement with those listed in Tables II and III and with the freezing point data, and, moreover, correspond to a La Mer "a" parameter[10] of only 2.4A—an extraordinarily small value. It seems to us that the most probable explanation of his results is that the copper sulphate in his most dilute solutions was partially hydrolyzed and that as a result his effective cupric ion concentrations were less than he supposed. The entry in Table III for 0.01 m, computed from freezing point and heat of dilution data, corresponds to an "a" of 3.9A—a more reasonable value in view of the results that have been obtained for other bivalent sulphates.[11]

[10] Gronwall, La Mer and Sandved, Physik. Zeits. **29**, 358 (1928).

[11] See, for example, La Mer and Parks, J. Am. Chem. Soc. **53**, 2040 (1931), Cowperthwaite and La Mer, J. Am. Chem. Soc. **53**, 4333 (1931), and reference 10.

JANUARY, 1937 JOURNAL OF CHEMICAL PHYSICS VOLUME 5

The Relaxation Time and Dipole Moment of Gliadin

SVEN ARRHENIUS, *Laboratory of Physical Chemistry, University of Upsala, Sweden*

(Received October 12, 1936)

THE dielectric constant of a medium depends not only on the temperature and concentration but also on the frequency. This is due to the fact that the molecules cannot orient themselves instantaneously with their electrical charges against the field when the latter changes rapidly. Accordingly Debye[1] writes the Clausius-Mosotti formula in the following manner:

$$\frac{\epsilon-1}{\epsilon+2}\frac{M}{d}=\frac{4\pi N}{3}\left(\alpha_0+\frac{1}{3kT}\cdot\frac{\mu^2}{1+i\omega\tau}\right). \quad (1)$$

In this equation $\epsilon=\epsilon'-i\epsilon''$ (ϵ' being the real part of the dielectric constant or that which is measured and ϵ'' the imaginary part which cannot be measured by capacity methods), M is the molecular weight, d is the density of the medium, N is the Avogadro number, α_0 is the optical polarisation, μ is the dipole moment, $\omega=2\pi\nu$ is the frequency, τ is the relaxation time, T is the absolute temperature and k is the Boltzmann constant.

If the frequency is of the order of that of light formula (1) reduces to

$$\frac{\epsilon_0-1}{\epsilon_0+2}=\frac{4\pi N\alpha_0}{3}, \quad (2)$$

and if the frequency is (small or) zero (direct current field) the formula reduces to the following

$$\frac{\epsilon_\infty-1}{\epsilon_\infty+2}=\frac{4\pi N}{3}\left(\alpha_0+\frac{\mu^2}{3kT}\right). \quad (3)$$

By combining formulas 1, 2, and 3 and solving for the real part of ϵ we obtain

$$\epsilon'=\epsilon_0+(\epsilon_\infty-\epsilon_0)\Big/\left(1+\left(\frac{\epsilon_\infty+2}{\epsilon_0+2}\right)^2\omega^2\tau^2\right). \quad (4)$$

By remembering that it is necessary to exert a torque to rotate a spherical molecule against the inner friction of the medium in which it is suspended the time of relaxation of such a molecule may be expressed in terms of its radius to give the following important result[8]

$$\tau=\frac{4\pi\eta r^3}{kT}=\frac{\epsilon_0+2}{\epsilon_\infty+2}\cdot\frac{1}{2\pi\nu_c}. \quad (5)$$

The frequency ν_c is that frequency for which $\epsilon=(\epsilon_\infty+\epsilon_0)/2$.

But if the molecule is a rotation ellipsoid with its long axis equal to a, and the short axis to b,

$(b/a=\rho)$ and it is rotating around its long axis in a medium with the viscosity η, then F. Perrin[7] has shown that the relaxation time is

$$\tau=\frac{4\pi ab^2\eta}{kT}\cdot\psi=\frac{4\pi ab^2\eta}{kT}\frac{4}{3}\times\frac{1-\rho^4}{1+(2\rho^2-1)(\rho^2/\sqrt{(1-\rho^2)})\ln(\sqrt{(1-\rho^2)}/\rho)}. \quad (6)$$

Now $4\pi ab^2/3=MV/N$ where M is the molecular weight and V the specific volume of the solute.

The molecular weight is obtained from centrifuge data according to the following formula:

$$M=RTs/D(1-Vd), \quad (7)$$

where s is the sedimentation constant, D is the diffusion constant, and d is the density, all in water at the temperature 20°C.

Finally, by combining Eqs. (6) and (7), we obtain

$$\tau=\frac{3\eta s}{D(1/V-d)}. \quad (8)$$

Preparation of gliadin

The object of this research was to study the relaxation time of gliadin with regard to the foregoing theory. The molecular weight and stability of this protein have been studied in this laboratory by Svedberg and Krejci[4] and its diffusion and viscosity in solution have been studied by Lamm and Polson,[5] also in this laboratory.

Neither the method of preparing gliadin of T. B. Osborne[6] nor that of Haugaard and Johnson[2] were suitable for our purpose; the former uses ether and absolute alcohol, which may probably denature the gliadin, whereas the latter separates the different components by flotation in LiCl and NaCl solutions. The high conductivity of solutions containing protein which had been in contact with appreciable electrolyte would render them unsuitable for capacity work.

The gliadin was prepared in the following manner: 1500 g flour was slowly added with constant stirring to 3000 cc aqueous alcohol (64 percent by weight). After having stirred for one-half day the solution was filtered through cotton cloth and put into a refrigerator at −8°C for four days. It was filtered at this temperature. It was then evaporated by using suction. When most of the alcohol had been removed the main part of the gliadin settled to the bottom of the vessel and the supernatant solution containing water soluble substances and some gliadin was discarded. The residue was fully dried and afterwards dissolved in alcohol. Three solutions were studied, one (A) containing 2.91 percent (weight) gliadin in 61.2 percent alcohol, a second (B) containing 1.70 percent in 46.9 percent alcohol, and a third (C) with 3.94 percent gliadin in 62.8 percent alcohol. (Maximum solubility = 4.01 percent in 61.7 percent alcohol.) Each sample was dialysed against alcohol of the same concentration. The outer liquids from dialyses were used as standards in all measurements.

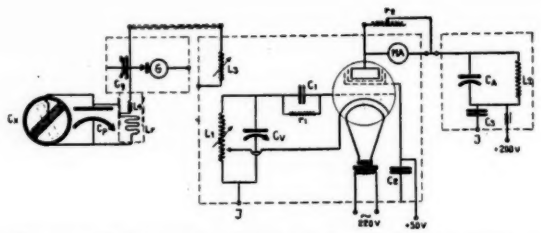

FIG. 1. Resonance apparatus for dielectric constant measurements.

C_x = Capacity cell (the positions marked)
C_p = Precision condenser 1500 $\mu\mu F$ or 500 $\mu\mu F$
C_v = Variable condenser, 100 cm
C_A = Variable condenser 450 cm
C_1 = Fixed condenser 250 cm
C_2 and C_3 = Fixed condenser 5000 cm
L_1, L_2, L_3, L_4, and L_7 = Variable inductances
r_1 = Fixed resistance, 5000Ω
r_2 = Variable resistance 0–310Ω (Shunt for A)
MA = Milliammeter
G = Galvanometer (Weston)
Tube = Philips E 446 transmitting tube
J = Earth connections of shield.

Ultracentrifuge measurements

The samples were run in the ultracentrifuge (70,000 r.p.m.) corresponding to 350,000 times gravity, and the sedimentation constants (reduced to water) were found to be, for solution A, $s=1.94\times10^{-13}$, for B, $s=2.01\times10^{-13}$, and for C, $s=2.04\times10^{-13}$. The corresponding molecular weights are $A=27{,}500$, $B=28{,}500$, and $C=28{,}900$. The ultracentrifuge diagrams showed no evidence of heavier particles or inhomogeneities. However, to make certain of a reproducible and homogeneous product, it is advisable to filter the sample at −11° and wash the precipitate with 5 percent alcohol.

Dielectric constant measurements

The dielectric constants of the several gliadin solutions under investigation have been measured

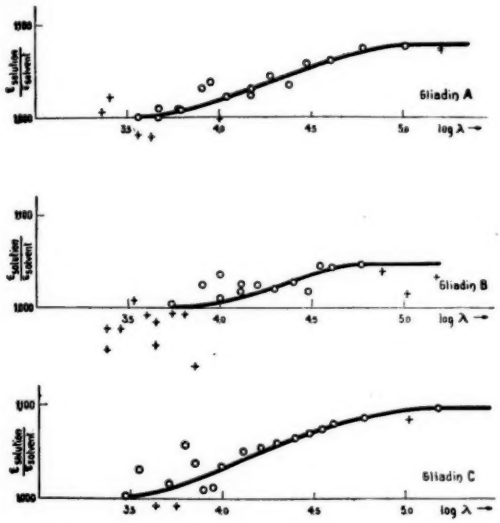

FIG. 2. Ratio of dielectric constant of solution to that of solvent as function of logarithm of wave-length. Actual dielectric constants may be obtained by multiplying the ratio by 43.8 for gliadin *A*, 57.5 for gliadin *B* and 42.7 for gliadin *C*.

with radiofrequency bridge or with resonance circuits, depending upon the frequency used. In the construction of the apparatus and in the capacity measurements directions given in a recent laboratory manual[9] were followed. The dielectric cells used were especially constructed to give proper shielding, rapid heat exchange with thermostat bath, low capacitative and inductive effects between leads, and exactness in operation. In these cells the capacity is measured with the rotor in two different positions without changing the external connections to the cell.

TABLE I. *Dielectric constant and time of relaxation data for gliadin solution A.*

λ_m	$\epsilon_{SOLUTION}/\epsilon_{SOLVENT}$	$\tau_{SEC.} \times 10^8$
1600	1.073	
1600	1.071	
1030	1.077	
591	1.074	7.0
403	1.067	10.5
300	1.057	9.0
240	1.035	13.1
191	1.044	8.3
149	1.030	9.3
149	1.024	11.0
110	1.022	8.7
89.5	1.038	4.5
80.5	1.031	4.9
62.2	1.008	9.1
54.7	1.009	7.5
47.0	1.010	
36.3	1.000	

Between $\lambda = 100$–1600 m the bridge method was used. A Hartley oscillator with modulated carrier wave (1000 cycles from amplified microphone hummer) was used as a generator. An ordinary radio receiver served as a detector for the wave-lengths 250–1600 m, but a specially built receiver was necessary for wave-lengths less than 250 m. Two mica condensers of 2000 cm capacity were used as the first two sides of the bridge; in the third a 2000 cm mica condenser parallel to a 0–1000Ω pressure resistance was used. The fourth side of the bridge contained the cell, the precision condenser, a simple variable condenser and an electrolyte resistance. The largest error in the measurement with this bridge is due to variations in the electric field of the laboratory.

The connections for the resonance circuit are

TABLE II. *Dielectric constant and time of relaxation data for gliadin solution B.*

λ_m	$\epsilon_{SOLUTION}/\epsilon_{SOLVENT}$	$\tau_{SEC.} \times 10^8$
1500	1.033	
1030	1.015	
761	1.039	
591	1.046	6.3
403	1.044	6.2
350	1.045	4.6
300	1.017	20.6
250	1.027	11.2
198	1.020	11.9
160	1.024	8.1
130	1.025	6.2
129	1.017	8.8
100	1.010	9.9
100	1.035	3.1
80.5	1.025	3.9

TABLE III. *Dielectric constant and time of relaxation data for gliadin solution C.*

λ_m	$\epsilon_{SOLUTION}/\epsilon_{SOLVENT}$	$\tau_{SEC.} \times 10^8$
1500	1.097	7.4
1030	1.085	19.5
591	1.087	10.2
403	1.080	9.3
350	1.075	9.4
300	1.070	9.2
250	1.065	8.6
197.5	1.060	7.6
160.5	1.055	6.9
130	1.051	6.1
100	1.035	6.5
89.5	1.012	11.6
79.1	1.010	11.4
71.8	1.038	4.4
62.2	1.058	2.5
36.2	1.031	2.6
30.0	1.003	8.2
57.6	1.016	5.7

shown in Fig. 1. The galvanometer is in the step over circuit, which is also tuned. The coupling coils to the resonance circuit are movable in a shielded box, so that any outside field will not cause disturbances.

Conclusions

The values of the dielectric constants of the solutions were never more than 1.1 times that of the solvent. Thus, an error in the third decimal place in capacity values will cause a large error in the relaxation time. All values are given for 20°C. The curves in Fig. 2 (gliadin solutions *A*, *B*, and *C*) show the variation of the ratio between the dielectric constant of the solution and that of the solvent with the logarithm of the wave-length.

In making the calculations for the times of relaxation of the gliadin molecules use has been made of refractive index data to evaluate the constant ϵ_0. We have taken arbitrarily $n^2=\epsilon_0$. The refractive indices for gliadin solutions are taken from an equation of Kent Jones and Amos[3] as follows:

$$n_{\text{gliadin}}=n_{\text{alcohol}}+0.0018C \quad (C=\text{concentration in weight percent}).$$

This equation gives practically the same value of $n^2=\epsilon_0$ for the solutions as for the solvent. The curves have been drawn by using all experimental points but only those for which $\epsilon_{\text{solution}}/\epsilon_{\text{solvent}}>1.000$ have been used in the calculation. Our choice of ϵ_0 is such that if this ratio is equal to or less than unity imaginary values of τ will result.

In order to calculate the τ values for gliadin solution *A*, ϵ_∞ has been fixed as $1.078\times43.8=47.2$; for gliadin *B*, $\epsilon_\infty=1.048\times54.9=57.5$; and for gliadin *C*, $\epsilon_\infty=1.098\times42.7=46.9$. The solvent dielectric constant values are 43.8, 54.9 and 42.7, respectively. The average values of τ are calculated to be 8.9×10^{-8} sec. for gliadin *A*, 8.9×10^{-8} sec. for gliadin *B* and 8.5×10^{-8} sec. for gliadin *C*. The values represent molecular weights of 28,000 for gliadin *A*, 25,500 for gliadin *B* and 27,000 for gliadin *C*. The dielectric constant data (Tables 1, 2 and 3) do not indicate any polydispersity of the gliadin.

On the other hand, if the values of *s*, *D*(6.78×10^{-7}, Lamm and Polson[5]), *b*/*a*(0.1041, Lamm and Polson[5]), and *V*(0.745, Krejci and Svedberg[4]) are substituted in the formula (8) we obtain for the relaxation time for gliadin *A*, $\tau=8.99\times10^{-8}$ sec., for gliadin *B*, $\tau=10.26\times10^{-8}$ sec. and for gliadin *C*, $\tau=9.37\times10^{-8}$ sec. The relaxation time for a gliadin suspended in pure water is calculated to be $\tau=3.7\times10^{-8}$ sec. at 20°C.

The times of relaxation given above are for the electrical field rotations of the gliadin molecule about the long axis. In order to obtain the constants characteristic of the rotation about the short axis dielectric constant measurements at longer wave-lengths are necessary. According to a private communication such data have been obtained recently for zein dissolved in aqueous alcohol solvent by Williams and Elliott working in the Wisconsin laboratory.

The dipole moment of the solute was calculated to be 14.3×10^{-18} e.s.u., 12.6×10^{-18} e.s.u., and 13.7×10^{-18} e.s.u. for gliadin *A*, *B*, and *C*, respectively. As an average value we give $\mu=13.5\times10^{-18}$ e.s.u.

I wish to express my sincere thanks to Professor J. W. Williams of the University of Wisconsin for his friendly help and his interest in opening this inspiring chapter of the physical chemistry to me, and to Professor The Svedberg, who has helped me in performing my work. I also wish to thank Mr. A. Polson of this institute for putting diffusion data at my disposal.

References

1. P. Debye, *Polar Molecules* (Chemical Catalog Co., New York, 1929).
2. G. Haugaard and A. H. Johnson, Compt. rend. de laboratoire Carlsberg **18**, 2 (1930).
3. D. W. Kent Jones and Amos, Am. J. Cereal Chem. **5**, 45 (1928).
4. L. Krejci and T. Svedberg, J. Am. Chem. Soc. **57**, 946 (1935).
5. O. Lamm and A. Polson, Biochem. J. **30**, 528 (1936).
6. T. B. Osborne, *Proteins of Wheat Kernel*, Carnegie Institute of Washington Publication, 84 (1907).
7. F. Perrin, J. de phys. **7**, 497 (1934).
8. J. W. Williams, Trans. Faraday Soc. **30**, 723 (1934).
9. F. Daniels, J. H. Mathews and J. W. Williams, *Experimental Physical Chemistry*, 2nd edition (McGraw-Hill Book Co., New York, 1934).

The Statistical Mechanics of Condensing Systems. I*

JOSEPH E. MAYER, *Johns Hopkins University, Baltimore, Maryland*

(Received October 21, 1936)

It is shown that for a system composed of N identical molecules with mutual potential energy, the assumption that the total potential energy can be expressed as the sum of that between pairs of molecules allows the derivation of simple, accurate formal equations for the thermodynamic properties of the system. Under certain conditions, generally fulfilled at low temperatures, the equations predict a region where the pressure and Gibb's free energy are independent of volume, the characteristic of condensing systems. The equations permit calculation of the Gibb's free energy of the liquid in equilibrium with the vapor and all the properties of the saturated vapor, but not the volume or volume dependence of the condensed phase.

WE seek a theoretical equation of state for a system composed of N identical molecules. This can be done by calculating A, the work function, or Helmholtz free energy, a function of volume, V, and temperature, T, from Q, variously called the partition function, sum of states, or phase integral. The first partial derivative of A with respect to V gives the negative of the pressure, P. The equations are

$$A = -kT \ln Q, \tag{1}$$

$$P = -(\partial A/\partial V)_T, \tag{2}$$

$$Q = \frac{1}{N!h^f}\int\int\cdots\int e^{-H(p,\,q)/kT}dp_1\cdots dp_f dq_1\cdots dq_f. \tag{3}$$

In Eq. (3) f is the number of degrees of freedom of the complete system, and $H(p_1, \cdots, p_f, q_1, \cdots, q_f)$ is the Hamiltonian, or energy expressed as a function of the f momenta and f coordinates of the complete system. The integration extends over the complete phase space. The division by $N!$ times the f power of h, Planck's constant, leads to an absolute value of A consistent with quantum-mechanical equations. The Eq. (3) for Q holds only for systems for which the classical mechanical approximations are valid.

For a gas containing internal degrees of freedom Q may be expressed as a product, and A as a sum, of the contributions due to the cartesian coordinates of the center of gravity and those due to the internal coordinates of the molecule. For the multiplicative part of Q due to internal motion the form (3) can usually not be employed but the more general quantum-mechanical sum over quantum states must be used. We shall be interested only in the factor of Q due to the $3N$ translational coordinates and momenta. Furthermore, we shall restrict ourselves to cases in which this part of the Hamiltonian can be written as

$$H(p, q) = \sum_{k=1}^{k=3N}\frac{1}{2m}p_k^2 + \sum_{i=j+1}^{i=N}\sum_{j=1}^{j=N-1}v_{ij}. \tag{4}$$

The expression for the part dependent on the momenta, the p's, is quite general. The other part assumes that the total potential energy can be expressed as a sum of terms each due to the mutual potential energy of a pair of molecules, (i, j), which is a function only of the differences of the coordinates of these molecules. This assumption would be unjustifiable in a gas composed of atoms or radicals which had a tendency to form valence bonds with each other (as monatomic hydrogen gas), but is presumably valid for all gases in which what are normally referred to as van der Waals forces only, occur. The v_{ij}'s are assumed to be functions of the coordinates of i and j alone. It is not necessary that they be functions of the coordinates of the centers of gravity alone, the mutual orientation angles may play a role, as they certainly do in all diatomic molecules. In the second paper of this series, in which numerical evaluations are made we shall assume spherically symmetrical molecules, essentially noble gases, but this assumption is nowhere needed in the more general discussion of this paper. Presumably the results of this paper may be considered to be applicable to all systems composed of chemically saturated molecules.

If we use the symbol $d\tau_i$ for the volume element of the ith particle (if spherically symmetrical

* Contribution from the Chemical Laboratory of The Johns Hopkins University.

atoms alone are considered $d\tau_i \equiv dx_i dy_i dz_i$) we can write

$$Q=\frac{1}{N!h^{3N}}\left\{\int_{-\infty}^{+\infty} e^{-p^2/2mkT}dp\right\}^{3N} Q_\tau = \left(\frac{2\pi mkT}{h^2}\right)^{\frac{3}{2}N}\frac{Q_\tau}{N!}, \tag{5}$$

with

$$Q_\tau=\int\left\{\prod_{i>j}^{N(N-1)/2 \text{ terms}} e^{-v_{ij}/kT}\right\}d\tau_1\cdots d\tau_N. \tag{6}$$

In the event that if $v_{ij}\equiv 0$, Q_τ becomes equal to V^N and the complete equation is that for a perfect gas.

By a trick which is commonly employed Q_τ may be expanded into a sum. The trick is to write

$$e^{-v_{ij}/kT}=1+e^{-v_{ij}/kT}-1=1+f_{ij}, \tag{7}$$

$$f_{ij}=e^{-v_{ij}/kT}-1, \tag{8}$$

$$Q_\tau=\int\int\cdots\int\left[1+\sum_{i=j+1}^{i=N}\sum_{j=1}^{j=N-1} f_{ij} + \sum_{i'}\sum_{j'}\sum_{i}\sum_{j} f_{ij}f_{i'j'}+\cdots\right]d\tau_1\cdots d\tau_N. \tag{9}$$

This trick makes possible an easy numerical evaluation of a first-order approximation to Q_τ.[1] However, although an entirely arbitrary mathematical decomposition of Q_τ into a sum of terms, it also aids in a qualitative discussion of the phenomena of condensation into liquid or crystalline phases.

Consider a general term of the sum in which P pairs f_{ij} occur, and L $(L/2\leq P\leq L(L-1)/2)$ *different* indices (molecules) occur in these P pairs. (Whereas no single pair, (ij), may occur more than once in a single term, any one index i may occur frequently, paired with different indices j' and j'' etc.) The L indices may be grouped into "clusters," such that all the indices occurring in one cluster are directly or indirectly connected with each other through a series of pairs, but no index occurring in one cluster occurs paired with an index occurring in any other cluster. Now let us collect all these terms together in which the same identical indices occur grouped together in the same clusters, and call the sum of these terms a constituent T of the sum. The significance of this particular grouping is the following. Suppose the indices 1 to 10 inclusive are connected together in one cluster. Integration of any or all of these terms contributes nothing in that part of the phase space where any of the molecules numbered 1 to 10 are far removed from any other of the cluster, since the function f_{ij} becomes zero for large values of its variable, r_{ij}. The complete value of the term can be obtained by limiting our integration to that part of the phase space where the molecules 1 to 10 are "reasonably" close to each other. This is connected with the fact that in a system of N molecules of which the stable configuration corresponds to M molecules in the liquid phase and $N-M$ in the gas phase, integration of the phase integral over that part of the phase space in which M molecules are "near" to each other contributes practically the whole of the phase integral, integration over the remainder giving only the vanishingly small contribution of the unstable supersaturated vapor to the complete free energy.

Integration over the volume element of any of the particles not occurring in the term contributes exactly V as a factor to the integral. Integration over the volume elements of $l-1$ indices of a cluster of l indices gives a value independent of the volume V, provided only that V is reasonably large compared to the "size" of the cluster. Integration over the lth index of the cluster contributes V (as a factor) to the integral. We wish now to define b_l as $1/l!$ times the integral over $l-1$ of the l indices occurring in the sum of all the terms which can be written as products of at least $l-1$ of the $l(l-1)/2$ functions f_{ij} between l definitely selected indices, consistent with the condition that the product correspond to a single cluster.

$$b_l=\frac{1}{l!}\int\int\cdots\int\Sigma\left[\prod_{l\leq i>j} f_{ij}\right]d\tau_1\cdots d\tau_{l-1}. \tag{10}$$

(Sum over all products consistent with a single cluster.)

The condition that the product is consistent with the existence of a single cluster means that there exists no single index or group of indices that is

[1] The usual method of treating the first term of the sum of Eq. (9) as small compared to unity, but as the only important term is unjustifiable. It is neither small, nor the most important term. A satisfactory treatment is given in Fowler's book *Statistical Mechanics* (Cambridge University Press, 1929), p. 168.

not at least indirectly connected to all the other indices, so that the integral (10) is independent of the volume of the system.

A single constituent T, as it has been defined, is characterized by having m_2 clusters, each of two definitely numbered particles; m_3 clusters each of three numbered particles; $\cdots$; m_l clusters each of l numbered particles; with $M=\sum m_l$, the total number of clusters, and $L=\sum l m_l$ the total number of particles involved in clusters. The additive contribution of this constituent to Q_τ will be.

$$T=\prod_{l\geq 2} l!b_l V^{N-L+M}. \tag{11}$$

The numerical value of the integrals b_l depend only on l, the number of particles in the cluster, and not on the particular particles involved. Therefore the same contribution T will occur several times, arising from all the terms characterized by the same set of numbers of the different size clusters $t\equiv(m_2, m_3, \cdots, m_l, \cdots)$ but differing from each other by the molecules involved. The sum of the contributions of all the constituents of the type t we shall call a term T_t, its numerical value will be

$$T_t=\frac{N!}{(N-L)!\prod_l m_l!l!}T$$

$$=\frac{N!}{(N-L)!\prod_l m_l!}\prod_{l\geq 2} b_l^{m_l}V^{N-L+M}, \tag{12}$$

and the total phase integral Q_τ will be the sum of these terms,[2]

$$Q_\tau=\sum_t T_t. \tag{13}$$

By this grouping the number of terms P_N occurring in the sum Q has shrunk considerably, it is, namely, the "partitio numerorum" of N, the number of ways that N can be expressed as a sum of numbers irrespective of the order of writing the numbers in the sum. This follows from the fact that N is the sum of $(N-L)$1's, plus m_2 2's $+\cdots+m_l$ l's$+\cdots$. The logarithm of P_N is known[3] to approach $\Pi(2N/3)^{\frac{1}{2}}$.

Were all the terms of the sum (13) positive we could call the largest single term of the sum T_{t^*}, and write

$$\ln T_{t^*}\leq \ln Q_\tau \leq \ln T_{t^*}+\Pi(2N/3)^{\frac{1}{2}}, \tag{14}$$

and since $\Pi(2N/3)^{\frac{1}{2}}$ is negligible compared to $\ln T_{t^*}$ which increases linearly with N we may write

$$\ln Q_\tau = \ln T_{t^*}. \tag{15}$$

We shall not wish to limit ourselves to the case that all the terms are positive. Nevertheless the derivation of the equation for $\ln Q_\tau$ on this assumption of equating it to the logarithm of the largest single term is so simple, and leads to such valuable intuitive results that we shall follow it here. In the appendix it is shown that a more careful derivation of the value of Q_τ independent of the assumption of only positive terms leads to identical equations.

We will find it convenient to introduce the Stirling approximation for the factorials in Eq. (12) and to introduce some new symbols, for quantities which do not depend on N. the total number of particles,

$$\mu_l=m_l/N, \tag{16}$$

$$\lambda=L/N=\sum_{l\geq 2} l\mu_l, \tag{17}$$

$$\mu=M/N=\sum_{l\geq 2}\mu_l, \tag{18}$$

$$v=V/N, \tag{19}$$

in which case we can rewrite Eq. (12) as

$$\frac{T_t}{N!}=\left\{\frac{v^{1-\lambda+\mu}e^{1-\lambda+\mu}}{(1-\lambda)^{(1-\lambda)}}\prod_{l\geq 2}\left(\frac{b_l}{\mu_l}\right)^{\mu_l}\right\}^N. \tag{20}$$

We define $\tau(\mu_2, \cdots, \mu_l, \cdots, b_2, \cdots, b_l, v)=(1/N)\ln(T_t/N!)$

$$=\sum_{l\geq 2}\mu_l[\ln b_l-\ln\mu_l-(l-1)(\ln v+1)]-(1-\lambda)\ln(1-\lambda)+\ln v+1], \tag{21}$$

and also define the convenient quantity q_τ,

$$q_\tau=(1/N)\ln(Q_\tau/N!)=\tau(\mu_2{}^*, \cdots, \mu_l{}^*, \cdots, b_2, \cdots, v) \tag{22}$$

[2] Up to about this point the treatment is not original; identical equations are derived, for instance, by Ursell, Proc. Camb. Phil. Soc. **23**, 685 (1927).

[3] Hardy and Raman Nujan, Proc. London Math. Soc. **16**, 130 (1917).

in which the $\mu_l^*=\mu_l$ (maximum), are determined by the equations

$$\partial\tau/\partial\mu_l=0(\text{at all } \mu_l=\mu_l^*)=\ln b_l-\ln \mu_l^*-(l-1)\ln v+l\ln(1-\lambda^*), \tag{23}$$

with

$$\lambda^*=\sum_{l\geq 2} l\mu_l^*. \tag{24}$$

Then

$$\mu_l^*=b_l(1-\lambda^*)^l/v^{l-1}, \tag{25}$$

and

$$q_\tau=1-\lambda^*+\mu^*-\ln(1-\lambda^*)+\ln v, \tag{26}$$

with,

$$\mu^*=\sum_{l\geq 2}\mu_l^*. \tag{27}$$

Using Eq. (22) we find, for the derivative of q_τ with respect to the logarithm of v,

$$v(\partial q_\tau/\partial v)=v(\partial\tau/\partial v)_{\mu_l=\mu_l^*}+\sum_l(\partial\tau/\partial\mu_l)_{\mu_l^*=\mu_l^*}(\partial\mu_l^*/\partial v), \tag{28}$$

but since $\partial\tau/\partial\mu_l=0$ at $\mu_l=\mu_l^*$.

$$v(\partial q_\tau/\partial v)=v(\partial\tau/\partial v)_{\mu_l=\mu_l^*}=1-\lambda^*+\mu^*. \tag{29}$$

For the second derivative one obtains

$$v^2(\partial^2 q_\tau/\partial v^2)=-[1-\lambda^*+\mu^*+v(\partial\lambda^*/\partial v)-v(\partial\mu^*/\partial v)]. \tag{30}$$

If now both sides of Eq. (25) are differentiated with respect to $\ln v$, multiplied by l, or by unity, and summed over l.

$$v(\partial\lambda^*/\partial v)=\sum_l lv(\partial\mu_l^*/\partial v)=-\sum_l l^2\mu_l^*-l\mu_l^*+[v/(1-\lambda^*)](\partial\lambda^*/\partial v)l^2\mu_l^* \tag{31}$$

$$=-\{h^*-\lambda^*+[h^*/(1-\lambda^*)](\partial\lambda^*/\partial v)\},$$

with

$$h^*=\sum_l l^2\mu_l^*, \tag{32}$$

from which

$$v(\partial\lambda^*/\partial v)=-(1-\lambda^*)(h^*-\lambda^*)/(1+h^*-\lambda^*). \tag{33}$$

Also

$$v(\partial\mu^*/\partial v)=\sum_l v(\partial\mu_l^*/\partial v)=-\sum_l l\mu_l^*-\mu_l^*+[v/(1-\lambda^*)](\partial\lambda^*/\partial v)l\mu_l^* \tag{34}$$

$$=-\lambda^*+\mu^*-[\lambda^*/(1-\lambda^*)]v(\partial\lambda^*/\partial v)$$

$$=-(\lambda^*-\mu^*-\mu^*(h^*-\lambda^*)/(1+h^*-\lambda^*)).$$

Substitution of (33) and (34) in (30) leads to

$$v^2(\partial^2 q_\tau/\partial v^2)=-(1-h^*-\lambda^*)^{-1}. \tag{35}$$

Returning now to Eqs. (1), (2), (5) and (22); and using (26), (29) and (35) we can write, for one mole of gas.

$$A=RT[\ln(h^2/(2\pi mkT))^{\frac{3}{2}}(N_0/Ve)+\lambda^*-\mu^*+\ln(1-\lambda^*)], \tag{36}$$

$$P=(RT/V)(1-\lambda^*+\mu^*), \tag{37}$$

$$(\partial P/\partial V)_T=-(RT/V^2)[1/(1+h^*-\lambda^*)], \tag{38}$$

$$((\partial\ln P)/(\partial\ln V))_T=(V/P)(\partial P/\partial V)_T=-1/((1-\lambda^*+\mu^*)(1+h^*-\lambda^*)). \tag{39}$$

The Gibb's free energy F is $A+PV$, adding V times Eq. (37) to (36) after eliminating V from (36) by means of (37), one obtains

$$F=RT\left\{\ln\left(\frac{h^2}{2\pi mkT}\right)^{\frac{3}{2}}\frac{P}{kT}-\ln\left(1+\frac{\mu^*}{1-\lambda^*}\right)\right\}. \tag{40}$$

Substitution of (37) for $v=V/N$ in (25) leads to

$$\mu_l^*=\frac{b_l(1-\lambda^*)^l}{v^{l-1}}=\frac{b_l(1-\lambda^*)^l P^{l-1}}{(kT)^{l-1}(1-\lambda^*+\mu^*)^{l-1}}. \tag{41}$$

Between h^*, λ^* and μ^* the relationship holds

$$h^*=\sum_{l\geq 2} l^2\mu_l^*>\lambda^*=\sum_{l\geq 2} l\mu_l^*>\mu^*=\sum_{l\geq 2}\mu_l^*, \quad \text{and also} \quad \lambda^*\leq 1. \tag{42}$$

With the definition of b_l, Eq. (10) the Eqs. (36) to (42) form a perfectly general and sufficient set from which the thermodynamical properties of any pure substances could, in principle, be calculated, provided: firstly, that the condition of Eq. (4) that the total potential energy be expressible as a sum of the potential between pairs of molecules be fulfilled; and secondly, that the volume of the system be greater than that of the condensed phases. This second requirement is needed because of the use of the condition that b_l be independent of the volume. Were the total system restricted to a volume comparable with the "natural" size of the cluster[4] this condition would not be fulfilled. The equations hold only for the condensed phases in equilibrium with their vapor, and cannot be used for the condensed phases under greater external pressure. Such cases might, however, be handled by the integral inclusion into the system of molecules of a second kind (an inert gas) with appropriate potentials between pairs of the two kinds of molecules.

The differences between the values of A, P, $(\partial P/\partial V)_T$ and F, in Eqs. (36) to (40), and the values of these quantities for a perfect gas, are all simple functions of the three quantities h^*, λ^* and μ^*. The results of the appendix show that the Eqs. (41) and (42) can be used for these quantities even if any of the b_l's have a value less than zero. In this event it is difficult to find a simple physical interpretation for these quantities. If all the b_l's happen to be positive, as they will at low temperatures (below the critical point), their physical significance is easy to see. λ^* is the (most probable) fraction of the material existing in clusters, that is, it is the fraction of the material, in excess of that expected from a random space distribution, which is spacially concentrated so that the molecules are close to each other.

μ^* is the number of these clusters divided by the total number of molecules, and h^* the product, number of molecules per cluster times fraction of material in the clusters, summed over all clusters. Perhaps $\lambda^*-\mu^*$ is of more significance than either λ^* or μ^* alone, it is the fraction of material which has been constrained to a dependent motion, so that $1-\lambda^*+\mu^*$ may be regarded as the number of independent entities in the system divided by the total number of molecules. Similarly $h^*-\lambda^*$ is the number of constrained molecules per cluster (since one, so to speak, is free) multiplied by the fraction of material in the clusters, summed over all clusters. The ratio which occurs in the expression for F is the ratio of the number of clusters to the number of completely independent molecules. It appears that if any of the b_l's are negative these quantities are to be interpreted in the opposite sense, that is λ^* as the fraction of the material which is not in clusters of size l compared to a certain amount which would be expected from considerations of random space orientation.

The phenomenon of condensation is easily explained by means of these equations. For small values of l the values of b_l can be individually calculated, or at least estimated. For very large values of l, $\ln b_l$ becomes asymptotically equal to $(l-1)\ln b_0$, in which b_0 is a constant, dependent on the temperature but independent of l or v, whose value can, in some cases at least, be estimated. The value of b_l for any value of l can always, then, be written as $b_l=b_0{}^{l-1}/f(l)$ in which $\ln f(l)\ll l-1$ for large values of l.

[4] Integration over $l-1$ volume elements of a cluster of l particles leads to b_l independent of the volume provided the integrand product, (Πf_{ij}), is zero before the boundary of the vessel is reached. Integration over the lth element leads to something like $V-v_l$ where v_l is the "natural" volume of a cluster of l particles. This correction, however, is entirely negligible since if V is greater than the volume of the condensed phase, which is about the natural volume of a cluster of N particles, then $v_l\ll V$ except for a very few (few compared with N) of the largest clusters. We are really interested in $(1/N)\ln Q_T$, and an error in Q_T of a good many fair size factors can be safely neglected.

Now from Eq. (41), using this form for b_l, the equation determining λ^* can be written in the form

$$\frac{\lambda^*}{1-\lambda^*}=\sum_{l\geq 2}^{l=N}\frac{l}{f(l)}\left\{\frac{b_0(1-\lambda^*)}{v}\right\}^{l-1}. \tag{43}$$

This equation, with b_0 and all $f(l)$'s positive, has obviously a solution with $0\leq\lambda^*/(1-\lambda^*)\leq+\infty$, or $0\leq\lambda^*\leq 1$, for all positive values of v. We shall define as v_s that value of v for which $b_0(1-\lambda^*)/v$ becomes exactly equal to unity. At $v=v_s$ from (43) $\lambda^*/(1-\lambda^*)=\sum l/f(l)$, and since the number of terms is finite this sum will have a finite, although possibly very large, value.

Anticipating the results of the following article, we find that, at low temperatures at least, $l/f(l)$ decreases with increasing l more rapidly than $l^{-\frac{3}{2}}$, so that the sum of $l/f(l)$ which we shall call σ has a relatively small value. Under these conditions, at $v=v_s$, the value of λ^*, which we shall call λ_s^* is appreciably smaller than unity.

For values of v equal to, or smaller than v_s the quantities μ_l^* and $l\mu_l^*$ decrease with increasing values of l. However, if v becomes even slightly smaller than v_s, so that $b_0(1-\lambda^*)/v$ becomes even very slightly larger than unity, say equal to $1+\epsilon$, the last terms in the sum (43) tend to become enormous. If $\epsilon=(1/N)[\ln(f(N)/N)+23]$ (for $N=10^{23}$) the last term alone would be 10^{10} and $1-\lambda^*=10^{-10}$. Now $\ln(f(N)/N)$ is a number very much smaller than N, so that we can say that for values of λ^* between $\sigma/(1+\sigma)$ and unity, $b_0(1-\lambda^*)/v$ is equal to unity and $(1-\lambda^*)/v$ remains constant. In this range the very large clusters, corresponding to the condensed phase, appear with increasing probability as v decreases.

Now the additive contribution μ_l^* of the large clusters to μ^*, as can be seen from the fact that we must always have μ_l^* less than $1/l$, is negligible. For small values of l we can say that $[(1-\lambda^*)/v]^l$ is constant (although not for $l\leqq 10^{23}$) so that, from Eq. (41), for $l\ll N$, μ_l^* and therefore μ^* is proportional to v. With both μ^* and $1-\lambda^*$ proportional to v we see from Eq. (37) that P, and from (40) that F remain constant during the condensation process. h^* very rapidly becomes large compared to unity and $\partial P/\partial V$ becomes zero, as of course must be the case if P is to be constant.

The volume of condensation, that is, the volume of the saturated vapor per molecule is v_s, determined by the condition that $b_0(1-\lambda^*)/v=1$ when $\lambda_s^*/(1-\lambda_s^*)=\sum l/f(l)$. Indicating all values corresponding to the saturated vapor by a subscript s, and defining the two sums

$$\sigma=\sum_{l\geq 2} l/f(l) \tag{44}$$

with $f(l)$ and b_0 defined by

$$f(l)=b_0^{l-1}/b_l;\quad (l-1)\ln b_0=\ln b_l (l\to\infty) \tag{45}$$

and

$$\phi=\sum_{l\geq 2} 1/f(l), \tag{46}$$

we have for λ_s^* and v_s the equations

$$\lambda_s^*=\sigma/(1+\sigma);\quad 1-\lambda_s^*=(1+\sigma)^{-1}, \tag{47}$$

$$v_s=b_0(1-\lambda_s^*)=b_0/(1+\sigma). \tag{48}$$

Substitution of these values in (41) leads to

$$\mu_s^*=\phi/(1+\sigma). \tag{49}$$

Using the above values in Eqs. (36), (37) and (40), one obtains, for one mole of the saturated vapor.

$$A_s=RT\left[\ln\left(\frac{h^2}{2\pi mkT}\right)^{\frac{3}{2}}\frac{1}{e}-\ln b_0+\frac{\sigma-\phi}{1+\sigma}\right]. \tag{50}$$

$$P_s=kT((1+\phi)/b_0), \tag{51}$$

$$(PV)_s=RT((1+\phi)/(1+\sigma)), \tag{52}$$

$$F_s=F_{\text{liq}}=RT[\ln(h^2/2\pi mkT)^{\frac{3}{2}}-\ln b_0]. \tag{53}$$

In Eq. (53), F_s, the Gibb's free energy of the saturated vapor is equal to that of the liquid (or solid) in equilibrium with it. For other conditions of pressure our equations tell us nothing about the thermodynamic properties of the liquid. Indeed, in the discussion of the condensation process it appeared, according to our equations, that $(1-\lambda^*)/v$, μ^*/v, and therefore P and F remain constant down to zero volume. This is due to the oft reiterated fact that we have assumed b_l to have a value independent of the volume. There is nothing in our equations to show us the volume of the liquid.

One can, however, calculate $\partial P/\partial T$ for the liquid vapor equilibrium, and, under the assumption that the volume of the liquid is negligibly small compared with that of the saturated vapor, from this the value of ΔH and ΔS for the condensation process. One obtains, for one mole,

$$\Delta H = T\Delta V\frac{\partial P}{\partial T} = TNv_s\frac{\partial P}{\partial T}$$

$$= \frac{RT}{1+\sigma}\left[(1+\phi)\left(1-\frac{\partial \ln b_0}{\partial \ln T}\right)+\phi\frac{\partial \ln \phi}{\partial \ln T}\right], \quad (54)$$

$$\Delta S = \Delta H/T$$

$$= \frac{R}{1+\sigma}\left[(1+\phi)\left(1-\frac{\partial \ln b_0}{\partial \ln T}\right)+\phi\frac{\partial \ln \phi}{\partial \ln T}\right]. \quad (55)$$

The above equations are, of course, only approximate, due to the neglect of the volume of the liquid. At low temperatures they become asymptotically exact.

Eq. (48) enables us to calculate the volume of the saturated vapor, v_s, provided b_0 can be calculated, and provided the sum σ converges rapidly enough to allow it to be evaluated. This is actually the case for temperatures somewhat below the critical point. Such a value of v_s will presumably correspond to the experimental value of the volume per molecule of the saturated vapor provided it is larger than v_l, the volume per molecule of the liquid at the same temperature and pressure. This is obviously not the case at the critical point. We cannot expect the equations of this article, then, without further extension, to give us correct values at the critical point. The behavior of the system in the neighborhood of this temperature will be discussed in a later paper.

In the following paper it will be shown that b_0, σ and ϕ can be estimated, and that the observable values of v_s, $(PV)_s$ and P_s so calculated are in reasonable agreement with experimental values, at least over a short temperature range.

APPENDIX.[5]

We wish to calculate the function $Q_\tau/N!$ defined by Eqs. (13) and (12) of the text,

$$\frac{Q_\tau}{N!} = \sum_{m_l=0}^{\Sigma lm_l=N}\frac{\Pi_l b_l^{m_l} V^{N-L+M}}{(N-L)!\Pi_l m_l!} \quad (1)$$

We define $v = V/N$, and $B_l = b_l v$,

$$\frac{Q_\tau}{N!} = \sum_{m_l=0}^{\Sigma lm_l=N}\frac{\Pi_l B_l^{m_l} v^{N-L} N^{N-L+M}}{(N-L)!\Pi_l m_l!} \quad (2)$$

and notice that

$$\frac{\partial}{\partial B_k}\left(\frac{Q_\tau}{N!}\right) = \frac{1}{N^{k-1}}\left(\frac{\partial}{\partial v}\right)^k_{B_l}\left(\frac{Q_\tau}{N!}\right). \quad (3)$$

If now we define

$$q = \frac{1}{N}\ln\frac{Q_\tau}{N!}, \quad (4)$$

then

$$\frac{\partial}{\partial B_k}\left(\frac{Q_\tau}{N!}\right) = \frac{Q_\tau}{N!}N\frac{\partial q}{\partial B_k} \quad (5)$$

and $$\left(\frac{\partial}{\partial v}\right)^k\left(\frac{Q_\tau}{N!}\right) = \frac{Q_\tau}{N!}N^k\left(\frac{\partial q}{\partial v}\right)^k\left(1+\frac{1}{N}\times\cdots+\cdots\right) \quad (6)$$

in which we can neglect the terms divided by N. Combining (5), (6) and (3) we obtain

$$(\partial q/\partial B_k)_{v,\ B_l} = (\partial q/\partial v)^k_{B_l}. \quad (7)$$

Now independently of all this we can write

$$\frac{Q_\tau}{N!} = v^N f(B_2/v^2, \cdots, B_l/v^l, \cdots), \quad (8)$$

from which we can derive that

$$v(\partial q/\partial v)_{B_l} = [1-\Sigma lB_l(\partial q/\partial B_l)_{v,\ B_m}], \quad (9)$$

and substitution of this in (7) leads to

$$(\partial q/\partial B_k)_{v,\ B_l} = [1-\Sigma lB_l(\partial q/\partial B_l)_{v,\ B_m}]^k v^{-k}. \quad (10)$$

We now reintroduce our old variables $b_l = B_l/v$, so that

$$(\partial q/\partial B_k)_{v,\ B_l} = (\partial q/\partial b_k)_{v,\ b_l}/v, \quad (11)$$

$$(\partial q/\partial v)_{B_l} = (\partial q/\partial v)_{b_l} - v^{-1}\Sigma_l b_l(\partial q/\partial b_l)_{v,\ b_m}. \quad (12)$$

Eq. (7) now becomes

$$\frac{1}{v}\frac{\partial q}{\partial b_k} = \left[\frac{\partial q}{\partial v}-\frac{1}{v}\sum_{l\geq 2} b_l\frac{\partial q}{\partial b_l}\right]^k, \quad (13)$$

in which case we can now safely drop the subscript indications of what is kept constant during the partial differentiation, and (10) becomes

$$\frac{1}{v}\frac{\partial q}{\partial b_k} = \frac{1}{v}\left[1-\sum_{l\geq 2} lb_l\frac{\partial q}{\partial b_l}\right]^k. \quad (14)$$

Equating (13) and (14) and taking the kth root,

$$\frac{\partial q}{\partial v} = \frac{1}{v}\left[1-\sum_{l\geq 2}(l-1)b_l\frac{\partial q}{\partial b_l}\right]. \quad (15)$$

We now define $$\mu_l^* = b_l(\partial q/\partial b_l), \quad (16)$$

$$\mu^* = \sum_{l\geq 2} l\mu_l^* \quad (17)$$

$$\lambda^* = \Sigma l\mu_l^*, \quad (18)$$

in which case (14) becomes

$$\mu_l^* = (b_l(1-\lambda^*)^l)/v^{l-1}, \quad (19)$$

and (15) $$v(\partial q/\partial v) = (1-\lambda^*+\mu^*). \quad (20)$$

Eqs. (17), (18) and (19) are identical with (27), (24) and (25) of the text, respectively, and Eq. (20) is identical (29) of the text. In the above derivation no use was made of any assumption that the b's were positive quantities. The above equations are sufficient to determine q completely since the integration constant at infinite volume is $\ln V$.

[5] The treatment here was suggested by that of Fowler (reference 1), which in turn apparently originated from Ursell (reference 2). The discussion in Fowler's book is more complete than given here.

The Statistical Mechanics of Condensing Systems. II*

JOSEPH E. MAYER AND PHILIP G. ACKERMANN, *Johns Hopkins University, Baltimore, Maryland*

(Received October 21, 1936)

It is shown how the quantities entering into the equations for the thermodynamic functions of a saturated vapor, given in the previous article, may be calculated. It is necessary to evaluate certain integrals which enter into the final expressions as the terms of an (almost) infinite, but rapidly convergent series. The first two of these integrals have been evaluated with fair accuracy for a gas obeying the inverse seventh power law of force attraction. The third integral has been estimated. The coefficients with which these integrals enter into the final expression have also been estimated. The results of the calculation have been compared with the experimental values for CO_2 and CH_4. Specifically, the volume of the saturated vapor in units of the volume of the molecules, and the ratio $(PV)/(RT)$ for the saturated vapor have been calculated on an arbitrary temperature scale. The agreement between the calculations and the experimental values is not unencouraging.

IN the preceding article equations giving the thermodynamic functions of an imperfect gas, and in particular, a saturated vapor, were derived in terms of certain integrals over the coordinate space of varying numbers of molecules. In this paper we shall proceed to show how these integrals may be evaluated.

We seek the value of b_l, which is defined by the equation

$$b_l=\frac{1}{l!}\int\int\cdots\int\sum\left\{\prod_{\triangleright i} f_{ij}\right\}d\tau_1\cdots d\tau_{l-1}, \quad (1)$$

(Sum over all products consistent with the existence of a single cluster.)

where $d\tau_i$ is the volume element of the ith particle, f_{ij} is a certain function of the difference in the coordinates of the ith and jth particle, and the sum is to be taken over all products of the f_{ij}'s in which every one of the l particles is linked (by means of an f) directly or indirectly to all other of the $l-1$ particles. The function f_{ij} is

$$f_{ij}=\exp\left(-v_{ij}/kT\right)-1, \quad (2)$$

and in the following it will be explicitly assumed that v_{ij}, the mutual potential energy of the pair of particles i and j is a function only of the distance between their centers of gravity r_{ij}, so that $d\tau_i=dx_i dy_i dz_i$.

For small values of l we can consider the various b_l's and the terms that go to make them up individually.

The smallest cluster is that of two particles. This cluster can be formed in only one way. The integral over the coordinates of one of the particles will be

$$b_2=\tfrac{1}{2}\int_0^\infty 4\pi r^2 f(r)dr=\gamma_1/2, \quad (3)$$

since this integral will occur as a constituent of the terms making up the higher b_l's we shall invest it with a new symbol, γ_1.

The cluster of three particles can be formed in four ways by combining the three indices 1, 2, 3, in pairs in the following manner 1st (12)(13); 2nd (12)(23); 3rd (13)(23); 4th (12)(23)(13). In the first of these arrangements integration over the coordinates of particle 2, or of particle 3, gives γ_1 independently of the position of the remaining two particles. Subsequent integration over the volume of one of the remaining two particles again yields γ_1. The value of the term is γ_1^2. The same is true of arrangements 2 and 3. The contribution of all three of these arrangements to b_3 is then $3\gamma_1^2/6$ or $\gamma_1^2/2$. The integration of the fourth arrangement is more difficult and yields a new integral which we shall designate by γ_2,

$$\gamma_2=\int\int f(r_{12})\cdot f(r_{23})\cdot f(r_{13})d\tau_1 d\tau_2, \quad (4)$$

$$b_3=\gamma_1^2/2+\gamma_2/6. \quad (5)$$

The integrals of the type γ_1 and γ_2 we shall refer to as "irreducible integrals" and also as "constituent integrals." The irreducible integrals, which in general will be designated by two subscripts (km), will be integrals over the volume elements of k particles of a certain

* Contribution from the Chemical Laboratory of The Johns Hopkins University.

definite product of the possible f_{ij}'s of $k+1$ particles. To be irreducible the product must be such that every one of the $k+1$ particles is connected by means of an f with at least two other particles, and in addition, of course, all $k+1$ particles must be at least indirectly connected with each other.

The irreducible integrals of $k=3$ are the following

$$\gamma_{30}=\int\int\int f_{12}\cdot f_{23}\cdot f_{34}\cdot f_{14}d\tau_1 d\tau_2 d\tau_3, \tag{6}$$

$$\gamma_{31}=\int\int\int f_{12}\cdot f_{23}\cdot f_{34}\cdot f_{14}\cdot f_{13}d\tau_1 d\tau_2 d\tau_3, \tag{7}$$

$$\gamma_{32}=\int\int\int f_{12}\cdot f_{23}\cdot f_{34}\cdot f_{14}\cdot f_{13}\cdot f_{24}d\tau_1 d\tau_2 d\tau_3. \tag{8}$$

Each irreducible integral corresponds to a certain pattern of bonds between $k+1$ particles, the integral γ_1 corresponds to a line ——, γ_2 to Δ, γ_{30} to $\square$, etc. In their additive contribution to b_{k+1} it can be seen that each irreducible integral γ_{km} occurs just as often as one can draw (in three dimensions) different patterns (km) between $k+1$ numbered points, i.e., γ_{30} occurs 3 times, γ_{31}, 6 times, and γ_{32}, once. If we call this number d_{km}, the number of ways that we can draw the pattern (km) between $k+1$ numbered points, and define as the "constituent integral" γ_k the sum $d_{km}\gamma_{km}$ over all values of m,

$$\gamma_k=\sum_m d_{km}\gamma_{km}, \tag{9}$$

the contribution of γ_k to b_{k+1} will be just $\gamma_k/(k+1)!$

We need two other facts. Just as every irreducible integral corresponds to an irreducible pattern, so any one of the products, (Eq. (1)), making up b_l can be said to correspond to a certain configuration of bonds between l numbered points in space, and each configuration can be analyzed as a sum of singly connected irreducible patterns. The number of irreducible patterns (km) we shall designate by n_{km}. From the fact that the patterns are singly connected it follows that

$$\sum_{km} kn_{km}=l-1. \tag{10}$$

It can also be seen that for every configuration in which the irreducible pattern km occurs once, there are $d_{km}-1$ other configurations exactly identical except that in the same $k+1$ particles the pattern km is drawn $d_{km}-1$ different ways, and there are also $d_{km'}$ other configurations identical with the first except that the pattern km' has replaced km, and in $d_{km'}$ different ways. It follows from this that the sum of terms making up b_l contains only powers of the constituent integrals so that we can write, designating the general term $s=(n_1, n_2, \cdots, n_k, \cdots)$

$$b_l=(l!)^{-1}\sum_s C_s\prod_k \gamma_k{}^{n_k}. \tag{11}$$

Detailed analysis shows that

$$b_4=2\gamma_1{}^3/3+\gamma_1\gamma_2/2+\gamma_3/24, \tag{12}$$

$$b_5=25\gamma_1{}^4/24+5\gamma_1{}^2\gamma_2/4+\gamma_2{}^2/8+\gamma_1\gamma_3/6+\cdots, \tag{13}$$

$$b_6=9\gamma_1{}^5/5+3\gamma_1{}^3\gamma_2+3\gamma_1\gamma_2{}^2/4+\gamma_1{}^2\gamma_3/2+\gamma_2\gamma_3/12+\cdots, \tag{14}$$

$$b_7=2401\gamma_1{}^6/720+343\gamma_1{}^4\gamma_2/48+45\gamma_1{}^2\gamma_2{}^2/16+\cdots. \tag{15}$$

The next task is to obtain an asymptotic value for the general coefficient C_s, or at least for the logarithm of this coefficient, as l becomes very large.

From general considerations it can be seen that it will be possible to write the asymptotic value of the logarithm of C_s in the form

$$\ln C_s=l\ln l+\sum_k n_k[\ln(l/n_k)+\ln c_k-k+1], \tag{16}$$

where c_k is a constant independent of l. If then the quantities β_k are defined as

$$\beta_k=c_k\gamma_k, \tag{17}$$

we can write Eq. (11) in the form

$$\ln b_l=\ln\{\sum_{k\geq 1}(\beta_k{}^{n_k}l^{n_k}/n_k!)\}. \tag{18}$$

In the above, use has been made of the fact that $\sum kn_k=l$ in which the difference between l and $l-1$ for large values of l has been neglected.

We shall, for the moment, neglect the problem of determining the value of c_k, the ratio of β_k

to γ_k, and confine our attention to the problem of obtaining a more manageable equation for $\ln b_l$ from (18). The sum under the logarithm in Eq. (18) has as many terms as the "partitio numerorum" of l, a number whose logarithm is negligible for large values of l, compared to the logarithm of any single term (see preceding article, Eqs. (14) and (15)). For all values of β_k positive we could therefore, set the value of the logarithm of b_l equal to the logarithm of the largest term in the sum, and since the values of n_k maximum will obviously be proportional to l we would obtain, defining

$$\nu_k^* = n_k^*/l, \quad n_k^* = n_k \text{ (maximum)}, \tag{19}$$

$$\ln b_0 = (\ln b_l)/l = \sum_{k\geq 1} \nu_k^*(1+\ln \beta_k - \ln \nu_k^*), \tag{20}$$

with

$$\sum_{k\geq 1} k\nu_k^* = 1. \tag{21}$$

The condition that ν_k^* be a maximum is obtained by setting the variation of Eq. (20) equal to zero, subject to the condition that the variation of (21) is also zero. Using the method of undetermined multipliers, multiply (21) by minus logarithm of ρ, and adding its variation to that of (20) we obtain that $(\nu_k^*/\beta_k)^{1/k}$ is independent of k, and equal to ρ, a value which we can then insert in Eqs. (21) and (20). We obtain

$$(\nu_k^*/\beta_k)^{1/k} = \rho, \quad \nu_k^* = \beta_k \rho^k, \tag{22}$$

$$\sum_{k\geq 1} k\beta_k \rho^k = 1, \tag{23}$$

$$\ln b_0 = \sum_{k\geq 1} \beta_k \rho^k - \ln \rho. \tag{24}$$

Eq. (23) can be used to determine ρ and Eq. (24) to determine $\ln b_0$. The above derivation assumes positive values of β_k, and is essentially the same as the method of obtaining q_τ in the previous article. In the appendix of this article a derivation of the two equations (23) and (24) is given which is independent of the assumption of positive values of β_k, and which is essentially similar to the derivation of the equation for q_τ given in the appendix of the preceding article.

For purposes of evaluation we shall find it convenient to introduce the dimensionless ratios between the various constituent integrals and the kth power of the first integral, namely,

$$r_k = \gamma_k/{\gamma_1}^k, \tag{25}$$

and

$$s_k = \beta_k/{\beta_1}^k = (c_k/{c_1}^k) r_k. \tag{26}$$

We can then write (23) as

$$x + 2s_2x^2 + 3s_3x^3 + \cdots = 1, \quad x = \beta_1\rho, \tag{27}$$

and (24) as

$$\alpha = e\beta_1/b_0 = x \exp(1 - x - s_2x^2 - s_3x^3 - \cdots). \tag{28}$$

We see that as $s_2, s_3, \cdots s_k$ approach zero, x and also α become unity, and b_0 becomes equal to $e\beta_1$.

We are finally forced to undertake the evaluation of the numbers c_k. To do this we must calculate the general coefficient C_s of the terms making up the sum of Eq. (11). This problem has not been solved satisfactorily. We can, in general, calculate a minimum value for the general coefficient C_s. For the term which we shall call $s = l-1$ for which $n_1 = l-1$, $n_2 = 0$, $\cdots$, $n_k = 0$ we can also calculate an upper limit to the value of C_{l-1}. The upper and lower limit bracket the value of the ratio c_1 between the values of $2/e$ and $e/2$, between two values, then, that differ by almost twofold. Fortunately it can be seen that the coefficient $C_{l-1}/l!$ for $l = 2$ to 7 inclusive, the numerical coefficient of ${\gamma_1}^{l-1}$ in Eqs. (3), (5) and (12) to (15), inclusive, obeys the equation

$$C_{l-1} = l^{l-2}, \tag{29}$$

from which, using Eq. (16), with $n_1 = l$, and all other n_k's $= 0$, we would derive that $c_1 = 1$. Although the authors realize that a deduction of the general term in a series from the value of the first six members is not exactly in the highest tradition of mathematical rigor they feel that it is highly probable that this method gives the correct value of the ratio c_1.

The bracketing process, referred to in the previous paragraph by which one obtains that c_1 lies between $e/2$ and $2/e$ is as follows. Firstly C_{l-1}, the number of ways that one can draw $l-1$ single bonds between l numbered points so as to have all the points indirectly connected to each other, but so as not to close any rings (which would lead to integrals other than γ_1), must be less than the total number of ways one can draw $l-1$ bonds between l numbered points. This total number is just the binomial coefficient, the coefficient of the $(l-1)$th term in the ex-

pansion of $(1+x)$ raised to the $[l(l-1)/2]$th power. Using Eq. (16) this leads to c_1 less than $e/2$.

In order to show that $c_1>2/e$ one may use the following argument. Consider l particles with $n-1$ bonds between them, making up a certain configuration. The configuration is not presumed to be such that only one cluster is formed, but it is presumed that no rings are closed, so that integration of the corresponding function would lead to ${\gamma_1}^{n-1}$. Assume that there are g_{n-1} such configurations. We now seek the ratio g_n/g_{n-1}. It is first apparent that any configuration of n bonds can arise from n different configurations of $n-1$ bonds. We shall determine the minimum number of ways that we can produce different configurations of n bonds out of any given configuration of $n-1$ bonds and divide this by n.

Assume we start with a configuration of $n-1$ bonds in which there are j clusters. There are then $n+j-1$ particles already in some way bonded, and $l-(n+j-1)$ particles which are not bonded. We have to pick 2 particles, but avoid closing a ring, which means only that we must avoid picking two particles out of the same cluster. We can pick two free particles, one bonded and one free, or two bonded particles, but from different clusters. The first we can do $[l-(n+j-1)]\times[l-(n+j)]/2$ ways, the second $(n+j-1)\times[l-(n+j-1)]$ ways, and the third *at least* $(n+j-1)\times 2(j-1)/2$ ways, since we can make our primary choice from any of the bonded particles and our second choice from any of the particles in the remaining $j-1$ clusters which have at least two particles per cluster. Summing these three ways, and dividing by n, we have

$$\begin{aligned} g_n/g_{n-1} &> (1/2n)[(l-n)(l+n-1)+j(j-1)] \\ &> (1/2n)[l-n](l+n-1), \end{aligned} \tag{30}$$

and since $g_1=l(l-1)/2$, we find for $g_{l-1}=C_{l-1}$,

$$C_{l-1}>\frac{1}{2^{l-1}}\frac{(2l-2)!}{(l-1)!}, \tag{31}$$

or finally, using (16), with $n_1=l-1$, $n_k=0$,

$$c_1>2/e. \tag{32}$$

The method which we use to obtain the general coefficient C_s is essentially similar to the method by which the equations (30), (31) and (32) were derived. It can be used to give a definite lower limit for C_s, or, by a slight alteration, to give an approximate probable value which we shall adopt to calculate the various c_k's. We consider l numbered particles in space and assume that between these l particles a certain number of bonds are drawn making up a certain configuration, $s-(km)$ characterized by the numbers n_1, n_2, $\cdots$, $(n_{km}-1)$, the numbers of the different irreducible patterns occurring in the configuration. The number of such configurations having the same characteristic numbers of irreducible patterns we shall call g_{s-km}. We now attempt to calculate g_s/g_{s-km}, g_s being the number of configurations with $s=n_1, n_2, \cdots, n_{km}, \cdots$ as the numbers of the different patterns. As before, any one configuration s may originate from n_{km} different configurations $s-(km)$, so we must divide the number of ways that we can make a configuration s out of one $s-(km)$ by n_{km} to obtain the desired ratio.

Assume that in a particular configuration $s-km$ there are J globs, so that if $K=\sum kn_{km}$ there are $K+J-k$ particles involved with bonds and $l-(K+J-k)$ free particles. The number of different configurations s we can make out of this configuration $s-(km)$ will be d_{km} times the number of ways that we can pick $k+1$ particles out of the configuration $s-km$ to add to it a single pattern km. We can pick all $k+1$ particles from the free particles, k from the free particles and one from any of the already bonded particles, $k-1$ free particles and two bonded particles, but from different globs, etc. Assuming that each glob has an average of m particles we find that to obtain the required number we must sum

$$S=\frac{(l-K-J+k)!}{(l-K-J-1)!(k+1)!}+\sum_{i=0}^{i=k}\frac{(l-K-J+k)!(K+J-k)m^i(J-1)!}{(l-K-J+i)!(k-i)!(J-1-i)!(i+1)!}. \tag{33}$$

If now m is given its minimum value of 2 we can obtain a lower limit for the ratio g_s/g_{s-km} which leads to a lower limit for C_s and the c_k's. Replacing m by 2, and doing some algebraic juggling in which

the small integers i and k are neglected compared to the large, K and J values, so that the factorials are replaced by powers, one arrives finally at the equation.

$$g_s/g_{s-km} > d_{km}(l-K)^k(l+kK)/n_{km}(k+1)!. \tag{34}$$

If one remember the definition of the constituent integrals as $\gamma_k = \sum_m d_{km}\gamma_{km}$, and uses

$$\sum_{n_{km}}(n_k!/\prod_m n_{km}!)\prod_m(d_{km}\gamma_{km})^{n_{km}} = \gamma_k{}^{n_k}, \quad (\text{with } \sum_m n_{km} = n_k) \tag{35}$$

one arrives at the expression for the general coefficient C_s

$$C_s > l!\prod_k[(k+1)^{1/k}l/ek!]^{n_k}/n_k!. \tag{36}$$

Use of this expression in Eq. (16) leads to

$$c_k > (k+1)^{1/k}/ek!. \tag{37}$$

This, of course, gives the same minimum value for c_1 that had been previously obtained, namely $2/e$.

We shall return to Eq. (33) and replace m, the average number of particles per glob by $K+J/J$, the ratio of the total number of bonded particles to the number of globs. We then obtain, in place of (34) Eq. (38), namely

$$g_s/g_{s-km} = d_{km}l^{k+1}/n_{km}(k+1)! \tag{38}$$

which leads to

$$c_k = e^k/(k+1)!. \tag{39}$$

This equation gives us $e/2$ as the value of c_1, which was the upper limit previously found. We have already shown that there is reason to believe that c_1 is equal to unity. We shall then use $c_1 = 1$, but for c_2 and c_3 the values derived from (39), namely,

$$\begin{aligned} &c_1 = 1, \qquad c_2 = e^2/6, \qquad c_3 = e^3/24; \\ &s_2 = (c_2/c_1^2)r_2 = 1.23r_2, \qquad s_3 = (c_3/c_1^3)r_3 = 0.835r_3. \end{aligned} \tag{40}$$

The sum σ of the previous article, Eq. (44), was the sum over all values of l of $lb_l/b_0{}^{l-1}$. Using Eq. (40) for c_1, Eq. (17) and (27) and (28) for b_0, and using the Eqs. (3), (5) and (12) to (15) for b_l from $l=2$ to 7, we can write the first few terms of σ. We obtain

$$\begin{aligned} \sigma = \sum_{l\geq 2} lb_l/b_0{}^{l-1} &= \sum(lb_l/\gamma_1{}^{l-1}e^{l-1})\alpha^{l-1} = \alpha/e + \alpha^2(3/2e^2)(1+r_2/3) + \alpha^3(8/3e^3)(1+3r_2/4+r_3/16) \\ &\quad + a^4(125/24e^4)(1+6r_2/5+3r_2{}^2/25+4r_3/25+\cdots) + \alpha^5(54/5e^5)(1+5r_2/3+15r_2{}^2/36 \\ &\quad + 5r_3/9+5r_2r_3/36+\cdots) + \alpha^6(3.334\times 7/e^6)(1+15r_2/7+0.842r_2{}^2+\cdots) \\ &= 0.368\alpha + 0.202\alpha^2(1+0.333r_2) + 0.133\alpha^3(1+0.75r_2+0.0625r_3) + 0.0955\alpha^4(1+1.20r_2+0.12r_2{}^2 \\ &\quad + 0.16r_3+\cdots) + 0.0726\alpha^5(1+1.60r_2+0.417r_2{}^2++0.555r_3+0.139r_2r_3\cdots) \\ &\quad + 0.0579\alpha^6(1+2.14r_2+0.842r_2{}^2+\cdots). \end{aligned} \tag{41}$$

The sum ϕ, Eq. (46) of the previous article is

$$\phi = \sum_{l\geq 2} b_l/b_0{}^{l-1}, \tag{42}$$

which can also be readily evaluated.

If it is generally true that the coefficient of $\gamma_1{}^{l-1}$ in b_l is $l^{l-2}/l!$ then the numerical coefficient multiplying α^{l-1} in the terms of σ will be $l^{l-1}/e^{l-1}l!$, which becomes asymptotically $e/l^{\frac{1}{2}}(2\pi)^{\frac{1}{2}} = 1.083l^{-\frac{1}{2}}$. In the last term given, for which $l=7$, the numerical coefficient has the value 0.0579 which is within about one percent of this asymptotic value. The use of this asymptotic value enables one to make

fairly accurate estimates of the sum of the contributions of the unevaluated terms in σ, and of course also in ϕ, which, however, converges appreciably more rapidly.

When all the r_k's are zero, as has previously been noted, α becomes unity. σ has then the value 1.70, of which 0.772 is contributed by the terms beyond those evaluated. ϕ has the value 0.355 of which 0.032 is contributed by the unevaluated tail. The value of $(PV)_s/RT$ (see Eq. (52) of the previous article) is $(1+\phi)/(1+\sigma)$, which under the condition that all the r_k's be zero, has the numerical value 0.501. This occurs, experimentally, in most gases, at a temperature slightly below the critical temperature, and we have chosen this temperature $T_{0.5}$ as a reference temperature from which to measure our temperature scale.

The Constituent Integrals

We now come to the problem of determining the constituent integrals, γ_k. To this problem there is, of course, no generally exact solution, since the exact form of the potential energy $v(r)$ as a function of the distance r between the centers of gravity of two molecules or atoms is not known. We shall assume a certain form

$$\begin{aligned} v(r)=v_1(z)&=6u\{(2/3z^6)(1/z^6-1)\}, \quad \text{for } (2/3)^{1/6}\leq z\leq\infty, \\ v_1(z)&=75u-72(3/2)^{1/6}uz, \qquad \text{for } 0\leq z\leq(2/3)^{1/6}, \\ z&=r/r_0. \end{aligned} \tag{43}$$

This function is of the general form $A/r^{12}-B/r^6$ in the range for which the exact value is of significance. The paramater r_0 is so chosen that $v(r)=0$ when $r=r_0$, $z=1$, and $-u$ is the minimum value of the potential which occurs at $z=(2)^{1/6}$ or $r=(2)^{1/6}r_0$. This potential function we shall refer to as the exact potential function, v_1, and the subscript 1 will be used in the left hand lower side of any integrals derived from it. We shall find it convenient to express our integrals in terms of the volume

$$v_0=4\pi(r_0/2)^3/3=\pi r_0^3/6, \tag{44}$$

which may be called the volume of the molecules. The quantity u/kT we shall call

$$\theta=u/kT. \tag{45}$$

Using Eqs. (2) and (3) we can evaluate ${}_1\gamma_1$ from this form of v_1 as accurately as we please. The integration is actually done directly from $z=0$ to $z=(2/3)^{1/6}$ and by expanding the exponential for larger values of z. The equation for ${}_1\gamma_1$ so obtained is

$$\begin{aligned} {}_1\gamma_1(\theta)/8v_0=-(2/3)^{\frac{1}{2}}\{1-e^{-3\theta}&(1/24\theta-1/864\theta^2+1/62208\theta^3)+(1/62208\theta^3)e^{-75\theta} \\ &-[3\theta+(69/70)\theta^2+(9/770)\theta^3+(5409/40040)\theta^4 \\ &+0.1504\theta^5+0.02108\theta^6-0.00726\theta^7+0.00273\theta^8\cdots]\}. \end{aligned} \tag{46}$$

The sudden occurrence of alternating signs is real.

This form of the potential function, however, leads to hopelessly complicated integrals in the determination of γ_2. We shall therefore introduce a new potential function $v_2(z)$, such that

$$\begin{aligned} v_2(z)&=-kT\ln(1+az^{-6}), \quad & f_2(z)&=az^{-6}, \quad & \text{for} \quad & 1\leq z\leq\infty, \\ v_2(z)&=+\infty, & f_2(z)&=-1, & \text{for} \quad & 0\leq z\leq 1. \end{aligned} \tag{47}$$

This function is also so chosen that $v(z)$ changes sign at $z=1$. The integration of ${}_2\gamma_1$ using this function is, of course, trivial. ${}_2\gamma_2$ can be obtained by using the coordinates r_{12}, r_{23}, r_{13}, with the volume element $d\tau_2 d\tau_3=8\pi^2 r_{12}r_{23}r_{13}dr_{12}dr_{23}dr_{13}$ and the integration limits for the first coordinate to be integrated, say

$$r_{12}, \qquad |r_{13}-r_{23}|\leq r_{12}\leq|r_{13}+r_{23}|.$$

The integration is extremely tedious, even with so simple a function as $f_2(z)$, so the steps will not be shown here. The results are,

$$ {}_2\gamma_1(a)/8v_0 = a - 1, \tag{48} $$

$$ {}_2\gamma_2(a)/(8v_0)^2 = 4.5[0.014356a^3 - 0.075455a^2 + 0.10748a - 0.104167]. \tag{49} $$

It is now possible by numerically equating (49) to (46) to find the "best" value of a to correspond to any given value of θ. By this means we obtain γ_1 exactly, and γ_2 fairly satisfactorily in terms of the two parameters θ and r_0 (or v_0), of the "exact" potential function (46). This method is undoubtedly fairly satisfactory as a means of determining γ_1 and γ_2 in terms of two parameters of a potential function.

However, the authors had no desire to continue the integration of $f_2(z)$ to obtain γ_3. With sufficient patience this could be done, but the chore is rather tedious. Considerable time was spent in integrating the three parameter function

$$ f_3(z) = \beta[(z/R) - 1] \exp(-z/\alpha R). \tag{50} $$

As long as $f_3(z) \geq -1$ this corresponds to the potential

$$ v_3(z) = -kT \ln [1 + \beta\{(z/R) - 1\} \exp(-z/\alpha R)]. \tag{51} $$

This function is much too "soft," that is it has no sufficiently pronounced deep minimum but a rather broad band where $v_3(z)$ is negative and $f_3(z)$ positive. The only use which we wish to make of the integrals obtained from this function is to point out the qualitative fact that most reasonable choices for the parameters give the ratio ${}_3\gamma_2/{}_3\gamma_1{}^2 = {}_3r_2$ as very much smaller than ${}_2\gamma_2/{}_2\gamma_1{}^2 = {}_2r_2$. With these values ${}_3r_3 = {}_3\gamma_3/{}_3\gamma_1{}^3$ is, in general, over the range in which we wish to work, very much smaller than ${}_3r_2$. If the parameters are so chosen that the ratio ${}_3r_2 = {}_2r_2$ we find that ${}_3\gamma_3$ and r_3 remain negative to much lower temperatures than γ_2 and r_2. The general impression obtained from attempting to work with this function $f_3(z)$ is that for the "soft" function γ_3 remains negative to lower temperatures than γ_2 (which with any function chosen is negative at lower temperatures than γ_1) and that r_3 is smaller than r_2 except at extremely low temperatures when both are greater than unity.

We then attempted to investigate

$$ \begin{array}{llll} f_4(z) = -1, & v_4(z) = \infty, & \text{for} & 0 \leq z \leq 1, \\ f_4(z) = a/3\delta, & v_4(z) = -kT \ln [(a/3\delta) + 1], & \text{for} & 1 \leq z \leq 1 + \delta, \\ f_4(z) = 0, & v_4(z) = 0, & \text{for} & 1 + \delta \leq z \leq \infty, \end{array} \tag{52} $$

in which δ is regarded as an infinitesimal. This function is too "hard" in contradistinction to the "soft" $v_3(z)$, and should show deviations in the opposite direction from the true integrals. The integrations are relatively simple for γ_1, γ_2, γ_{30} and γ_{31}. γ_{32} was obtained by making a few approximations which are of no great importance to discuss here since it contributes relatively little to $\gamma_3 = 3\gamma_{30} + 6\gamma_{31} + \gamma_{32}$. The equations obtained are

$$ {}_4\gamma_1(a)/8v_0 = a - 1, \tag{53} $$

$$ {}_4\gamma_2(a)/(8v_0)^2 = a^3/6 - 3a^2/4 + 15a/16 - 15/32, \tag{54} $$

$$ {}_4\gamma_{30}(a)/(8v_0)^3 = a^4/6 - 2a^3/3 + 6a^2/5 - 34a/35 + 34/105, \tag{55} $$

$$ {}_4\gamma_{31}(a)/(8v_0)^3 = a^5/36 - a^4/4 + 11a^3/16 - 39a^2/40 + 0.70837a - 0.2361234, \tag{56} $$

$$ {}_4\gamma_{32}(a)/(8v_0)^3 = 0.001805a^6 - 0.064815a^5 + 0.2882a^4 - 0.4862a^3 + 1.25a^2 - 0.885a + 0.295, \tag{57} $$

$$ {}_4\gamma_3(a)/(8v_0)^3 = 0.001805a^6 + 0.101852a^5 - 0.7118a^4 + 1.6388a^3 - a^2 + 0.885a - 0.295. \tag{58} $$

Numerical comparison shows that a is to be identified with the a of $v_2(z)$. ${}_4\gamma_2$ becomes positive at much higher temperatures than ${}_2\gamma_2$, and ${}_4\gamma_3$ is positive at all reasonable temperatures, but very small in numerical value until about the temperature at which ${}_4\gamma_2$ becomes positive. For lower temperatures than this it increases rapidly in value, with decreasing temperature. The fact that ${}_4\gamma_3$ is positive at high temperatures may be due to an error in estimating ${}_4\gamma_{32}$, but if so this will make little difference at the lower temperatures at which it is unimportant. Plotting ${}_4\gamma_2$ and ${}_2\gamma_2$ against a shows that a shift of scale of a in ${}_4\gamma_2$ will bring the two curves into remarkably good agreement. The shift is by a factor of 1.31 such that

$$ {}_4\gamma_2(a/1.31) \cong {}_2\gamma_2(a). \tag{59}$$

We have therefore chosen, as an empirical estimate of γ_3 to use Eq. (59) but with substitution of $a/(1.31)^2$ for a in the equation. We shall not trust any numerical calculations in temperature ranges where s_3 is large, and since we are entirely omitting s_4 in any event this rather crude estimate of γ_3 is probably sufficient for our purposes. It will at least give us a rough indication of the temperature range for which we can make calculations with some degree of confidence in the results.

Numerical Results

In Table I the most important steps in the evaluations, and the values of some of the observable properties of the saturated vapor are given. In column 1 the value of a is given for which the subsequent values in the same row are calculated. In column 2 are the values of $\gamma_1/8v_0$ calculated from Eq. (48), namely $a-1$. In column 3 the values of $\theta=u/kT$ are given, calculated from Eq. (46). r_2 obtained from Eqs. (49) and (48), and r_3 from (59) and (48), as well as s_2 and s_3 are listed in columns 4, 5, 6 and 7, respectively. $x=\beta_1\rho$, Eq. (27), and α, Eq. (28), as well as b_0/v_0 are in columns 8, 9 and 10. It is to be noted that from Eq. (28), $\partial\alpha/\partial x=0$ when (27) is fulfilled, so that the error introduced into α and b_0 by the omission of s_4 and subsequent terms may be expected to be of the order of magnitude of s_3x^3 rather than of $3s_3x^3$. For the row $a=6.5$ we have $s_3x^3=0.026$ and for the last row, $a=9$, $s_3x^3=0.035$. The sums σ, Eq. (41), and ϕ, (42), are tabulated in columns 11 and 12. Finally v_s/v_0, the ratio of the volume per molecule of the saturated vapor to the volume of the molecules as defined by Eq. (44), is given in column 13, $(PV)_s/RT$, which is $(1+\phi)/(1+\sigma)$, a measure of the degree by which the saturated vapor deviates from the perfect gas law, is listed in column 14. In the last column an arbitrary linear scale of temperature is given. The scale is so chosen that the temperature, $T_{0.5}$, at which PV/RT is 0.5 is chosen as unity.

On this scale of temperature, the temperature at which $\gamma_1/8v_0$ becomes zero is 3.562. One predicts then, that for gases obeying an A/r^7 attractive law of force between the molecules, the temperature at which the second virial coefficient changes sign, the Boyle temperature, should be

Table I.

1	2	3	4	5	6	7	8	9	10	11	12	13	14	15
a	$\gamma_1/8v_0$	$\theta=u/kT$	$r_2=\gamma_2/\gamma_1^2$	$r_3=\gamma_3/\gamma_1^3$	$s_2=\beta_2/\beta_1^2$ $=1.23r_2$	$s_3=\beta_3/\beta_1^3$ $=0.836r_3$	$x=\beta_1\rho$	$\alpha=e\gamma_1/b_0$	b_0/v_0	σ	ϕ	v_s/v_0	$\frac{PV}{RT}=\frac{1+\phi}{1+\sigma}$	$T/T_{0.5}$
1.0	0.0	0.286												3.562
2.0	1.0	0.606												1.681
3.0	2.0	0.857												1.190
3.5	2.5	0.960	−0.027		−0.034									1.064
3.8	2.8	1.020	0.000	δ	0.000	δ	1.000	1.000	60.9	1.70	0.35	22.5	0.502	1.000
4.0	3.0	1.056	0.019	0.02	0.023	0.02	0.915	0.961	67.8	1.13	0.32	31.8	0.620	0.967
4.5	3.5	1.140	0.060	0.04	0.074	0.03	0.841	0.919	82.8	0.94	0.29	42.7	0.667	0.895
5.0	4.0	1.220	0.095	0.06	0.117	0.05	0.784	0.882	97.5	0.84	0.27	53.0	0.690	0.837
5.5	4.5	1.294	0.130	0.07	0.160	0.06	0.746	0.859	114	0.79	0.26	63.7	0.706	0.790
6.0	5.0	1.358	0.166	0.08	0.205	0.07	0.717	0.833	130	0.74	0.25	75.0	0.719	0.753
6.5	5.5	1.411	0.201	0.09	0.248	0.07	0.690	0.820	146	0.71	0.24	85.2	0.725	0.723
7.0	6.0	1.466	0.234	0.10	0.288	0.08	0.668	0.797	164	0.67	0.23	98.0	0.736	0.697
8.0	7.0	1.556	0.301	0.14	0.371	0.12	0.625	0.763	199	0.62	0.22	123	0.754	0.652
9.0	8.0	1.636	0.379	0.20	0.467	0.17	0.583	0.729	239	0.57	0.21	152	0.773	0.624

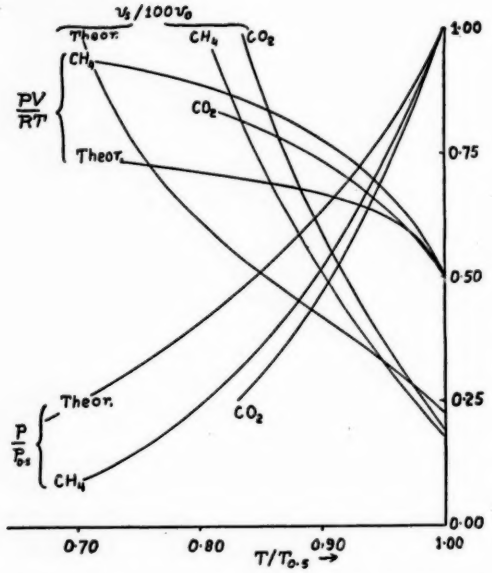

FIG. 1. PV/RT, P and $v_s/100_0$ for the saturated vapor plotted against $T/T_{0.5}$. The temperature scale is so chosen that unity is the temperature at which PV/RT of the saturated vapor is equal to 0.5. The pressure scale is so chosen that P is unity when T is unity. The volume ratio is obtained by assuming that in liquid CO_2 and CH_4 the volume per molecule is 2.5 times v_0.

about 3.5 times the temperature for which PV/RT of the saturated vapor is one-half. Experimentally it appears that this ratio is about 3.5 in N_2.

In Fig. 1 a plot showing the agreement, or disagreement, between the results of these calculations, and the experimentally observed values for the two gases CO_2 and CH_4 is shown. The temperature scale is so chosen that $PV/RT=0.50$ at $T=1.00$. The pressure scale is also chosen so that $P=$unity at this temperature. The volume scale is, however, not arbitrary. It was assumed that the volume of a liquid at ordinary temperatures, (P_s about 1 atm.) would be about 2.5 times our v_0, per molecule. It is to be remembered that the v_0 which we chose is the volume of a sphere the diameter of which is equal to the distance of the centers of two molecules when their mutual potential just changes sign. This volume is some $\sqrt{2}$ fold less than the volume corresponding to the minimum of the potential energy curve. The value 2.5 then assumes that the volume of the liquid is about 25 percent greater than "close packing." The free energy of the gas changes by only about RT ln 2 for a two-fold change in pressure or volume. The fact that, from $T=1.00$ to about $T=0.8$ the ratio v_s/v_0 appears to agree within 2-fold with the experimental values indicates that within this temperature range our equations should give the free energy of the liquid to within about RT ln 2. This appears to the authors to indicate some degree of success. It is, however, obvious from the plot of Fig. 1 that considerable improvement can be made before the agreement with experiment can be said to be excellent.

CONCLUSION

It is obvious that the present paper shows lacks, both in the rigor of some of the proofs and in the accuracy of the numerical evaluations. The value $c_1=1$ is probably exact, but certainly not proven, the values of other c_k's, c_2 and c_3 are extremely uncertain, in fact it can be safely said that they are rather certainly inexact. Although the value of γ_1 can be said to be exactly correct for a gas of molecules with the mutual potential given by Eq. (43), the value of γ_2 is certainly somewhat in error, and that of γ_3 is little more than a guess. Better evaluations of these integrals is largely a matter of patience, although considerable patience was needed to go as far as has been done!

In addition to these faults the question of the volume dependence of b_l at small volumes has been entirely neglected as yet. The discussion of the slightly complicated behavior of the gas in the neighborhood of the critical point has been avoided in this paper.

The authors hope that some of these questions will be handled in later papers.

In conclusion the authors wish to thank Dr. M. Goeppert Mayer, who has listened patiently, but critically, to many false theories, and has offered many constructive suggestions.

Note added in proof: P. G. Ackermann has discovered that the value of the general coefficient C_s (Eq. (36)) appears to be

$$C_s=(l!/l^l)\Pi(l/k!)^{n_k}(1/n_k!)$$

which leads to $c_k=1/k!$. This can probably be proven. Work on the integrals γ_3 by S. F. Harrison indicates that the values chosen in this article are too small. It is to be hoped that

better numerical agreement with experiment can now be obtained. Harrison and Mayer have also observed that Eqs. (22), (23) and (24) contain an explanation of the phenomena of fusion, a prediction of a second change of phase, highly temperature dependent, arising in a manner similar to the condensation phenomena.

APPENDIX

We seek a more satisfactory form for $\ln b_l$, than Eq. (18) of the text. We define a function B, as
$B(l, \beta_1, \cdots, \beta_k, \cdots, x, j)$

$$=\sum_{n_k}\{\prod_k \beta_k^{n_k} x^{kn_k} j^{n_k}/n_k!\}, \text{ with } \Sigma k n_k = l, \quad (1)$$

and obtain, by direct differentiation of the sum

$$\beta_k \frac{\partial B}{\partial \beta_k} = \beta_k x^k j B(l-k, \beta, x, j), \quad (2)$$

$$x\frac{\partial B}{\partial x} = \sum_k k\beta_k \frac{\partial B}{\partial \beta_k} = lB, \quad (3)$$

$$j\frac{\partial B}{\partial j} = \sum_k \beta_k \frac{\partial B}{\partial \beta_k}. \quad (4)$$

The introduction of b_0, with $x \equiv 1$,

$$\ln b_0(l, \beta, j) = (1/l) \ln B(l, \beta, j), \quad (5)$$

allows us to transform (3) into

$$\Sigma k\beta_k(\partial \ln b_0/\partial \beta_k) = 1, \quad (6)$$

and (4) into

$$\partial \ln b_0/\partial j = (1/j)\sum_k \beta_k(\partial \ln b_0/\partial \beta_k). \quad (7)$$

Taking the logarithm of (2), setting $x=1$ and $j=l$, and using $\ln b_0((l-k), \beta, j) = \ln b_0(l-k), \beta, (j-k) + k(\partial \ln b_0/\partial j)$ we obtain, after neglecting one term which is multiplied by k/l,

$$\ln(\partial \ln b_0/\partial \beta_k) = -k \ln b_0 + k\sum_k \beta_k(\partial \ln b_0/\partial \beta_k)$$

$$+l\{\ln b_0(l-k, \beta, j-k) - \ln b_0(l, \beta, j)\}. \quad (8)$$

The last term in this expression is negligible, since it is just $-k(\partial \ln f(l)/\partial l)$ which is of the order of magnitude $(k/l) \ln f(l)$ and negligible compared to $\ln b_0$. We find that $(\partial \ln b_0/\partial \beta_k)^{1/k}$ is independent of k, and can abbreviate it with the symbol ρ, in which case (6) and (8) become

$$\sum_{k\geq 1} k\beta_k \rho^k = 1, \quad (9)$$

$$\ln b_0 = \sum_{k\geq 1} \beta_k \rho^k - \ln \rho, \quad (10)$$

identical with Eqs. (23) and (24) of the text.

Errata: The Role of Molecular Orientation in Photochemical Reactions in Monolayers

JOSEPH S. MITCHELL, *Laboratory of Colloid Science, Cambridge, England*

(J. Chem. Phys. **4**, 725 (1936))

ON page 727 of my article with the above title, the last sentence of the paragraph preceding the paragraph headed "General Features of the Absorption of Light by Monolayers," should read "For any value of θ_0, the deviation of the observed ϕ_a from that calculated on the assumption of negligible thermal oscillation is proportional to the absolute temperature, but owing to the usual variation of θ_0 with molecular area, it is only at and near the limiting area that such an effect could be detected."

LETTERS TO THE EDITOR

This section will accept reports of new work, provided these are terse and contain few figures, and especially few halftone cuts. The Editorial Board will not hold itself responsible for opinions expressed by the correspondents. Contributions to this section must reach the office of the Managing Editor not later than the 15th of the month preceding that of the issue in which the letter is to appear. No proof will be sent to the authors. The usual publication charge ($3.00 per page) will not be made and no reprints will be furnished free.

Infrared Absorption by Formaldehyde Vapor

The absorption by formaldehyde vapor has been remapped from 1.0μ to 11.0μ using an absorption cell of Pyrex glass to which polished rocksalt windows were cemented with glyptal. The formaldehyde polymer may then be placed in the cell as a solid, the cell evacuated and sealed off. This has the definite advantage of insuring against oxidation or other decomposition of the formaldehyde by contact with air.

The observations verify the results of Nielsen[1] except in the region from 8.5μ to 10μ. The parallel type band reported in this work is apparently not due to H_2CO but instead a region of intense absorption is found extending from about 8.5μ to 9.8μ of which the region measured in emission by Nielsen near 9.6μ may be identified as a portion. The band resembles that of 7.5μ in general details, the average spacing between prominent lines being about 22.5 cm^{-1}.

The complete details of these measurements will be published in the near future together with the band spectrum of the deuteroformaldehyde on which preliminary measurements have already been made.

EARLE S. EBERS
Royal Canadian Fellow

HARALD H. NIELSEN

Mendenhall Laboratory of Physics,
Ohio State University,
Columbus, Ohio,
December 10, 1936

[1] "The Infrared Absorption Spectrum of Formaldehyde," Phys. Rev. 46, 117–121 (1934).

The Effect of Hydrogen Bond Formation on the Fundamental Frequency of the Hydroxyl Radical

Wulf, Liddell, *et al.*,[1] have shown that the first harmonic of the hydroxyl group is absent when hydrogen bonding or "chelation" occurs. This result has been confirmed by us for a number of compounds. The disappearance of the first harmonic, however, does not necessarily imply the absence of the fundamental.

Gordy[2] has suggested that the fundamental of the hydroxyl is shifted to shorter wave-lengths when a solution is made from two liquids belonging to different chemical types such that a hydrogen bond might be formed between two unlike molecules. While we do not question Gordy's experimental results, his interpretation may not be correct, since hydrogen bonding is already present in one of the pure liquids, and may actually be decreased in amount when the solution is made.

As a matter of fact, one might predict the opposite effect; *viz.*, a shift to longer wave-lengths for the OH fundamental when a hydrogen bond is formed. The writers have observed what appears to be such a shift in a number of cases. In a dilute carbon tetrachloride solution, the OH fundamental appears at about 2.75μ. This frequency is not greatly different from that observed in water vapor. When there is an opportunity for hydrogen bonding, this fundamental appears to shift and fuse with the C–H fundamental at 3.2μ. The resulting peak has a maximum near 3.0μ, and still shows a shoulder at 3.2μ indicative of the C–H absorption. With the limited resolving power of our apparatus, we cannot separate these two bands, if, indeed, this be possible, so that positive identification is difficult. A number of compounds of the type of *o*-nitrophenol have not failed to show this strong absorption in the neighborhood of 3.0μ, and when the hydrogen was substituted by deuterium under conditions under which it was hoped that only the hydroxyl would be deuterated, this new band was shifted almost completely to 4.2μ, leaving the C–H band apparently unaltered in location. While the utmost caution must be observed in interpreting results of this kind, we do not see how any other interpretation can be placed on these results, unless some unsuspected phenomenon is occurring. We hope, by further work, to confirm this result, or else discover the correct interpretation if our inference is incorrect.

It may be mentioned here that there are indications that the behavior of both the fundamental and perhaps even the first harmonic of the hydroxyl is somewhat different in the case where the hydrogen bond is between molecules. The results discussed above involve intramolecular hydrogen bonds. This latter point, however, also requires further investigation.

We wish to acknowledge our indebtedness to Drs. R. Bowling Barnes and Urner Liddell of the American Cyanamid Company for a profitable discussion of some of the results reported here.

A. M. BUSWELL
V. DEITZ
W. H. RODEBUSH

University of Illinois,
Urbana, Illinois,
November 25, 1936

[1] G. E. Hilbert, O. R. Wulf, S. B. Hendricks and U. Liddell, J. Am. Chem. Soc. **58**, 548 (1936).
[2] W. Gordy, J. Chem. Phys. **4**, 749 (1936).